DEVELOPMENT AND ANALYSIS OF A FLUID POWER TEST FACILITY

by

I.F. Jones B.Sc., B.E.(Hons.)

Submitted in partial fulfilment of the requirements for the degree of Master of Engineering Science in the Faculty of Engineering, University of Tasmania, Hobart.

January, 1972

Contents

Abstract

The work described in this thesis was undertaken as part of a project to design and build an electro-hydraulic vibration testing machine of unusual configuration using the limited manufacturing facilities of the departmental workshops of the Engineering School of the University of Tasmania. A sketch showing the basic concept of the vibrator design is shown in Chapter 1.

Technical limitations concerning available means of measurement and manufacture resulted in the development of a series of four-way spool valves featuring thin axial flutes milled in the spool lands to limit the area gradient and allow a long stroke relative to the flow rating of the valve.

An experimental rig to measure spool forces and flow characteristics under various static and dynamic conditions is described in detail. Difficulties experienced in the operation of the rig are discussed together with suggested lines of rig development.

Digital simulation of hydraulic servo-mechanisms by the Runge Kutta technique is examined in detail particularly with respect to the causes of numerical instability. An alternative approach based on the Method of Characteristics is also described and found to be particularly useful for systems containing long pipelines. The latter method is based on the velocity of pressure propagation in the fluid media and the results of an experimental investigation to determine this velocity as a function of pressure in a flexible high pressure hose are presented.

------ ooo ------

INTRODUCTION

In essence this thesis describes the first attempt by the Engineering Department of the University of Tasmania to enter the field of fluid power; in particular the field of high pressure oil power transmission and control. As such it possibly contains much rudimentary material. However this is included mainly as a background for those at a similar stage of development, or for those who follow.

The project had as its general aim the development of a variable flow, high pressure test facility to which hydraulic components and systems can be connected. However, as with any developmental project, it is preferable to have a more specific goal to work towards. This was the design and construction of a vibration testing machine to be used for testing machines and structural components. It was to be a small, compact unit consisting of an hydraulic servo-mechanism amplifying the output from an electromagnetic exciter. The frequency range was to be from 5 to 250 Hz and the output was to approximate a sinusoidal waveform with low distortion. Furthermore the unit was to be capable of high force levels, the force approaching 5000 lbf at the lower frequency limit.

With this specific aim in mind, it was therefore of considerable interest to find a French design of vibration testing machine [1], shown below, which was very similar to that envisaged. The article accompanying the diagram however, gave very little useful information about the design or construction of the device. Nevertheless it was decided to aim for a final design very similar to this. This decision ruled out the use of commercially available four-way valves for the control valve, and as a consequence the Engineering Department embarked on the development and construction of its own valve designs. At the same time the overall analysis of the servo-mechanism was commenced. This reduced to the analysis of a four-way valve controlling a double acting ram with inertia loading.

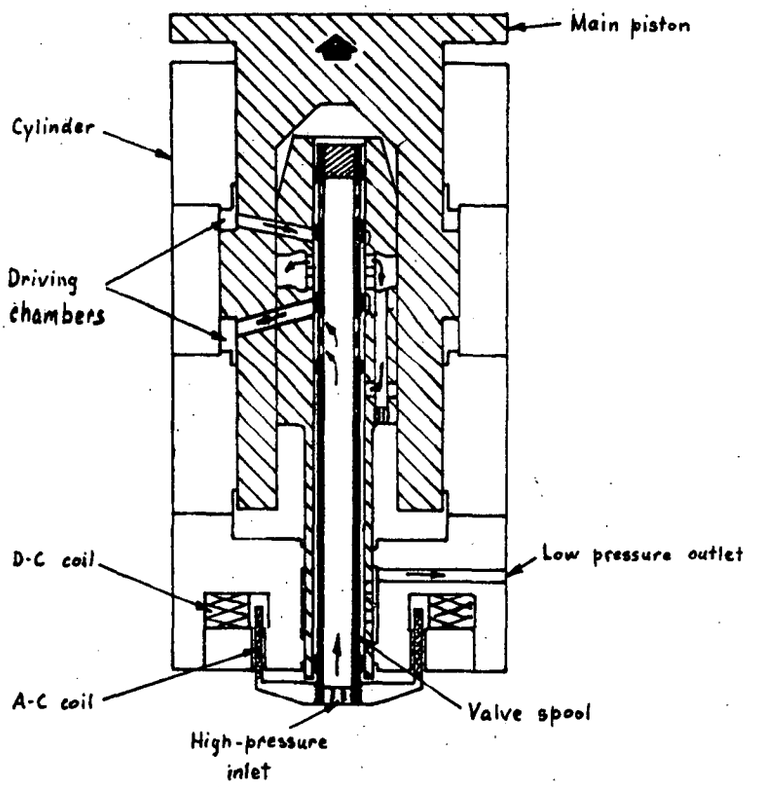

The analysis of such a servo-mechanism is of course in no way new. As long ago as 1947 Coombes [2] analysed a similar system. But, because of the difficulty in solving the equations which result from assuming a sinusoidal valve input, he used the rather interesting approach of assuming a sinusoidal output and deriving the required valve input. Royle [3] had more success by solving the problem with a sinusoidal input for a simple servo-mechanism without feedback and with an incompressible fluid. He obtained a series approximation to the solution which was valid under certain conditions. However when he added feedback, the increased complexity forced him to use an analogue computer to obtain a solution. Butler [4] also obtained a solution for the simple servo-mechanism with cavitation by numerical means. In fact the equations both Royle and Butler solved were similar to those discussed in this thesis under the heading of "Solid-slug models". However Butler makes no mention of numerical instability occuring as the valve closes; a problem which caused considerable trouble in this project. Turnbull [5] also solved the problem of the simple

servo-mechanism, with feedback included, by the graphical means of "phase-planes".

If compressibility is included in the models the equations become even more difficult to solve. Consequently most of the models which include it have been studied with the aid of analogue computers. Martin and Lichtarowicz [6] used this method to investigate the onset of cavitation in a servo-mechanism similar to that studied here, but without feedback. In this project it was unfortunate that a suitable analogue computer was not readily available. A fast, digital computer however, was, and consequently the solutions were attempted numerically. This lead to many interesting problems in itself, such as numerical instability.

Probably the most common method of solution is to linearize the equations [7, 8]. This has the great advantage that the conventional techniques of control engineering may then be employed in the analysis. The simple servo-mechanism without feedback was studied in this fashion by Reeves [9] while Ashley and Mills [10] investigated a much more complex servo-mechanism. The latter although not directly applicable to the servo-mechanism studied in this thesis is of interest because of the two-stage, flapper controlled valve used to control the ram. Ashley and Mills showed that the flow behaviour of this type of valve does not follow the classical dependence on the square root of the valve pressure drop. In fact the load pressure has only a small effect on the flow; a fact which could be of some value in a vibration tester. However the most useful linearization in relation to this project is one by Lambert and Davies [11]. The servo-mechanism they studied is identical to that in this project and the third-order, linearized model they derive has been used later to compare with the results obtained by numerically intergrating the non-linear equations of the system.

The main disadvantage with linearized models, however, is that the linearization tends to remove some of the distortion in the waveforms. This is not very important for simple servo-controls as the overall

response and time constants of the system are generally all that is required. However with a vibration tester, distortion is quite important and the linearized equations are consequently only of limited value in this respect.

------ ooo ------

CHAPTER 1

HYDRAULIC CIRCUIT AND INSTRUMENTATION

1.1 The Basic Hydraulic Circuit

A schematic diagram of the hydraulic circuit is shown in figure 1.1. Basically it consisted of a pump supplying oil at constant pressure to a "system" under study. This "system" normally required highly irregular flows, both of a relatively high frequency pulsating nature and of quite variable average flow rate. The accumulator was included to smooth out the high frequency pulsations while the variation in average flow was overcome, initially, by the relief valve diverting excess oil from the fixed displacement pump back to the reservoir, and later by a pressure compensated variable displacement pump. The latter adjusted its output to maintain a "constant" supply pressure. To monitor the supply pressure a Bourdon tube type pressure gauge was connected to the supply upstream of the "full-flow" ball valve used to isolate the system from the supply.

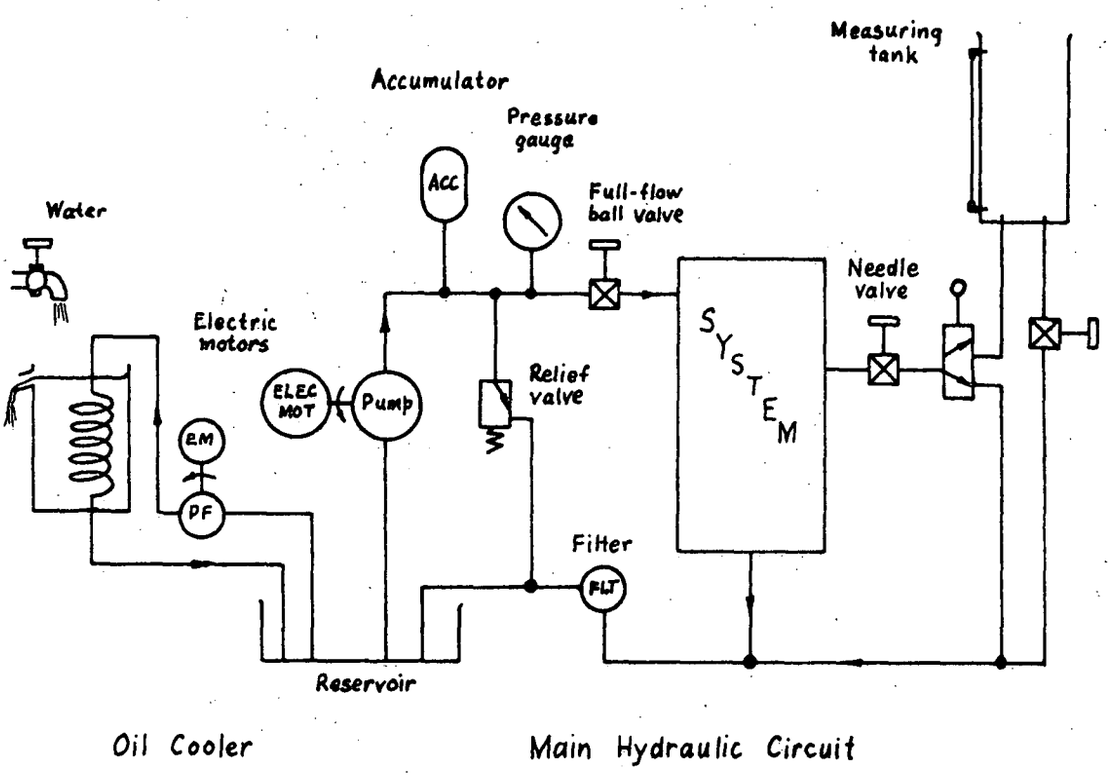

Figure 1.1

The hydraulic circuit

From the "system" the oil could be taken through a needle valve, which was used to apply back-pressures to the "system", to a two-way valve which either directed the flow into the measuring tank or back to the reservoir. Unfortunately this two-way valve was of the closed centre type; an open centre had been ordered but as there would have been a considerable delay in its delivery a closed centre was accepted. This was a bad mistake for the interruption to the oil flow as the valve passed through centre caused serious pressure pulses which not only upset the operation of the "system" but could also damage the pressure transducers used on the rig, particularly if, as is anticipated, the supply pressure is increased. It would be highly desirable to change this valve to an open centre type in the near future. Filtering of the oil was accomplished by a filter in the return line.

The other main feature of figure 1.1 is the oil cooling circuit on the left. The cooling was achieved by passing cold water over a copper coil through which the oil was pumped. This circuit is described in detail later (section 1.3) as it had many interesting features in itself.

The oil used in the circuit was a light "hydraulic" mineral oil (BP HLP65). It had addatives for antiwear, antirust, antifoam, anti-oxidation and a pour depressant. At 100°F the specific gravity was 0.85 and the viscosity 33 centistokes.

Originally the pump, accumulator, relief valve and reservoir were bought as a complete commercial unit. The pump was a fixed displacement vane pump capable of pressures up to 2000 psi and a maximum flow of between 3.5 and 4 gpm (imperial). The relief valve was adjustable and could be set to maintain, within limits, any pressure from 500 to 2000 psi.

There were several drawbacks with this unit. The main one was the continuous, constant, high power input required by the fixed displacement pump. As this power was dissipated in the oil, it represented a considerable heat input, and the oil temperature proved difficult to control, even with the oil cooler. Also the

relatively small maximum flow offered by this pump severely limited the results that could be obtained. This was very apparent in the early studies of the valve characteristics, for the valves had been designed on the assumption of significantly higher flows.

Late in the project it became possible to purchase a new pump. The type chosen was a pressure compensated, variable displacement, piston pump capable of maintaining pressures from 200 to 3000 psi at flows up to a maximum of over 6.5 gpm. Fortunately the motor supplied with the original unit had been excessively large and it was possible to use this same motor with the bigger pump.

This pump was found to be very satisfactory. Not only was the maximum flow now of the order of that assumed in designing the valves, but, because of the variable displacement, the average power input was greatly reduced, even though the pump was larger. This lower average power input was due to the considerable periods of time during which the flow requirements of the "system" were only small. With the fixed displacement pump this made no difference, for the flow not required by the "system" was diverted to the reservoir by the relief valve. However with the variable displacement pump the pressure compensator shut down the flow, and hence power input, to suit the requirements of the "system". This usually enabled the oil cooler to maintain the oil temperature within reasonable limits. The pressure compensator also meant that the relief valve was no longer really necessary. Nevertheless it was left on the rig and set to operate at a pressure approximately 50% above working pressure, which in this case had been limited to 1000 psi by the original pressure transducers, to safeguard against any pressure rise due to a malfunction in the pressure compensator.

Some photographs of the experimental rig are shown in figure 1.2. These show the rig set up for the dynamic tests on the four-way valve described in Chapter 2.

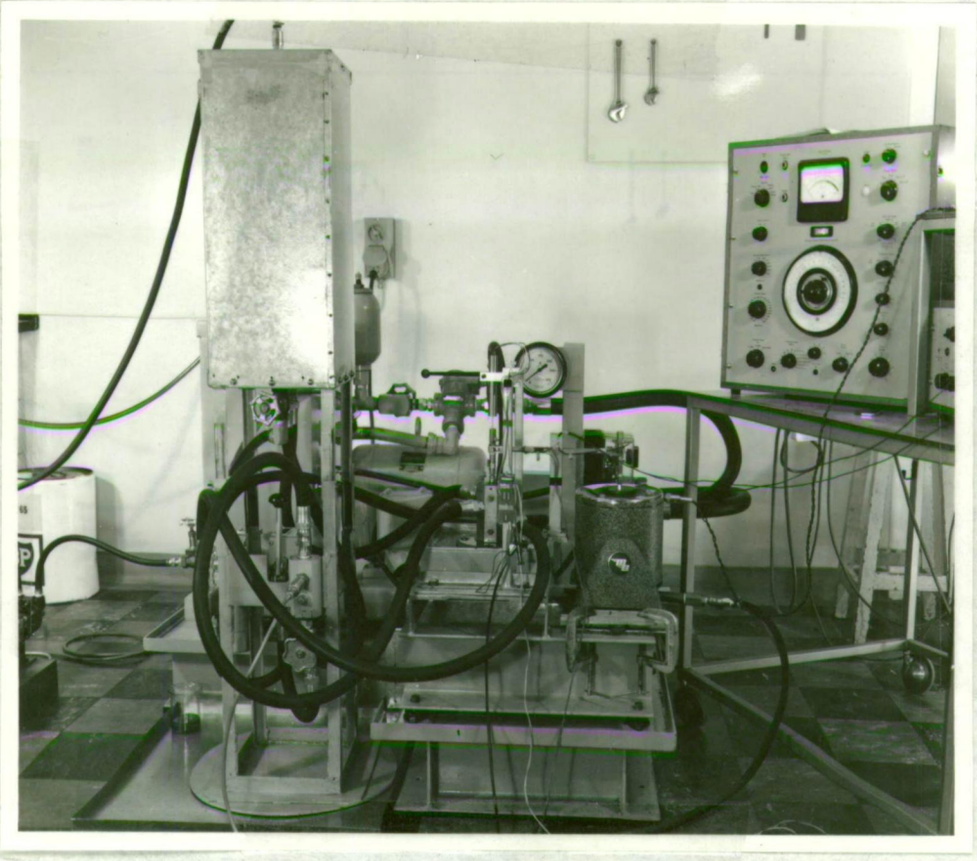

(a) The 4-way valve can be seen in the foreground centre. To the left is the measuring tank and the electromagnetic vibration exciter is on the right. The main pump and motor are behind the valve and exciter. At the extreme left, the rear of the oil cooler pump can be seen.

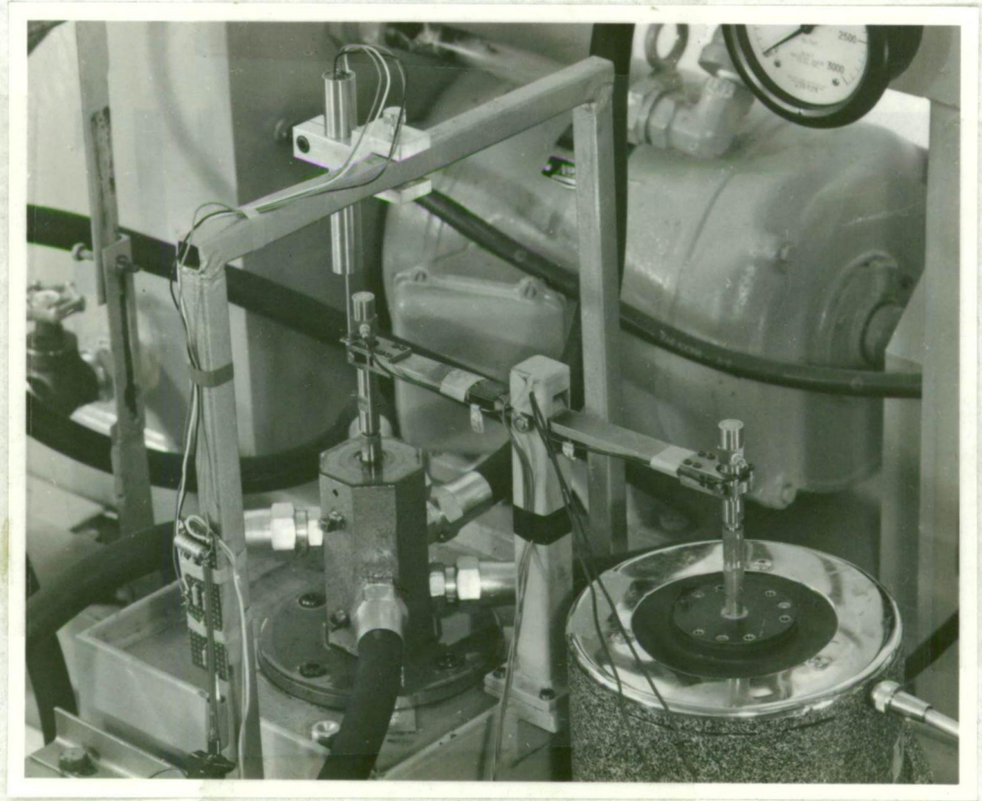

(b) The rocker arm can be clearly seen between the valve spool and exciter. The accelerometers are the small cylindrical objects at the end of the valve spool and exciter coupling. The large cylindrical device above the valve is the displacement transducer.

Figure 1.2
The hydraulic rig

1.2 The "System"

Up to the present, the "system" has in the main, consisted of a four-way valve, described in detail in Chapter 2. As such the "system" was rather ill-defined with respect to the hydraulic circuit, for this changed depending upon which valve characteristics were being studied at any given time. To facilitate these frequent alterations to the circuit, high pressure flexible hoses were used to make connections, both within the "system" and, to and from the supply. These hoses were fitted with threaded steel couplings and consequently changes could be carried out very easily and rapidly.

Eventually the "system" will be developed into the hydraulic amplifier for the vibration tester. This will probably be similar to the servo-mechanism shown in figure 1.3. In this a four-way valve

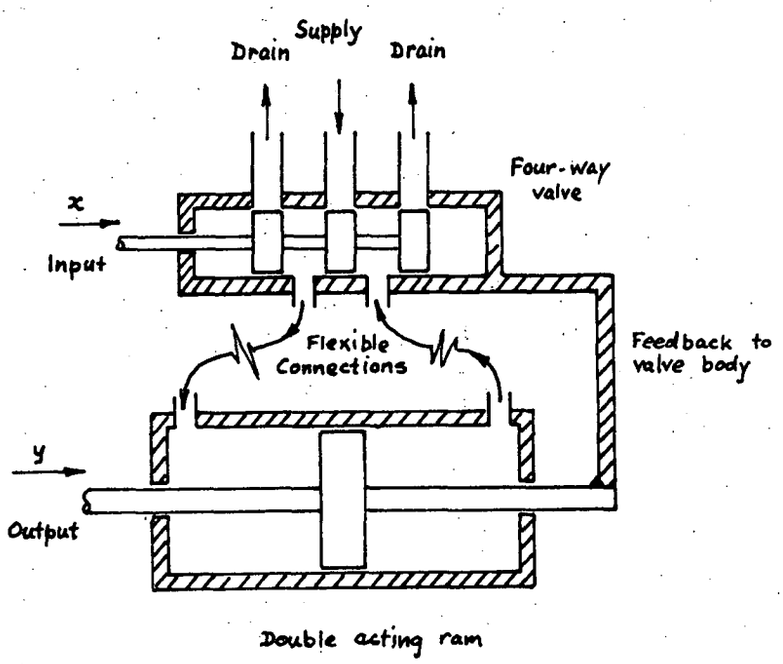

Figure 1.3

A possible hydraulic amplifier for the vibration tester

controls the motion of a double-acting ram. By oscillating the valve with an electromagnetic exciter the ram can be made to vibrate in sympathy.

1.3 The Oil Cooling Circuit

Originally it was thought that the heat loss from the pipework and particularly from the sides of the oil reservoir, might have been sufficient to maintain a reasonable oil temperature. This also appeared to be supported by the fact that the manufacturers of the original unit had not mentioned nor included any form of oil cooling for that unit. However it soon became apparent that there was almost no cooling afforded by heat loss from the pipework or reservoir and the temperature rose at a rather disturbing rate while the motor and pump were running. Presumably the painted surfaces of the reservoir and the fairly still air conditions in the laboratory resulted in a much lower heat transfer coefficient, between the surfaces and the air, than expected. In fact an estimate was made of the likely temperature rise assuming no heat loss to the surroundings and this was found to agree reasonably well with the observed temperature rise of approximately $2^{\circ}F$/min. This of course set a severe limit on the length of run that could be made, for it was observed that for oil temperatures above approximately $190^{\circ}F$, not only did the original pump, the vane pump, become excessively noisy but the relief valve also malfunctioned; it appeared to stick intermittently. Furthermore, the large temperature variation during a run caused significant differences to the results obtained, under what were otherwise identical conditions. The design of an oil cooler was therefore commenced. This was hampered by the somewhat vague and variable information on heat transfer coefficients and it was no real surprise to find this first design in error by almost an order of magnitude in heat transfer coefficient.

The design consisted of a coil of 3/8 in. diameter copper tube, approximately 20 ft. in length, immersed in the oil reservoir. Through this coil cold water was run. Measurements with this arrangement showed a very poor cooling efficiency. The heat absorption was only of the order of a third the heat input and the heat transfer coefficient was less than 20 BTU/hr$^{\circ}F$ sqft. It was also noted that the heat transfer coefficient was nearly independent of the rate of water flow

through the coil, for flows from approximately 0.2 gpm to over 2 gpm. This confirmed that the most significant heat transfer coefficient was on the oil side of the coil. With a thermometer it was observed that a thin, cool, viscous sheath of oil formed over the coil and even though the oil in the reservoir was kept in constant circulation by the steady flow of the vane pump, it was not sufficient to break up this insulating sheath of cool oil. This could be further confirmed by vigorously moving the coil in the oil, which improved the heat transfer.

Consequently the circuit was rearranged slightly. A small gear pump was obtained and coupled to a variable speed motor. This was then used to pump the oil through the coil, which was now immersed in cold flowing water. This showed a great improvement in heat transfer. Measurements made with this arrangement indicated that the heat transfer coefficient was approximately proportional to the oil flow, and a coefficient of almost 100 BTU/hr^{o}F sq ft. was measured at an oil flow of 1 gpm; very considerably higher than with the coil immersed in the oil! Unfortunately an attempt to measure the coefficient at an oil flow of 1.5 gpm failed when the light flexible hose connecting the pump to the coil came off the pump fitting and resulted in oil being sprayed all over the room. Nevertheless it was considered that this arrangement would be satisfactory until the new pump arrived, for although it did not remove all the heat being input, it removed enough to extend the useful run time by a factor of over three.

A further interesting observation was made with this arrangement. At low temperatures the oil cooler could very nearly cope with the heat inflow and the temperature could be kept rising at a low rate. However when the oil reached a critical temperature of approximately 120^{o}F, the oil seemed to rise in temperature much more rapidly and it was difficult to reduce the temperature even by lowering the oil pressure to below 500 psi. At this pressure the oil cooler should have coped reasonably well. It could be that some form of "core" flow was set up at these temperatures. By this is meant that the oil very

near the cold tube wall, being quite viscous, could form a thin insulating sheath, while the low viscosity hot oil from the reservoir might form a high velocity jet down the centre of the tube. Unfortunately, as this was not a primary aim of this project and time was running short, no measurements were taken to confirm or disprove this apparent change in oil cooler efficiency. However it is worth noting, perhaps for future investigation, particularly as the temperature at which it occurs is close to that at which the rig is usually run, namely 100°F. This could also seriously upset the operation of any automatically controlled oil cooling circuit using a similar arrangement.

With the arrival of the new pump the oil cooler was again modified to try and improve its efficiency. The old coil was cut into two new coils and these were then coupled in parallel. The reasoning behind this was as follows. With the same pressure drop across the coils as previously - it could not be increased because of the danger of the hose slipping from the pump fitting - the flow would be increased, for this pressure now acted across a shorter length of tube. Therefore provided the heat transfer coefficient kept rising with flow, as seemed likely from the measurements that had already been taken, the total heat transfer would be greater, for the two coils together still had the same surface area, but a higher coefficient. Measurements taken with this new arrangement confirmed that for the same oil velocity within the tubes the coefficient was the same. However the improvement expected was not obtained. The cause of this was the small flow capacity of the oil cooler pump. The maximum flow, which now had two paths to flow through, only resulted in an oil velocity within each tube, of the same magnitude as previously. Consequently there was no increase in the heat transfer coefficient, and hence no improvement in efficiency. Of course the pressure drop across the coils had decreased, but this was of little consequence, except perhaps, for the improved safety factor with regard to the hose connections!

This arrangement also suffered from another drawback. The hot oil returning from the "system" had a tendency to "float" to the surface

of the cool oil in the reservoir, instead of mixing with it. This was further aggravated by the oil cooler, for it drew off oil from the bottom of the reservoir and returned it at about mid-height. Hence there were two distinct layers in the reservoir; a hot layer at the top and a reasonably cold layer towards the bottom, with a fairly well defined interface. An attempt to mix these regions by discharging the oil from the oil cooler into the reservoir above the oil surface, was abandoned when it was found that the oil jet, impinging on the surface, entrained a large amount of air which it was considered desirable to keep out of the circuit. A better technique would have been to draw off the oil for the oil cooler, from near the top of the reservoir. However, when the measuring tank on the rig filled with oil, the level in the reservoir fell, and consequently the highest point that could be used was about mid-height. Even so, this should have been an improvement.

It could be that an oil cooler in the main return line would be a more suitable arrangement. In any case a new, or at least highly modified design will be required if there is to be any possibility, at high power inputs, of maintaining a constant oil temperature. There is also no reason why it should not be automatically controlled.*

1.4 Instrumentation

1.4.1 Pressure

Initially a great deal of difficulty was experienced in obtaining pressure recordings. This was not so much a fault of the pressure transducers themselves, but more a question of the reliability of the associated electronic equipment. This was of fairly old vintage and suffered from very poor drift and noise characteristics. These transducers also, because of their small pressure range, fixed the maximum supply pressure at 1000 psi.

---

* An investigation is currently being carried out on the feasability of an oil cooler in the pump suction line. This would automatically control the oil temperature at the pump inlet. Results to date have been quite encouraging.

Fairly late in the project two better pressure transducers were purchased to replace the original ones. However, even though these had a larger pressure range, the supply pressure was left at 1000 psi. This allowed the experimental results already obtained to be used in later work. The new transducers were of the diaphram-bonded strain gauge type (MB Electronics Model 510A). But unlike others, which required external bridge and amplifier circuits, these were completely self contained. Built into them was a d.c. bridge circuit with temperature and power supply compensation and a high gain d.c. amplifier. The pressure range was from 0 to 2500 psi (absolute), and the drift and power supply compensation was excellent. No data was supplied by the manufacturers on the dynamic performance of the transducers, but this is expected to be more than adequate, as the electronics is all d.c. and the resonant frequency of the diaphram assembly is stated to be greater than 20 KHz.

One of the most annoying aspects of these units, and a major drawback, was the need to isolate the input and output. This often proved difficult to accomplish if several instruments were being run off the same power supply. The reason was that if the output of another instrument were displayed together with the output of the transducer, on, say, a dual beam CRO then it was possible to complete an electrical circuit from the output to the input of the transducer, via the common earths on the CRO and the electrical circuit of the other instrument. To overcome this, small, individual, floating output, power supplies are to be made for each transducer.

1.4.2 Flow

Although no flow meter as such was used on the rig, average flows could be measured by directing the oil into a measuring tank and timing a given level change. The oil level in the tank was indicated by means of a clear plastic tube fixed to the outside of the tank and connected to the inside at the top and bottom. However this only showed the correct oil level under static conditions. During flow measurements the oil level was changing continually and therefore, because of the viscous drag on the oil in the plastic tube, a

difference between the oil levels in the tank and tube was needed to create the oil flow into or out of the tube. This difference in levels was obviously dependent on both the rate of change of the oil level and the length of tube involved, i.e. on the oil flow and the oil level. Measurements of this were made, at varying levels, by suddenly stopping an oil flow into the tank and observing the subsequent rise in oil level within the tube, as the oil in the tank and tube came to equilibrium. These measurements showed that the maximum error in a calculated flow, caused by ignoring this effect, was only of the order of 2%.

1.4.3 Force on the Valve Spool

To measure the force being transmitted to the valve spool a small, steel rocker arm was incorporated between the exciter and spool. This can be readily seen in figure 1.2(b). The force was infered from the deflection of the arm. To measure the deflection, strain gauges were glued to the upper and lower surface of the arm. Originally these strain gauges were connected to a commercial strain gauge unit, which used an a.c. bridge circuit. However this unit showed large drifts compared to the forces (more correctly strains) being measured. The drift was of the order of ± 1 lb compared to the maximum flow reaction force of approximately 8 lb. The unit also, because of the low frequency carrier used, had large phase shifts at frequencies well below 100 cps. It was therefore discarded and replaced by a d.c. bridge circuit and small integrated circuit d.c. amplifier. This worked well, although noise from the integrated circuit tended to be a little large. Later some high gain, high stability preamplifiers were purchased and one of these was coupled to the bridge in place of the integrated circuit. This was found to be highly satisfactory.

1.4.4 Acceleration

Accelerations of both the valve spool and the exciter were measured with small piezoelectric type transducers (Brüel & Kjaer - type 4334). These can be seen in figure 1.2(b); one screwed to the

end of the valve spool and the other to the top of the moving element of the exciter. The frequency response was limited by the preamplifiers coupled to the accelerometers (Brüel & Kjaer - type 2622) and was flat within ± 0.5 dB from 2 Hz to 10 KHz. These preamplifiers also scaled the output to 10 mV/g (g is the acceleration due to gravity). Besides being used to measure the accelerations, these accelerometers were incorporated in the feedback loop of the vibration exciter control. This is described later in section 1.4.6.

1.4.5 Displacement

In the static tests the displacement of the valve spool was determined by the use of a dial gauge. This however had one fairly serious drawback. That was, the dial gauge exerted a quite significant force on the valve spool and this had to be allowed for in the force measurements. Unfortunately this was complicated by the fact that the force-displacement characteristic of this gauge suffered from an hysteresis type effect. This caused the force exerted by the dial gauge to differ depending upon which way the spool had been moved to a given position. To a certain extent this was overcome by tapping the valve body with a small hammer (this had to be done in any case in order to overcome difficulties of valve sticking).

Displacements during dynamic tests were taken with a small differential transformer displacement transducer (Hewlett Packard Model 24DCDT 1000). Basically this consisted of a transformer coil assembly and a small core which, when displaced along the axis of the coil assembly altered the coupling between the windings of the transformer. This difference in coupling was used to produce an output voltage proportional to the core position. To excite the primary winding of the transformer a d.c.-powered oscillator was used. A quite compact, self-contained transducer was produced by incorporating the differential transformer, oscillator and demodulator all within the one case. To transmit the valve spool motion to the core a light connecting rod, cemented to the core, was employed.

The main disadvantage of this transducer was the very low frequency of the oscillator. This meant the filter in the output stage of the demodulator attenuated the output signal rather badly and also introduced large phase shifts, at quite low frequencies. To some extent allowance could be made for this as the nominal filter characteristics and 3 dB point were specified by the manufacturer. However for this particular transducer the 3 dB point occured at 100 Hz, whereas the rig was operated up to 150 Hz. At this frequency the amplitude was approximately one half of what it should have been and the phase shift was nearly 60°. It would be preferable to have a transducer with a considerably higher internal carrier frequency.

1.4.6 Exciter and Vibration Controller

The exciter was a conventional electromagnetic unit driven by a power amplifier (MB Electronics PM-50 exciter, 2250 MB amplifier). It had a maximum force capability of 50 lb, if air cooling was employed, and a maximum stroke of $\pm$ 0.5 ins. The power amplifier was driven by the output of the vibration controller.

The vibration controller was basically a sine wave signal generator, the output of which was controlled by a feedback loop (Brüel & Kjaer - type 1025). In this case the output from an accelerometer on the valve spool was used as the feedback signal to the controller. The controller, if necessary, integrated this signal to give velocity or displacement, and then rectified and filtered it to obtain an average input. This was compared to a preset level and an error signal used to control the output of the signal generator. Hence, this differed from the type of controller usually associated with this type of vibration equipment in that it only controlled the average level of the vibration, whether this was acceleration, velocity or displacement, and in no way controlled the actual wave shape. This was somewhat of a disadvantage during the dynamic tests on the valve, for the valve characteristics caused significant distortions to the wave shape of the valve spool motion.

Normally the controller was used in a mode that maintained a constant amplitude of only the acceleration, velocity or displacement. However it also had facilities to enable a cross-over frequency to be set at which the control changed from one input variable to another. Either a constant displacement-constant acceleration, or constant velocity-constant acceleration mode of operation could be selected. For the dynamic tests on the valve, the former mode was used, i.e. constant displacement-constant acceleration. The cross-over frequency was slightly less than 55 Hz corresponding to a displacement amplitude of $\pm$ 0.1 in and an acceleration of $\pm$ 30 g. The frequency range of the controller and exciter combined was from 5 Hz to 10 KHz. However power requirements limited the maximum frequency on the experimental rig to 150 Hz.

1.4.7 Ultra-Violet Recorder and Preamplifiers

For the permanent recording of most of the measured variables on the experimental rig a U.V. recorder was used. This consisted of a number of small galvanometers which deflected, by means of a little mirror attached to the galvanometer suspension, a fine spot of ultra-violet light onto a sensitised paper. This paper could be driven through the recorder at varying speeds. It was developed in ordinary light leaving the trace quite visible. If required the paper could also be "fixed" although this was not normally necessary provided the paper was stored in a dark place (to stop further development). The response of the galvanometers was flat to 300 Hz which was quite adequate for most of the signals being recorded. However some recordings, such as pressure, were so rapid that it was necessary to use a CRO to observe them, particularly the amplitude, as the galvanometers attenuated the peaks. The galvanometers were electrically damped by controlling the output impedance of the preamplifiers used to drive them.

The preamplifiers were designed and built in the department using integrated circuits. The original specification was for a d.c. preamplifier with an input impedance of at least 1 MΩ, variable gain

from 0.1 to 10 and impedance matched to the U.V. recorder galvanometers which had a resistance of only 120 Ω. It was also to have very low electrical and temperature drifts. The circuit sketched in figure 1.4 was built and tested. It was found to be quite satisfactory provided the output impedance of the source driving it was not too high. The reason for this was that the integrated circuit required an input bias current of approximately 20 nA. This was normally only important in the case of piezoelectric type transducers.

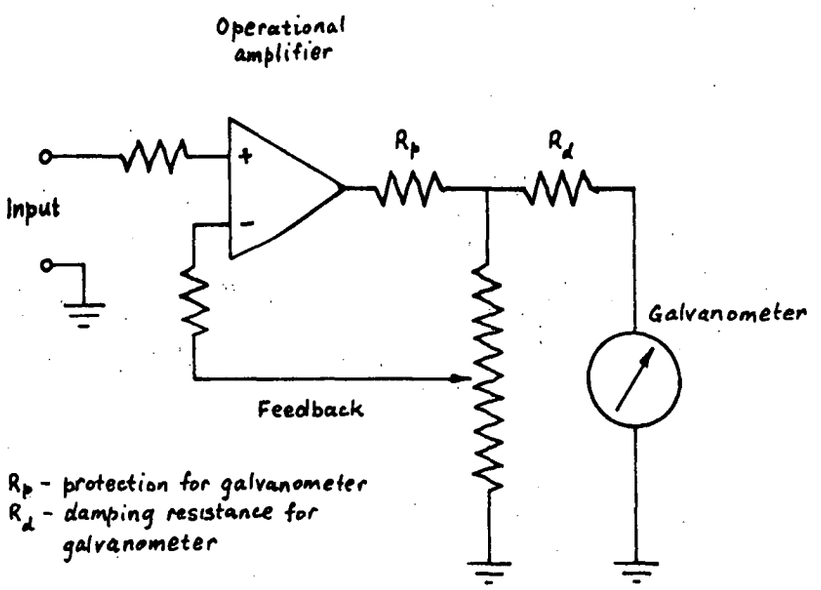

Figure 1.4

Galvanometer preamplifier

However, some of the equipment it was anticipated using with these preamplifiers was found to have a large d.c. offset voltage of the order of 11 V. Consequently the specification had to be modified to allow a.c. coupling at the input and this, in fact, caused very great problems. This was because of the bias current required by the input stage of the integrated circuit. With a capacitor coupling between the source and input the only means of supplying this current was via some form of bias resistor circuit. But the specification required an input impedance of greater than 1 MΩ. Consequently the bias resistance had to be at least 1 MΩ and as the

bias current was approximately 20 nA the voltage offset across this resistance was then 20 mV. This was quite large compared to the input signals expected. An idea of their range can be gained by observing that the galvanometers required only about 60 mV for full scale deflection and even at the lowest amplifier gain of 0.1 this represented only 600 mV at the input. Relative to the smallest signal expected the offset was a factor of three times larger! The final compromise arrangement is shown in figure 1.5.

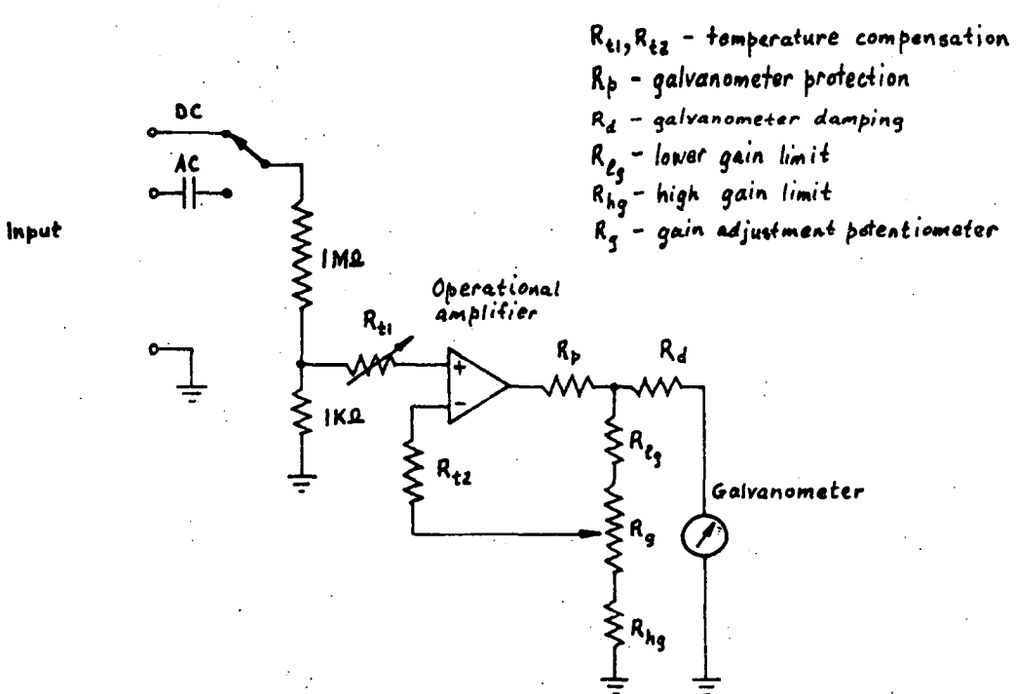

Figure 1.5

Modified galvanometer preamplifier

This was only moderately satisfactory because of the large attenuation of signal at the input. This meant the signal being fed to the operational amplifier was becoming comparable with noise and consequently at gains greater than about 5 the noise at the output became excessive. A further problem was that the circuit could only be temperature compensated for either d.c. or a.c. but not both as the impedance seen by the input to the operational amplifier was different in each case. Also although the input divider improved

the offset on switching from d.c. to a.c. it did not overcome the problem and consequently the trace had a quite considerable offset on switching over. Nevertheless as a considerable amount of time had been spent on this design it was decided to make do with it.

It is perhaps of interest to note that several attempts have been made since, both to design another preamplifier or to buy a reasonably priced commercial unit, which would satisfy the specification, but as yet none has been found that would be entirely satisfactory.

------ 000 ------

CHAPTER 2

THE FOUR-WAY VALVES

2.1 Valve Mk I

At the time this project was commenced a four-way, spool valve was already under construction in the departmental workshop. It had a three land type spool as shown in the detail drawing, figure 2.1. Essentially the valve consisted of three parts. A mounting flange and outer body which had the threaded holes for the high pressure hose fittings, an inner sleeve in which the valve ports were machined, and finally the valve spool itself. As it was not expected that a long component life would be required, in the first valve design anyway, all components were made from mild steel. This also meant they could be easily machined. The close radial fit between the spool and sleeve was achieved by first making them with a slight interference fit. The sleeve was then honed and finally the spool and sleeve lapped. A feature of this design was the ease with which it could be dismantled or altered. Considerable modifications to the valve characteristics, or even style, could be made by simply machining a new sleeve and spool.

An examination of this first valve design however showed that it had many faults. The most obvious one was the asymetrical nature of the valve ports (see section through sleeve, figure 2.1). With a supply pressure of 1000 psi it was anticipated that the valve would lock in the closed position due to the large side thrust caused by this. There was a problem, too, of the end lands of the valve spool fouling the drain holes. These drain holes had already been moved in order to clear some "O" ring seals that had been placed between the sleeve and body! Furthermore a quick estimate of the flow characteristics of the valve showed that the maximum flow would be developed at a displacement of only about 0.01 in. This was thought to be somewhat small for accurate measurements within the laboratory and particularly with respect to the tolerances expected on the valve ports and spool

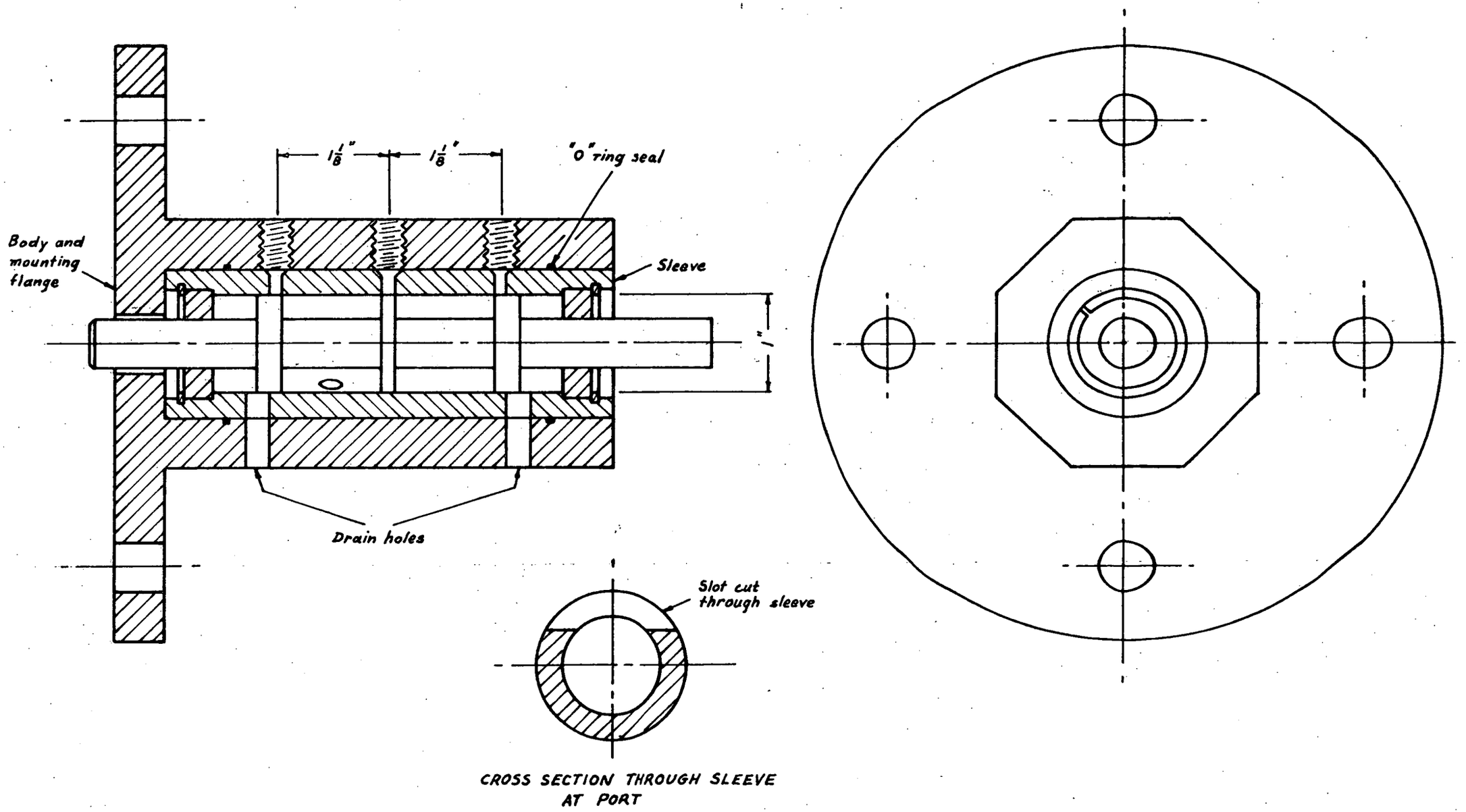

Figure 2.1

Valve Mk I

lands. Nevertheless it was decided to perservere with the fabrication of this valve so that the overall assembly of the hydraulic rig would not be delayed. It was also expected that the experience gained, not only in the manufacture of the valve components but also in the operation of the hydraulic rig, would be of great benefit in later valve designs and experiments. At the same time, possible modifications to this valve were investigated in an attempt to see if some of these difficulties might be overcome fairly simply. As well as this the design of a completely new sleeve and spool (Valve Mk II) was commenced.

As predicted, when the valve was tested on the rig, it was found to lock as it passed through centre. It could only be moved with a great deal of difficulty and very large forces. Also the full flow was reached within a very small valve travel as had been expected. The leakage on the other hand appeared to be fairly small which was a very encouraging result.

2.2 Valve Mk I Modified

In order to overcome the large side thrust on the valve spool of valve Mk I, two more slots were cut around the valve sleeve at the central port position, as shown in figure 2.2. This balanced the

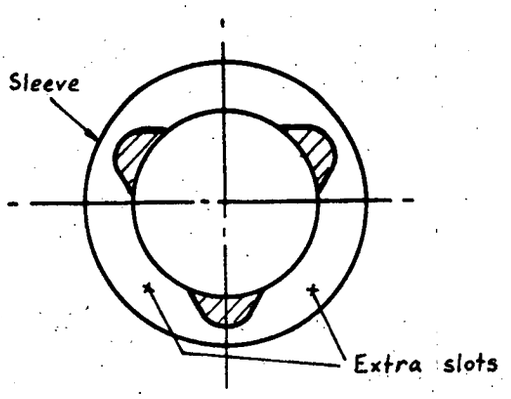

Figure 2.2

Section through central port of modified valve sleeve

pressure forces around the spool at this position. Unfortunately this could only be done on the central port as the resultant slot at the other two port positions would have touched the leakage drain holes! In any case, as the design of the new spool and sleeve was well advanced it was decided to concentrate on the central port only, and see how it behaved.

The valve was reassembled and connected to the high pressure supply. Tests on this modified valve proved reasonably satisfactory as far as the forces required to move the valve were concerned. However the pump could only manage to maintain 600 psi or less across the valve, even in the fully closed position. It was suspected that the majority of the flow was in fact leaking around the central land of the spool, but at the same time it was thought some might have been leaking between the sleeve and body. In order to determine just how important this leakage around the sleeve was, the valve spool was partially removed from the sleeve so that the large end land completely blocked the central port. The high pressure oil was again connected and the total leakage found to be very small, indicating that for all intents and purposes the flow previously observed was all past the central land.

A quick analysis of the flow and pressure drop showed that a valve underlap of some four thousandths of an inch was required. Consequently the valve was dismantled again and the sleeve and spool carefully examined. This showed that although the slot width and spool land dimension were very nearly identical, the two extra slots that had been cut around the sleeve, were axially displaced by several thousandths of an inch from the original slot. This together with the small radial clearance was sufficient to account for the results observed (remembering that the port width was now three times larger).

2.3 Valve Mk II

It was decided if possible, in this design, to use the existing outer casing of the old valve. With hindsight this was a mistake, for

it severely limited what could be done with the spool and sleeve. The main problem was the very large flow obtained at only very small displacements of a conventional type spool valve with large port widths. For this valve it was felt that, for the full pump flow at the supply pressure, a displacement approaching 0.1 in. was desirable. This was because the tolerances that could be held on the sleeve and spool were poor relative to those normally maintained in this field. Also, for accurate measurements of the spool displacement, particularly dynamic measurements, within the laboratory, a reasonably large displacement was necessary. However this meant a total port width of less than 3/16 in.! The problem was therefore to either decrease the spool diameter and hence port width, in the case of an annular groove type port, or to machine several very small rectangular ports in the sleeve. For the spool diameter it was decided that the minimum diameter that could be handled with any accuracy on the available equipment was of the order of 0.5 in. or greater. Therefore the desired maximum spool displacement had to be decreased unless very small width ports could be made. However the latter appeared quite difficult as the only convenient way of making a rectangular port was by slotting across the sleeve, and the tolerances that needed to be maintained to give the required port width accuracy, with a spool diameter greater than 0.5 in., were unrealistic.

By chance, at about this time, a slotted or fluted spool construction was discovered. This had spool lands much longer than the port size. Slots were then machined in the lands in such a way that the end of each slot just touched the edge of the port. See figure 2.3. This allowed the actual port width in the sleeve to be large and yet still present an effective port width, for the oil flow, of just the combined width of the slots in the spool land. The one major drawback with this technique was the difficulty in locating the ends of the slots accurately. With this particular valve the problem was partly overcome by measuring the average position of the ends of the slots on the completed spool and cutting the ports in the sleeve

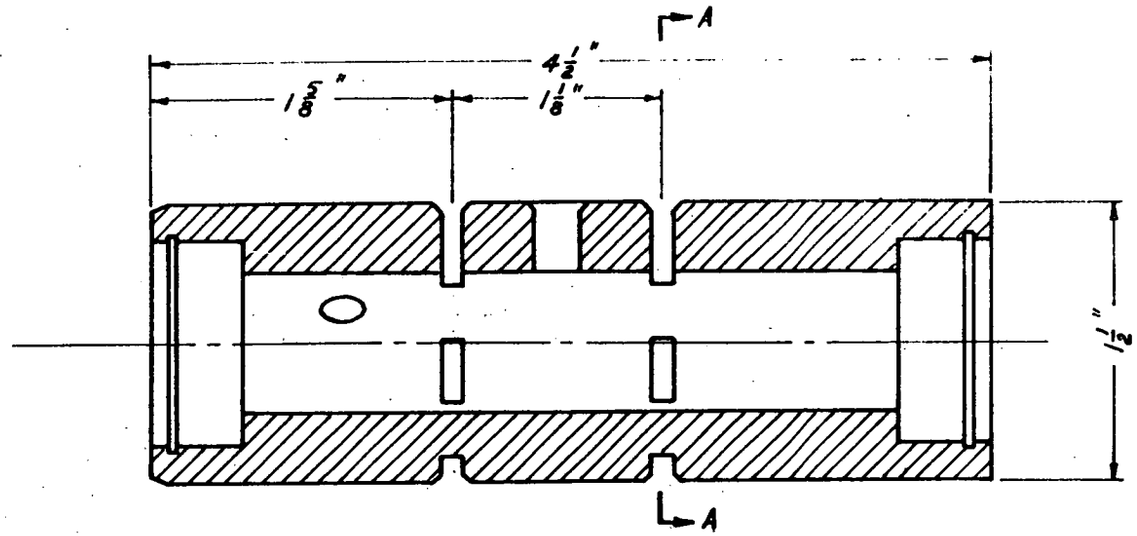

SLEEVE CROSS SECTION

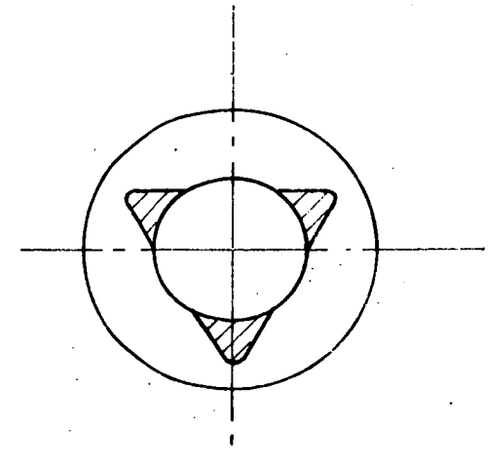

SECTION AA

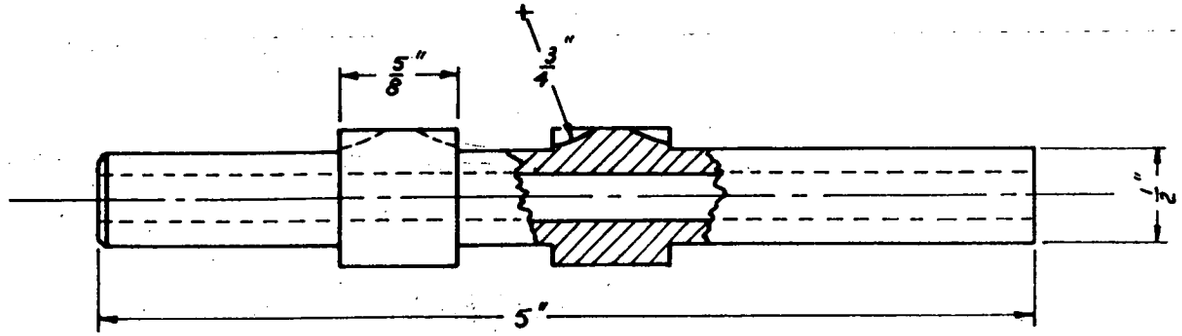

SPOOL

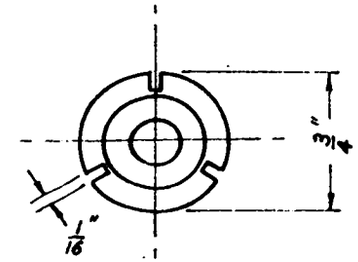

Figure 2.3

Valve Mk II

to match. However with later valves which are to be hardened by heat treatment, any distortion of the spool will result in non-uniformity of the slot end-positions around the spool, as these will have to be cut before hardening.

The other main feature that had to be considered was how many lands to have on the spool. As already mentioned in the discussion of valve Mk I, if a three land construction were used the end ports could not be placed uniformly around the sleeve as the resultant slot fouled the leakage drain holes. Consequently the only valve spool that could be constructed that would fit the existing outer body was a two land type, shown in figure 2.3. This was very unfortunate as it left oil trapped between the end caps and the valve spool. Normally this type of valve would be made with four lands as shown in figure 2.4. In this case

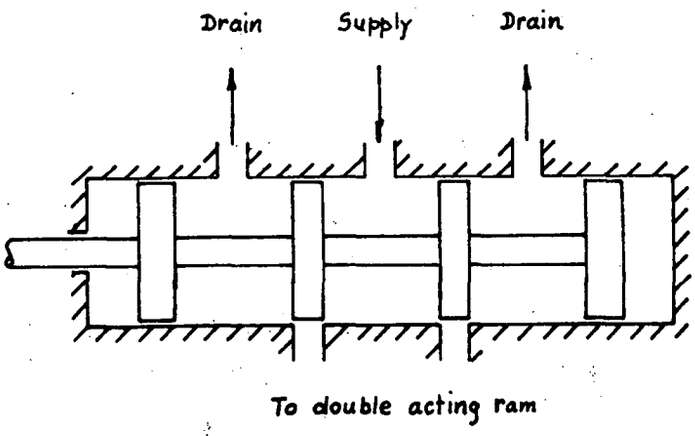

Figure 2.4

Conventional, four land, four-way valve

there was no room to place the extra two lands and this presented difficulties in later experiments due to slight pressures built up in these end chambers. These caused extra axial forces to be exerted on the valve spool.

As previously, the spool and sleeve were made from mild steel. The radial fit was also obtained as before, i.e. the spool was first made an interference fit with the sleeve, the sleeve then honed and finally the spool and sleeve lightly lapped. No accurate measurements

were taken of the radial clearance. However the fit was certainly reasonable, for the leakage flows were small, approximately 1.5% full flow, as can be seen from the results presented in the next chapter. In comparison the tolerances actually held on the other dimensions were not very good. The ends of the slots were within approximately ± 0.001 in. of each other and there was an average overlap of slightly greater than 0.001 in. on the high pressure side of the valve lands and an average underlap of approximately 0.001 in. on the low pressure side of the lands. As it turned out this was not very critical, for the full flow displacement was relatively large, being approximately 0.1 in. Also the slot effective area was not strictly determined by the displacement of the slot alone but by a throat area which was also determined by the slot shape, as described in the next chapter.

One further feature of the valve was the provision of an axial hole through the centre of the valve spool. This was done in readiness for hydrostatic bearings on the spool, if these were required later. This axial hole was to carry oil from the high pressure oil chamber to several small radial holes drilled through the lands, between the slots, as shown in figure 2.5. Restrictions were to be screwed into

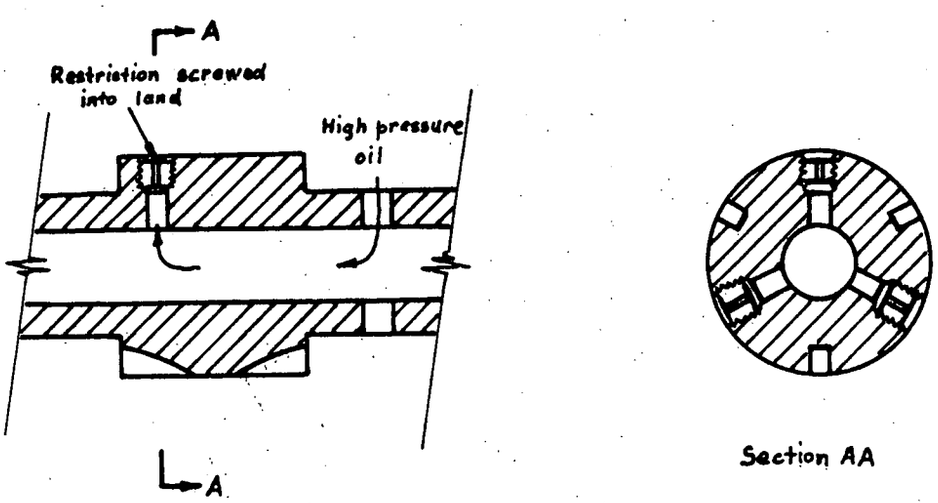

Figure 2.5

Hydrostatic bearing for valve spool

these radial holes in order to obtain the necessary pressure-flow characteristic. Small flats could also have been cut into the lands

to improve the efficiency of the bearing. In fact no such bearings were made for this valve, even though the experimental results indicated this was necessary. The reason was that at the time of these experiments a completely new valve, including a new outer body, was being designed. The necessary modifications and experimentation associated with these bearings was therefore not thought justified, particularly as this old valve suffered from many other faults.

A photograph of the dismantled valve is shown in figure 2.6. The

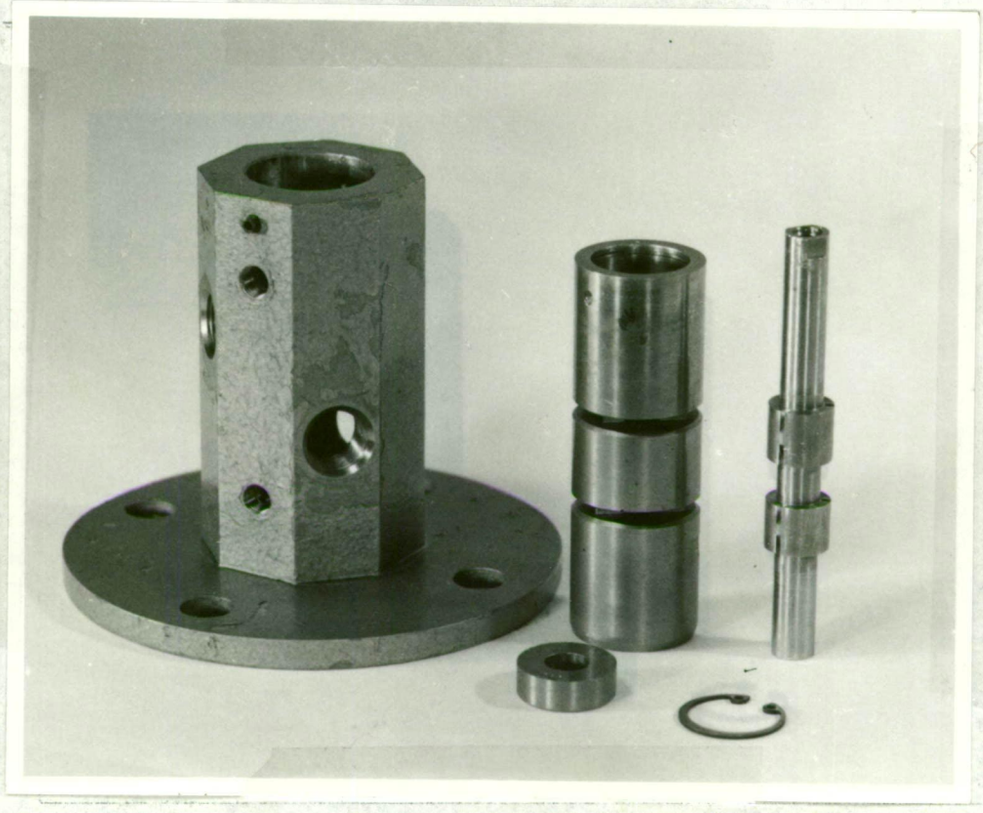

Figure 2.6

Dismantled valve Mk II

very small size of the slots in the spool lands can clearly be seen.

One further advantage of the fluted valve construction was the flexibility it afforded in valve characteristics. By simply altering either the number or width of the slots in the spool lands the valve characteristics could be changed. This meant that the different flow paths in the valve could all be made with different characteristics if

necessary. In fact something of this nature could possibly be used to overcome problems of cavitation in the hydraulic amplifier of the vibration test rig.

A further point of interest relevant to this section is the orifice flow nomograph presented in appendix 1. This was found to be extremely useful throughout the project. It allowed very easy rapid estimates of the flow behaviour of orifice-like restrictions to be made, and this was particularly handy during the valve designs. A small Algol computer program was written to produce the nomograph on the digital incremental plotter coupled to the Elliott 503 computer at the University. The program procedures or subroutines which were used to plot the axes were written fairly generally so that almost any nomograph could be produced with a minimum of time and effort.

------ ooo ------

CHAPTER 3

STATIC BEHAVIOUR OF THE VALVE

3.1 Flow Equation

If "steady-state" conditions are considered to exist within the valve and the flow in the vicinity of the metering orifice is incompressible, non viscous and turbulent, then the flow will follow the "orifice" equation:

$$Q = C_d A \sqrt{\frac{2 \delta p}{\rho}} \qquad (3.1)$$

where Q = rate of flow

C_d = discharge coefficient

A = valve orifice area

δp = pressure drop across valve

ρ = oil density

That this equation does in fact represent the behaviour of most valves of the type being considered here, i.e. valves with a large pressure drop across an orifice type restriction, has been shown by many workers in this area [7, 8, 12]. Indeed, as will be shown later in this chapter, the valve studied in this experiment was no exception.

In general the discharge coefficient, C_d, is taken to be constant. This is not strictly correct, particularly for very low pressure drops or small valve openings [12]. However other effects are usually much more important than this in causing discrepancies between the measured and calculated flows, and for most valves the assumption of constant C_d is very good. This was certainly true of the valve studied in this experiment. For an orifice with sharp edges a coefficient of 0.6 - 0.65 is usually observed; for slightly rounded edges it is 0.8 - 0.9 and varies somewhat. In respect to the fluted valve the metering orifice had as well as sharp edges a reasonably smooth flat "edge". See figure 3.1. Therefore, for design purposes a coefficient of 0.7 was assumed. This turned out to be close to the value actually measured, viz. 0.72 (see section 3.3.1).

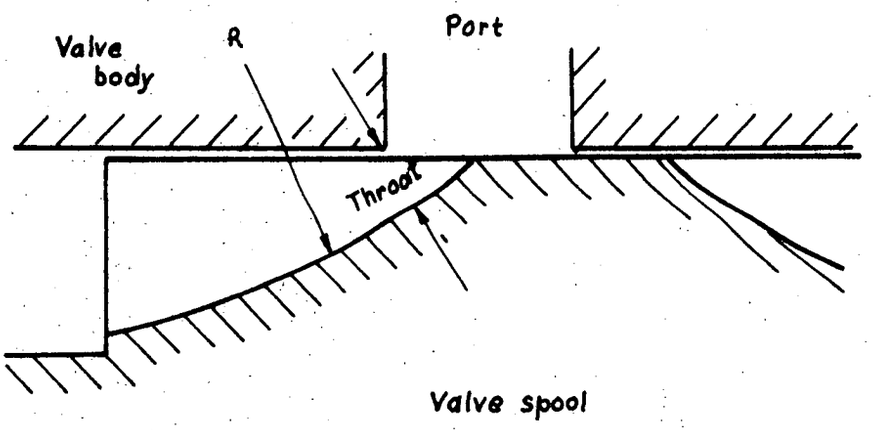

Figure 3.1

The valve metering orifice

A further point that needs examining more closely is the relationship between spool displacement and orifice area for a fluted valve spool. In the more conventional "square-land" type spool valve the orifice area is simply the product of the displacement and the port width. However with the fluted design there is in fact a "throat" of considerably smaller area than the displacement times the port width. This is clearly shown in figure 3.1. Moreover this throat is not a linear function of the displacement of the spool, as shown in figure 3.2.

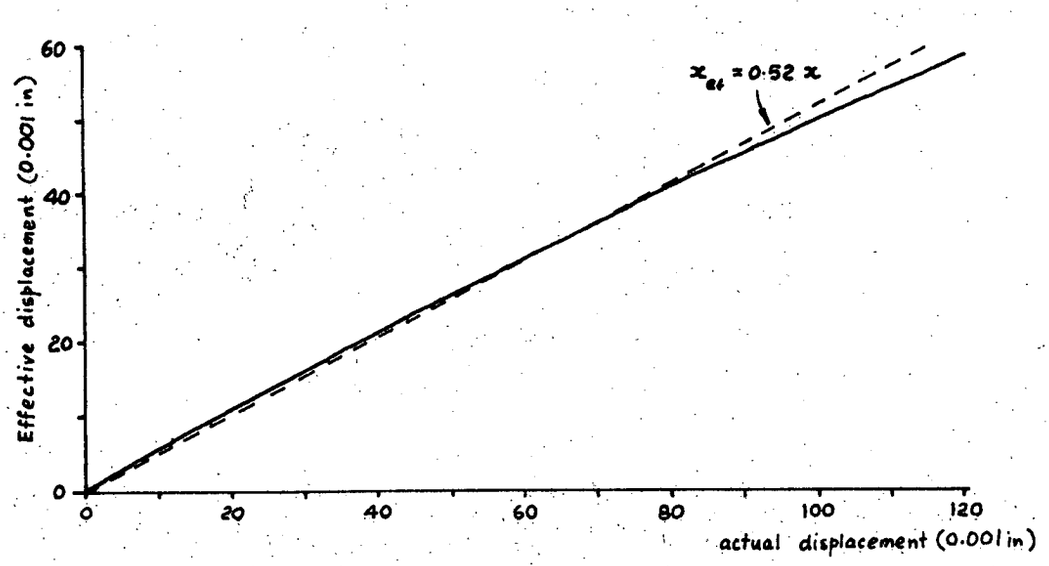

Figure 3.2

Effective displacement vs actual displacement

In this figure an effective displacement has been obtained by dividing the throat area by the port width (strictly speaking, by the combined slot width). This is the equivalent displacement that would be required to give the same orifice area with a "square-land" spool. Figure 3.2, however, also shows that over the range of displacements expected, i.e. displacements up to 0.1 in., the effective displacement can be approximated quite well by

$$x_{ef} = k\, x_{act}$$

where k = 0.52 approximately, for the valve considered here. In general k will be different for different valves and displacements. The orifice area is therefore given by

$$A = k\, w\, x$$

where w = port (combined slot) width

and the flow equation becomes

$$Q = C_d\, k\, w\, x \sqrt{\frac{2\,\delta p}{\rho}} \qquad (3.2)$$

As this equation is used later in deriving the equations for the dynamic behaviour of the system, it is perhaps pertinent to comment on the meaning of the "steady-state" assumption, originally used in deriving these equations. In the dynamic situation, steady-state conditions can not in reality be said to exist. However it is assumed that the speed with which the flow in the vicinity of the metering orifice changes, due to variations in the upstream or downstream pressure, or due to changes in spool position, is very much more rapid than the speed with which these "external" changes occur. Hence at any instant during changing conditions the flow through the valve is assumed to be the same as the flow that would have resulted had the same pressure drop and spool position existed during steady-state conditions.

3.2 Flow Reaction Force

Consider the schematic diagram, figure 3.3, showing one metering orifice of a spool valve. The oil flows in through duct A and out

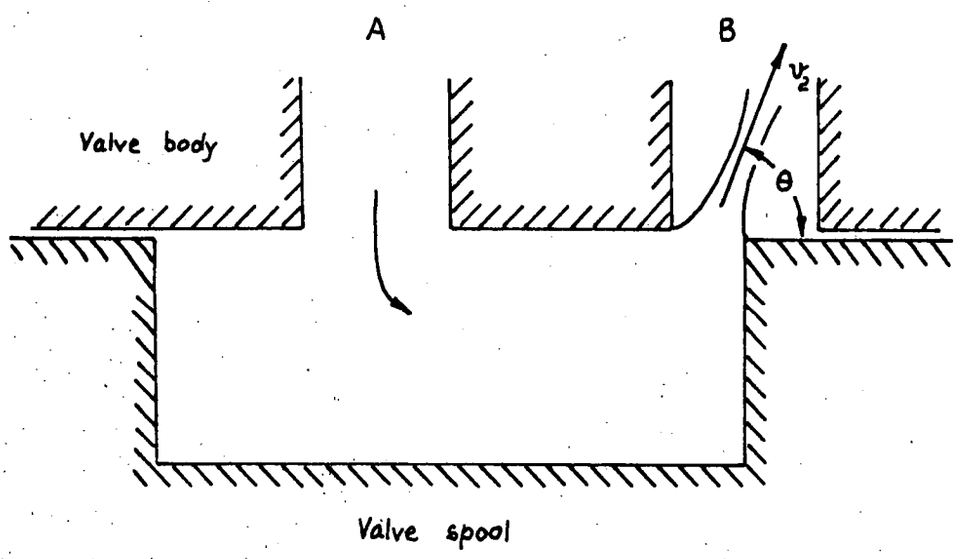

Figure 3.3

Section through spool valve

through duct B. In general the areas of the ducts and the chamber, are large compared to the area of the orifice and consequently the velocities are small with the exception of the velocity of the oil jet passing through the orifice. This jet is not only of high velocity but it enters duct B at an angle, $\theta \neq 90^{\circ}$, and therefore carries away some axial momentum. This it could only have gained from the "spool" chamber and consequently there must be a reaction force on the spool which tends to close it. This is very briefly the origin of the flow reaction force.

Referring back to figure 3.3, provided the angle of the jet, θ, is known, the axial force on the spool can be calculated. This force must be the net axial component of the rate of change of momentum of the oil passing through the valve. Because the velocity of the oil entering the chamber is very small compared to that of the jet leaving it, the momentum flux entering the chamber is usually ignored. The momentum flux, M, leaving the chamber can be determined at the vena contracta of the jet. It is

$$M = \rho Q v_2$$

where v_2 = velocity at the vena contracta.

By the Bernoulli equation

$$v_2 = \sqrt{\frac{2\,\delta p}{\rho}}$$

The axial force, F, is given by the net axial change in momentum flux, i.e.

$$F = \rho\, Q\, v_2 \cos\theta$$

Combining this with the flow equation (3.2) finally gives

$$F = 2\, C_d\, k\, w\, x\, \delta p \cos\theta \qquad (3.3)$$

If the direction of flow is reversed so that the jet flows into the chamber from duct B, the equation still holds and the force still tends to close the valve.

For a "square-land" valve when the valve opening, x, is small compared with the other dimensions of the chamber, but large compared with the radial clearance, the angle, θ, is found to be approximately 69° [12]. However, for the fluted valve under study, the land "edge" was nowhere near square, the angle being about 35° as shown in figure 3.4. The jet angle was therefore expected to lie somewhere between these angles, probably closer to 35° than 69° due to the effect of

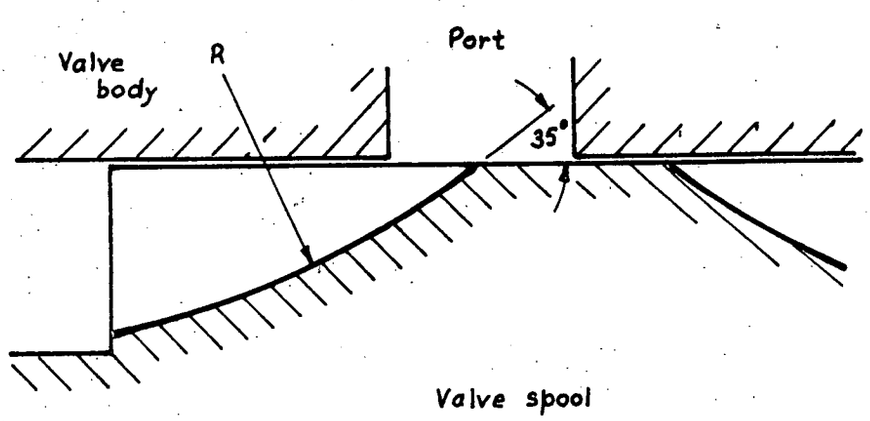

Figure 3.4

Spool land edge angle

the slot on the flow. As shown later, the angle in fact was approximately 40° (See section 3.3.2).

3.3 Experimental Results

3.3.1 Pressure-Flow Characteristics

Because of the peculiarities of valve Mk II, particularly in having only two lands, instead of the more usual four, it was difficult to find a satisfactory way of coupling it to the rig. The most satisfactory method seemed to be that sketched in figure 3.5. However even this had the disadvantage that any difference between

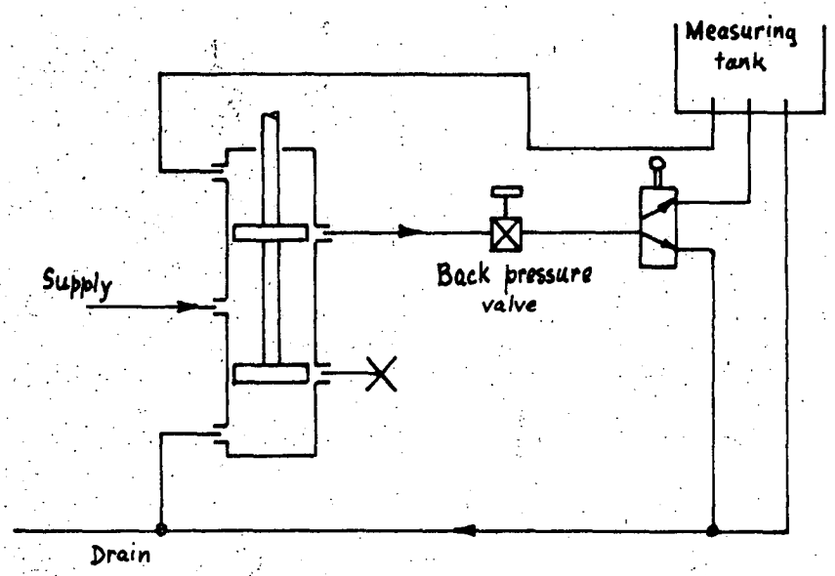

Figure 3.5

Hydraulic circuit for static tests

the oil pressures at the measuring tank and return line caused a resultant force on the spool, as these pressures were communicated to the chambers between the end-caps and the spool lands. Furthermore the leakage flow measured when the valve was closed was that across the whole land, not just from the high pressure land to the valve port. Fortunately this was not a very great disadvantage in this case as the only occasion for which the leakage flow could be measured was for "zero" back pressure. In all other cases the back pressure could not be maintained with only leakage flow, as the outside edge of the land opened the port to the end chamber and hence zero pressure. In any case, with "zero" back pressure the major part of the leakage flow should have been from the high pressure edge of the land to the port, as the pressure drop across the outside edge of the land should have been zero.

(Strictly speaking this was not quite correct, for the port did not extend continuously around the sleeve and consequently between port sections there would have been a slight pressure build up).

The "outside" land characteristics, i.e. the characteristics from the port to the end chamber, were not studied in this particular experiment. There were two reasons for this. Firstly, only the characteristics across the "inside" lands were required for the dynamic studies anticipated with this particular valve. Secondly, as a result of the two land construction, the results obtained for the "outside" lands were expected to be somewhat unreliable. This was because of the slight pressure increase that would have been created in the end chamber due to the oil flow through it. This would have upset the flow reaction force readings. Also the large clearance between the end-cap and the valve spindle would have resulted in a significant leakage flow past the end-cap.

One further point that should be made about this valve is that the characteristics of any metering orifice cannot be assumed to remain the same if the direction of oil flow is reversed. In fact it is very likely that there will be a difference, for in one case the oil flows through a convergent slot and throat into a fairly large duct, while for the reverse flow, the oil passes from the duct, through the throat into a divergent slot. In all that follows the "inside" land characteristics are considered for an oil flow out through the spool slots to the duct or port.

The raw data obtained from valve Mk II, with a supply pressure of 1000 psi, is shown plotted in figure 3.6. Positive flows were taken to be flows through one port, while negative flows were through the other port. At small flows the plots are reasonably linear; however at higher flows there is a marked roll-off or saturation effect as it is commonly called. At least some of this roll-off can be considered to be due to pressure drops within the hoses and fittings both upstream and downstream of the valve. These caused a drop in the total pressure across the valve orifice proper. (There was no justification at this

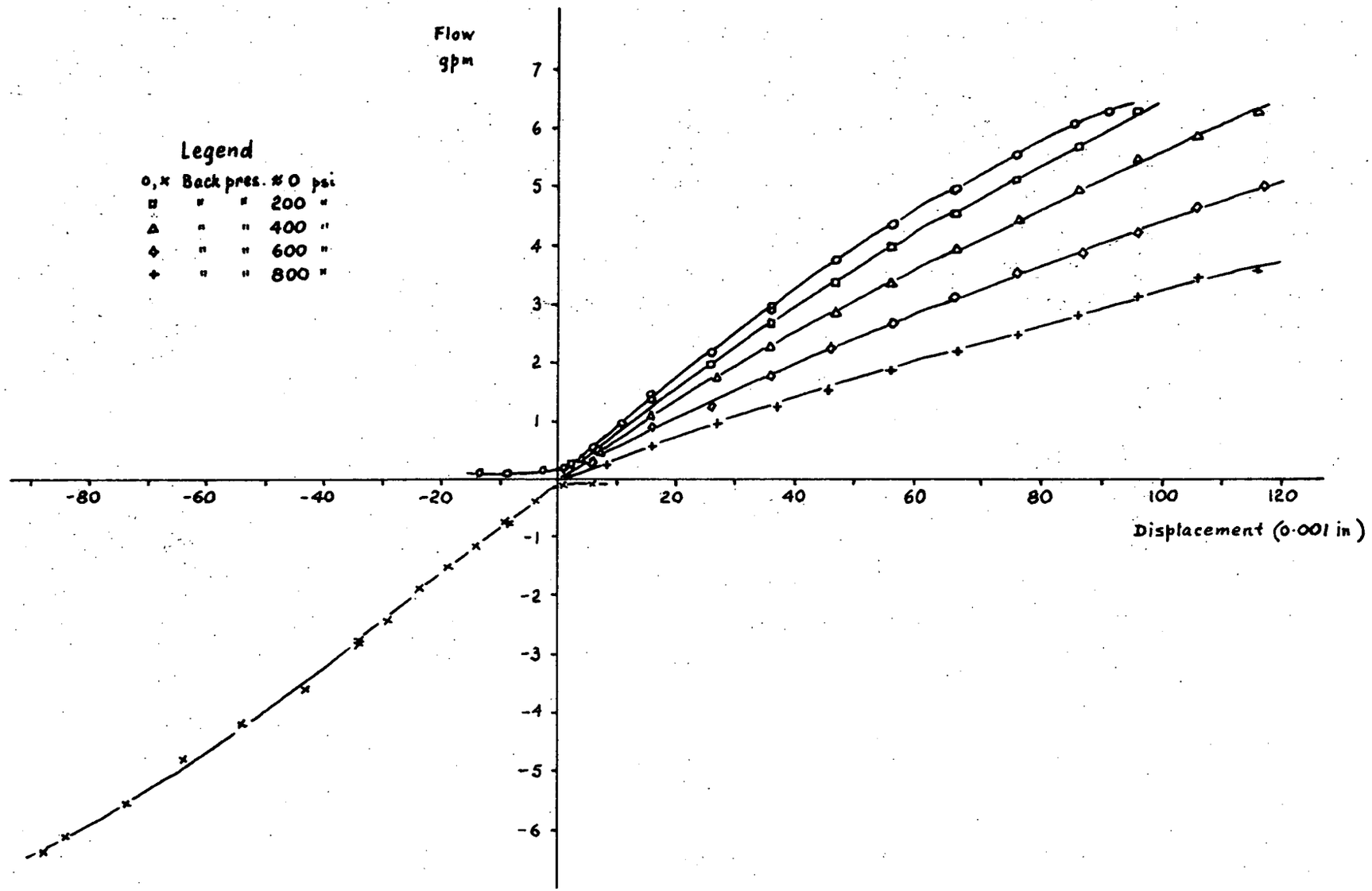
Flow
gpm
Legend
o, × Back pres. × 0 psi
□ " " 200 "
△ " " 400 "
◇ " " 600 "
+ " " 800 "
7
6
5
4
3
2
1
-1
-2
-3
-4
-5
-6
-80
-60
-40
-20
20
40
60
80
100
120
Displacement (0·001 in)

Figure 3.6

stage, in assuming the total roll-off to be due to this cause, as the valve need not have been linear. Indeed this was one reason for actually measuring the valve characteristics). With one exception the hoses and fittings upstream of the valve were large and should have offered only a small resistance to the flow. The exception was at the entry to the valve where the oil passed through a $\frac{1}{4}$ in. diameter hole into the central valve chamber. To estimate the likely pressure drop upstream of the valve, it was assumed that, as the $\frac{1}{4}$ in. hole was the most significant restriction, it caused most of the pressure drop. It was then assumed to behave as a sharp edged orifice of the same diameter.

Downstream of the experimental valve the oil had to flow through several fittings and valves. However in this case the pressure drop was measured directly by a pressure transducer placed just downstream of the experimental valve. This made it possible to calculate an equivalent orifice type restriction to represent the loses downstream of the valve. It should be noted, however, that this was only applicable to the "zero" back pressure results. (Strictly speaking, even though these results were obtained with the back pressure valve fully open, the back pressure was not zero due to the pressure drops downstream). For all other results the back pressure was maintained constant by the back pressure valve irrespective of the oil flow. The hydraulic circuit therefore looked somewhat like figure 3.7 (a) in the case of "zero" back pressure, and like figure 3.7 (b) in all other cases.

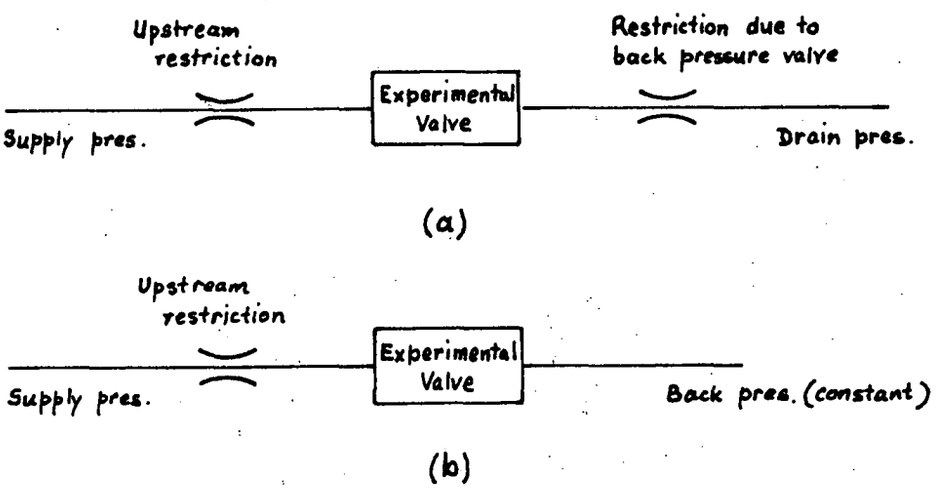

Figure 3.7

Hydraulic circuit for (a) "zero" back pressure,

and (b) non-zero back pressure, results

This explains the greater droop in the "zero" back pressure curve; the results in this case had the added effect of a flow dependent pressure drop downstream, as well as upstream. The estimates of the pressure drops upstream and downstream of the valve were used to evaluate the approximate pressures that actually existed across the metering orifice of the valve at any flow. This, together with the assumption that the valve behaved, at least to a first approximation, in accordance with the orifice equation (3.2), enabled a correction to be made to the flow results to give an estimate of the flows that would have resulted had there been no pressure drops upstream or downstream. That the valve did behave, at least to a first approximation, in accordance with the orifice equation, can be deduced from the results already presented in figure 3.6. In addition to this correction, a small correction was made for the non-linearity of the orifice area with displacement. The "corrected" results are plotted in figure 3.8. There is still a small amount of roll-off at the higher flows. This could no doubt be eliminated by assuming slightly higher losses. However this is hardly justified in view of the assumptions and estimates already made to obtain these curves. In new valve designs, one of which is presently under construction, provision has been made for pressure tappings into the valve body to enable the pressure drop across the metering orifice to be accurately measured.

Figure 3.8 also shows that the valve was slightly under lapped, i.e. the extrapolated flow curves reach zero flow, ignoring leakage, at a small negative displacement, $-x_o$. This is taken into account in some of the mathematical models presented in chapter 4 by displacing the origin of the orifice flow equation as below:

$$Q = C_d\, k\, w\, (x + x_o) \sqrt{\frac{2\,\delta p}{\rho}} \qquad (3.4)$$

The results presented in figure 3.8 also show that, with the exception of the 600 psi back pressure set, the coefficient of discharge is very nearly constant. The average value, excluding the 600 psi results, is 0.73. There is some doubt as to the accuracy of the back pressure in

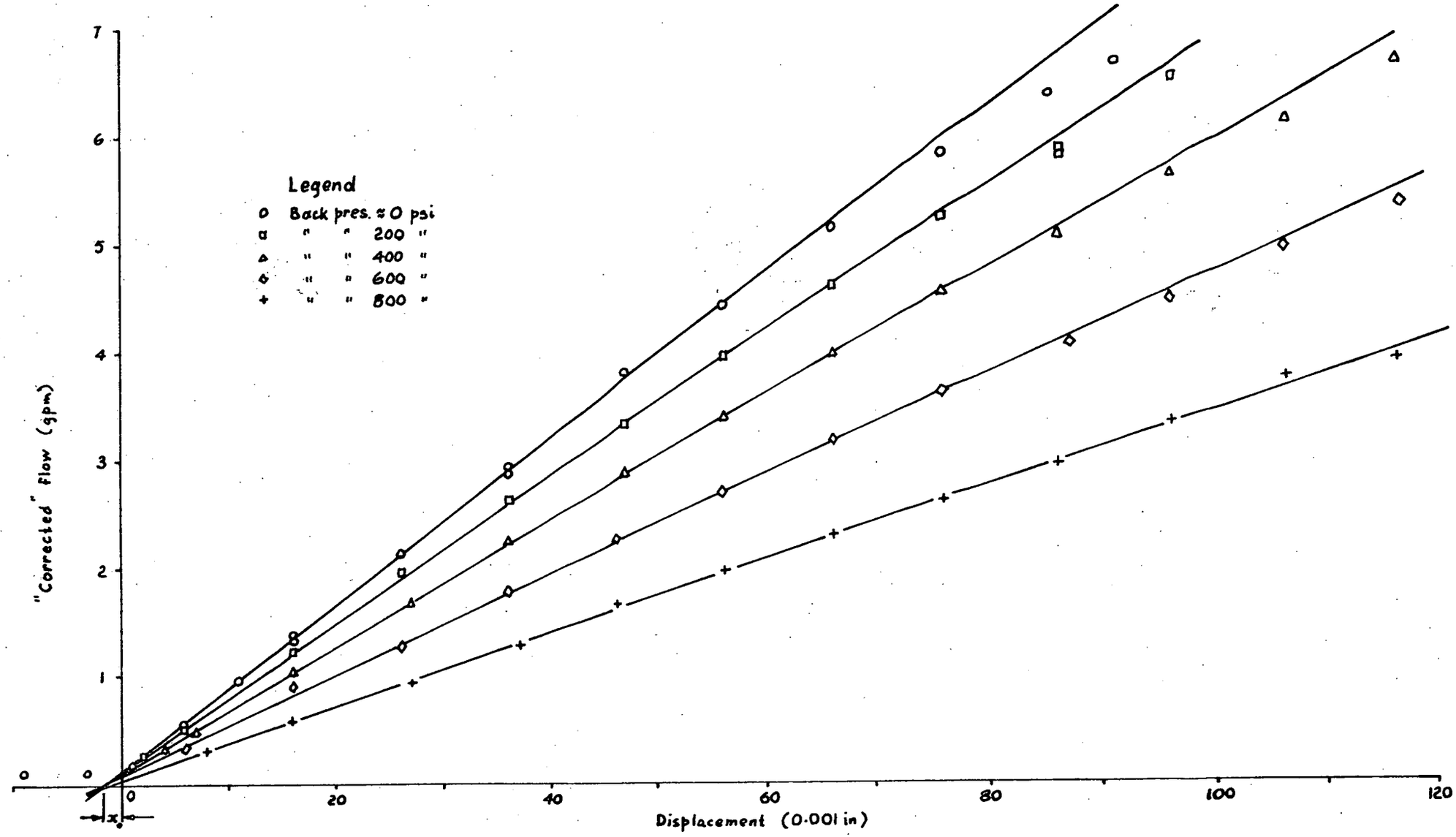
Legend
o Back pres. ≈ 0 psi
□ " " 200 "
△ " " 400 "
◇ " " 600 "
+ " " 800 "
"Corrected" Flow (gpm)
Displacement (0.001 in)
0
1
2
3
4
5
6
7
20
40
60
80
100
120
x

Figure 3.8

the case of the 600 psi set and this could explain why the discharge coefficient in that case is lower, at 0.69.

It should be noted however, that these discharge coefficients, and indeed figure 3.8 itself, do not in reality describe the actual, physical valve. They represent the behaviour that would be expected from a valve of similar design to the one discussed here, but with a linear displacement throat area characteristic and constant pressure drop across the metering orifice. In chapter 4 results from the mathematical models of the system are compared with those from the actual valve, hoses and fittings, and as such figure 3.6 represents the behaviour more correctly than this figure. The discharge coefficients used in chapter 4, therefore, have been chosen so as to best approximate the behaviour shown in figure 3.6. Figure 3.8 is included mainly to show that the actual metering orifice does in fact behave in accordance with the orifice equation, even though its physical appearance is more that of a restricting passage than an orifice.

3.3.2 Flow Reaction Force

As already mentioned, because valve Mk II had only two spool lands, it was possible that significant errors could occur in the flow reaction force measurements. These could arise as a result of different oil pressures within the chambers between the end caps of the valve and the valve spool lands (see figure 3.5). In addition, during the actual tests of the valve, two further effects were observed. The most significant effect was the valve spool sticking, often called hydraulic lock, particularly at high back pressures. To overcome this it was necessary to lightly tap the valve body with a small hammer to jar the spool free. This tapping, however, could itself introduce bias into the results as it was found that tapping the side of the valve body had very little effect; the tap had to be in an axial direction and in the case of high back pressures it had to be reasonably heavy. The other significant effect was the force exerted on the spool shaft by the dial gauge used to measure the spool position. This was complicated by the fact that the dial gauge force, besides

being position dependent, also showed a marked hysteresis effect, i.e. the force exerted was dependent on the direction and way the position of the dial gauge plunger had changed as well as on the actual position of the plunger. After movements towards the gauge body, static forces as high as 0.9 lb_f were measured, while after movements away from the gauge body, forces as low as 0.05 lb_f were measured. In this respect the tapping of the valve body was beneficial for it tended to reduce the hysteresis effect and hence, after a reasonable amount of tapping, the force could be estimated fairly well from the dial gauge reading. For readings near the low end of its travel, the force was approximately 0.1 lb_f; this increased to approximately 0.4 lb_f at the high end of its travel.

Figure 3.9 shows a plot of the "corrected" forces against spool position at various back pressures. Although a certain amount of

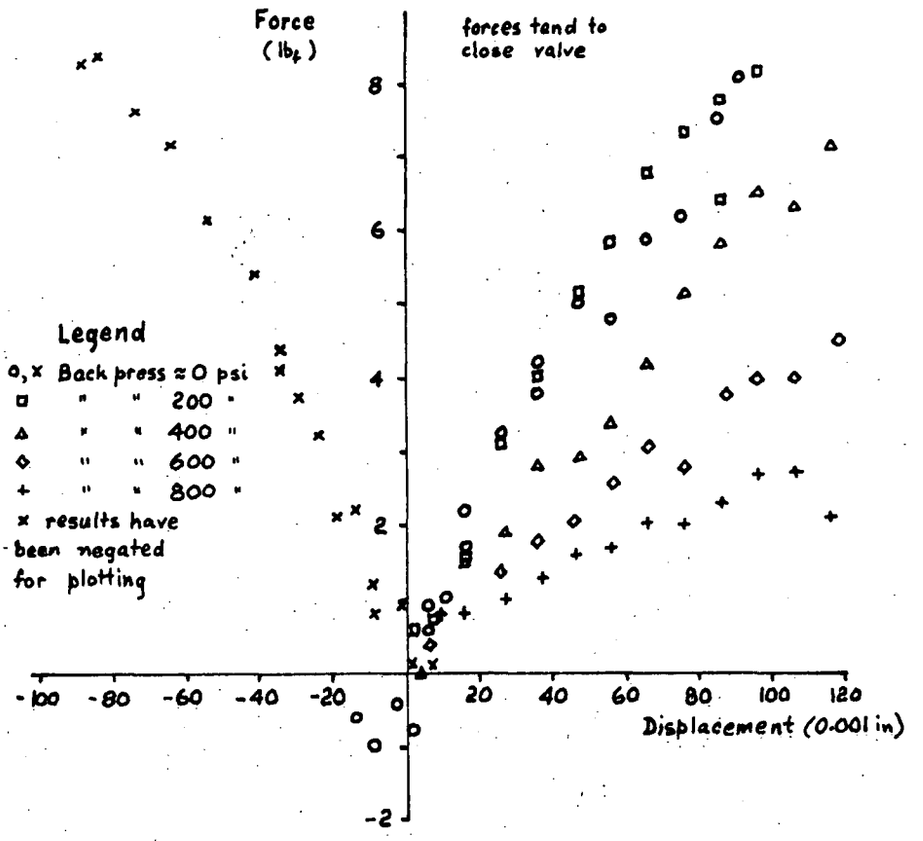

Figure 3.9

Flow reaction force

scatter is present the points lie roughly along straight lines. This

would be expected, provided the angle of the oil discharge jet did not alter significantly (see equation 3.3). At high flows there is once again a roll-off trend. This could at least, be partly explained by the pressure drops occuring in the hoses and fittings up and down-stream of the valve. Corrections could be made for this effect in the same way as in section 3.3.1. However it was not thought justified in this case as the results themselves show a fair variability.

An interesting point to note about these results is the way in which the 200 psi back pressure results tend to overlap and in places exceed the corresponding forces for the "zero" back pressure results. The reason for this is not clear. It could be that the oil discharges from the orifice at a different angle in the two cases, or it could possibly be due to a difference in the oil pressures in the end chambers of the valve, although why this should be affected by the setting of the back pressure valve is not obvious. By taking the "slope" of these graphs and applying the flow reaction force equation (3.3), i.e.

$$F = 2 C_d k w x \delta p \cos\theta$$

an estimate of the angle at which the jet is discharged from the metering orifice can be obtained. These results are given in the following table:

Pressure drop, δp psi	angle, θ degrees
1000	51
800	39
600	42
400	42
200	39

With the exception of the first result, i.e. the "zero" back pressure result, the angle is approximately 40°, which is about the angle expected (section 3.2).

No doubt the variability in the results presented in this section would be decreased if hydrostatic bearings were incorporated in the valve. However, as previously mentioned, this was not thought justified with this particular valve as it had many other faults. Also, for the dynamic tests, hydrostatic bearings did not appear necessary, for, while the valve spool was stroked, it did not appear to stick. In current valve designs provision has again been made for hydrostatic bearings and these will no doubt be incorporated; indeed it will be most interesting to compare the results of this valve with those of future ones.

3.3.3 The Oil Wave Velocity Within Flexible Hose

Some of the mathematical techniques of chapter 4, used to analyse the dynamic behaviour of the system, require an accurate measure of the speed with which small disturbances are propogated through the oil within the flexible hoses. Unfortunately this velocity is not only dependent upon the density and compressibility of the oil, but also on the stiffness of the hose or passage in which the oil is contained. It therefore becomes very difficult to make an accurate estimate of this velocity unless the hose or passage properties are well known. In this case the flexible hose used, was of rubber and steel wire-braid construction and consequently the only practical way to determine the wave velocity was to physically measure it. This also solved the problem of estimating the compressibility of the oil; estimates are usually poor due to the entrainment and absorption of air in the oil. This increases the compressibility[12].

To measure the velocity a length of flexible hose, call it B, was coupled between two pressure transducers as shown in figure 3.10. A further length of hose, A, terminated by a valve, V, was coupled to one end of this to enable the generation of small pressure pulses. The technique used to generate these pulses will be described presently. The two pressure transducers, T1 and T2, were of the same type and mounted as nearly as possible at the same distance from the centre-line of the hose. This ensured uniform delays between the

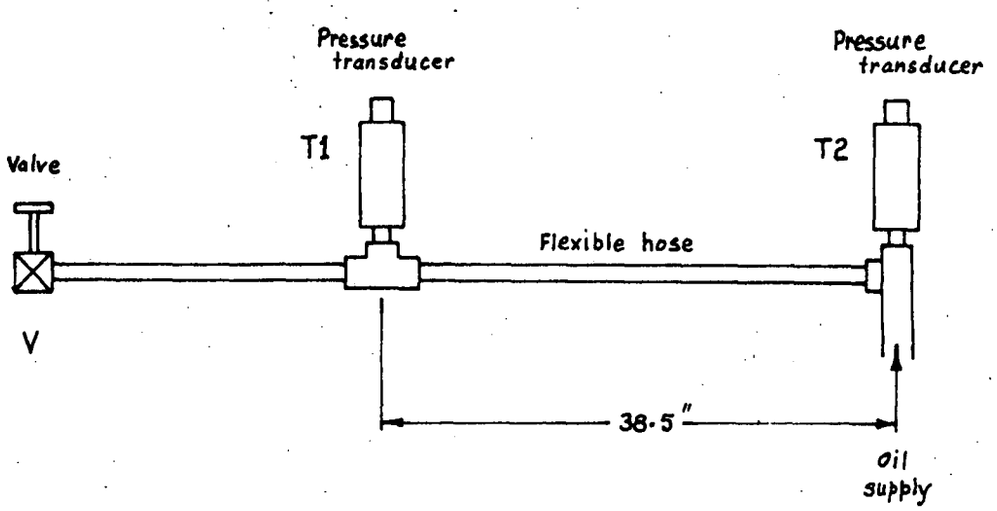

Figure 3.10

Experimental set up to determine the oil wave velocity within flexible hose

pressure pulses arriving at the transducer position and actually reaching the sensing element. By opening valve, V, a representative sample of hot oil could be drawn off from the hydraulic rig. The supply pressure to this experiment was controlled by valves and could be maintained at any pressure from 20 psi up to 1000 psi. The outputs from the transducers were observed on a dual beam CRO.

The first method used to create small pressure pulses was to strike the valve, V, in such a manner that hose A was slightly compressed longitudinally, thus generating a small pressure pulse which would travel down the hoses. This was not very satisfactory. Firstly there appeared to be some high frequency "ringing" effect set up in hose A which created a small train of waves, very nearly sinusoidal, instead of a pulse. This caused a considerable amount of difficulty in determining the time delay between the wave at the two transducers, as the corresponding peaks were difficult to identify. A sketch of the form of the traces observed, is given in figure 3.11. Presumably the "ringing" was in the hose proper, for if it were due to pressure waves soley in the oil, then either the wave velocity would have to be excessively great, or there would have to be a high order harmonic

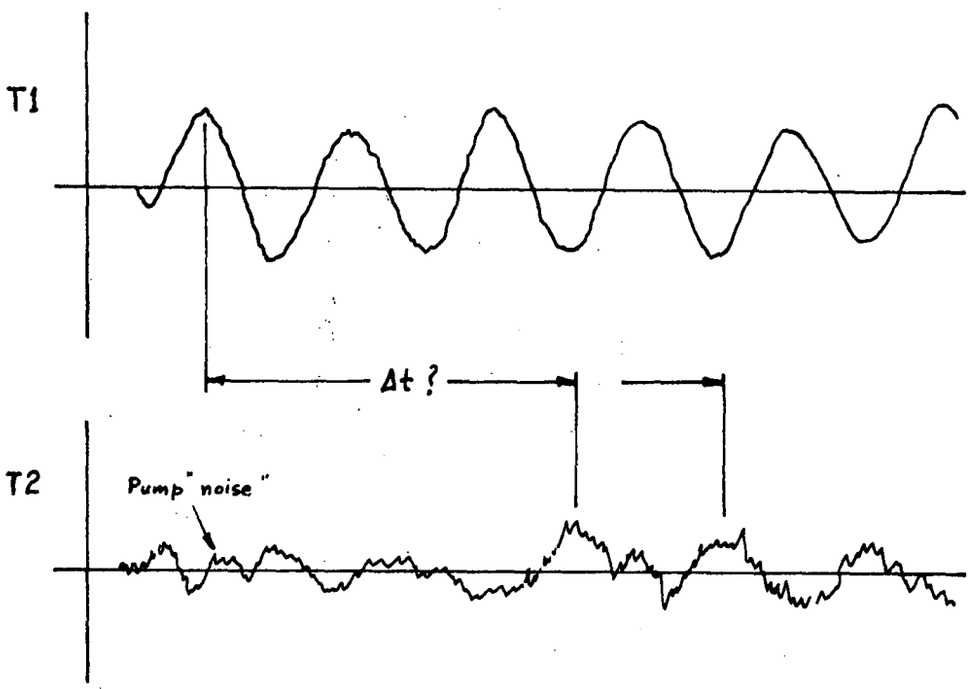

Figure 3.11

Wave trains at the first and second transducer

standing wave set up in the hose, and it is difficult to see how this could be sustained without some form of external excitation of approximately the correct frequency. Also at very low pressures the "ringing" did not occur. The hose had to have a reasonable pressure in it before any wave trains were observed; possibly the steel wire braid of the hose was the predominant "spring" in the system, and this required some pressure within the hose before it was "tensioned" and could contribute. Secondly the peak pressure disturbances produced by this method were small and it was difficult to detect them over the pump "noise" at the second transducer, T2.

A better waveform was found to be obtained by sharply striking the side of the flexible hose, A, with a small hammer. This created a fairly well defined, although broad, pulse which could be readily detected at both transducers. Figure 3.12 shows some photographs of the CRO traces occuring at various static pressures within the hose. A slight "ringing" effect can be seen in the trace of the first

(a)

Static pres. 20 psi

Scales:

100 psi/cm

50 psi/cm

0.2 ms/cm

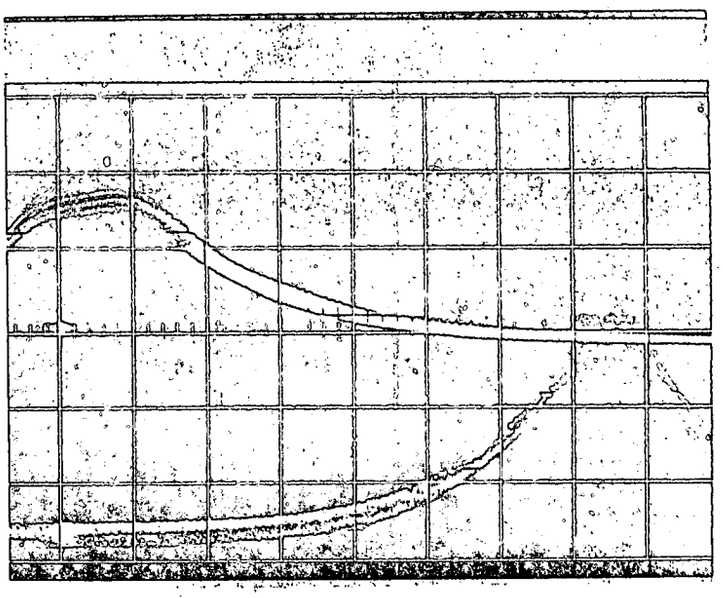

(b)

Static pres. 250 psi

Scales:

50 psi/cm

0.2 ms/cm

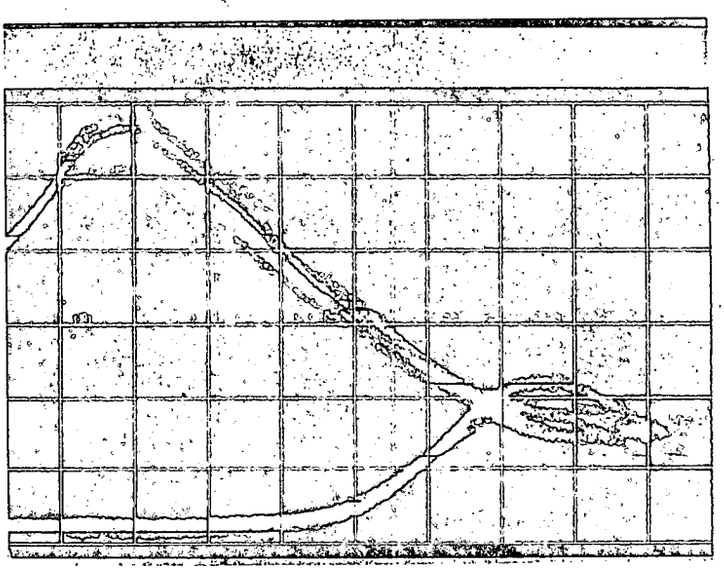

(c)

Static pres. 500 psi

Scales:

100 psi/cm

50 psi/cm

0.2 ms/cm

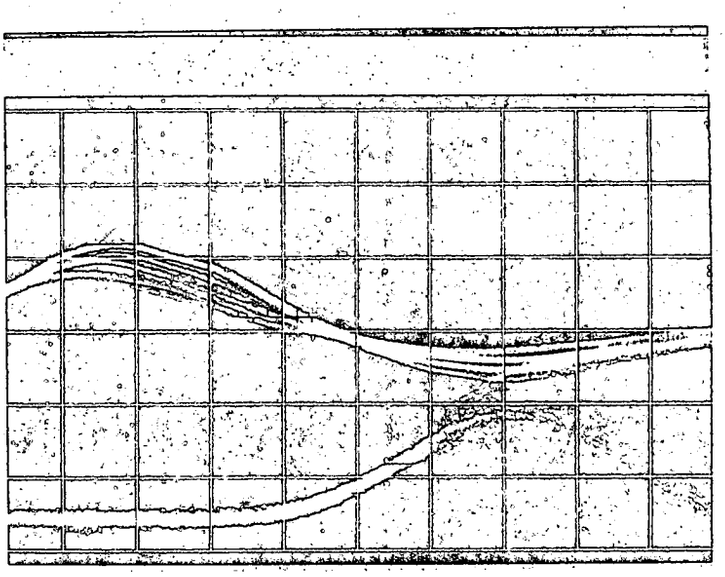

Figure 3.12 (i)

Wave velocity measurement. Upper traces - transducer 1, lower traces - transducer 2

(d)

Static pres. 750 psi

Scales:

50 psi/cm

0.2 ms/cm

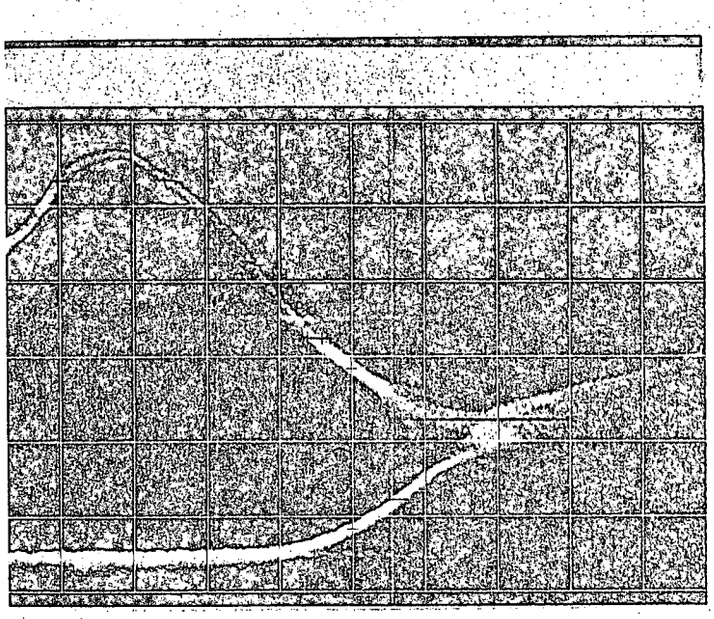

(e)

Static pres. 1000 psi

Scales:

50 psi/cm

0.2 ms/cm

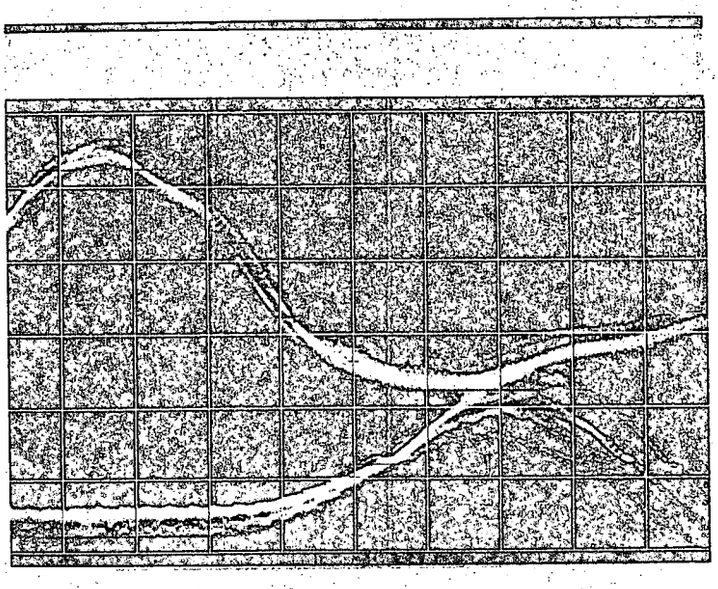

(f)

Static pres. 50 psi

Scales:

(not calibrated)

50 psi/cm

2 ms/cm

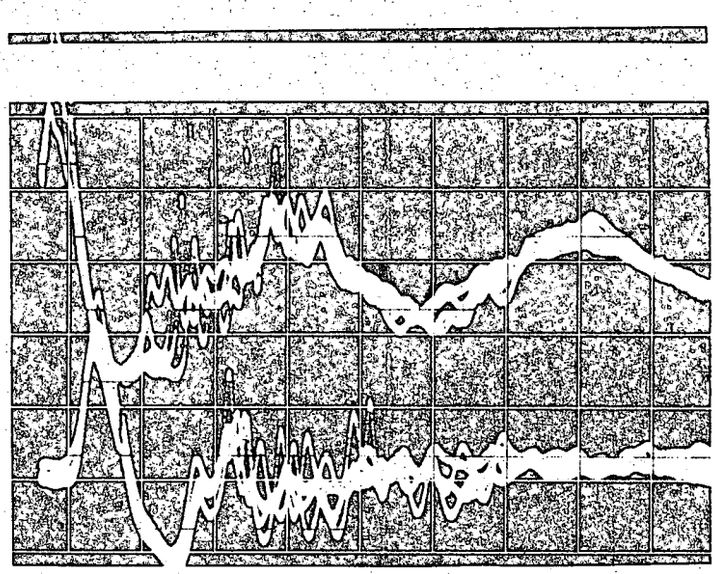

Figure 3.12 (ii)

Wave velocity measurement. Upper traces - transducer 1,

lower traces - transducer 2

transducer, T1, in some of the photographs. This became worse the harder the hose was hit. In figure 3.12 (f) the time scale has been compressed. This gives some idea of the effect of reflections and "ringing" after the initial wave has passed both transducers. By measuring the time delay between the pulse reaching the first transducer and the second, the wave velocity can be deduced, for a given static pressure. Of course this relies on the accuracy of the CRO time base. To calibrate this a signal generator and electronic counter were used. The counter was connected to the signal generator, and gave an accurate measure of the average frequency over a small counting interval, while the output of the signal generator was displayed on the CRO. The time base was then adjusted to give the correct trace wavelength for the particular frequency used. The time base setting during this was naturally that to be used for the photographs.

Figure 3.13 shows the results of these measurements. The velocity

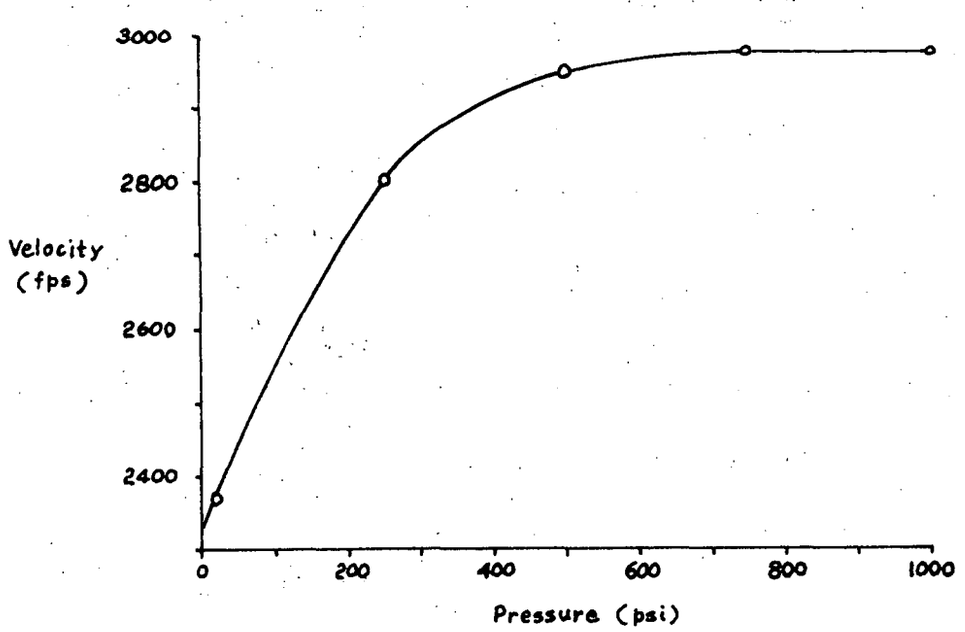

Figure 3.13

Wave velocity in flexible hose vs static pressure

increases initially at low static pressures and then levels off with higher pressures at a velocity of 2970 fps. Presumably this effect was caused by the particular construction of the flexible hose; it was

rubber with steel wire braiding. As the pressure increased the steel braid probably carried a larger and larger proportion of the load and thus the hose appeared to stiffen with pressure.

It is interesting at this stage to compare the effective compressibility of the oil-hose combination with that of the oil alone. It will be shown later that the effective bulk modulus, i.e. the reciprocal of the effective compressibility, is related to the wave velocity by the following equation:

$$a = \sqrt{\frac{\beta_e}{\rho}}$$

where a = wave velocity

β_e = effective bulk modules

ρ = density of oil

Inserting the plateau velocity of 2970 fps, gives an effective compressibility of 1×10^{-5} in^2/lb_f compared to the value normally taken for oil itself of 5×10^{-6} in^2/lb_f [12] ; that is the hose has effectively doubled the compressibility of the oil! This is a point well worth remembering, particularly if there are large quantities of oil contained within flexible hose in any system.

------ ooo ------

CHAPTER 4

DYNAMIC BEHAVIOUR

Introduction

As has already been mentioned, the original aim of this project was to design and construct an hydraulically powered vibration testing machine. Furthermore, because of the ready availability of a high speed digital computer, in comparison to an analogue machine, an attempt was made to solve the dynamic equations describing the system by numerical means rather than analogue means. This chapter presents some of the models and the problems associated with them. The results obtained from the current experimental rig are also presented.

Broadly speaking the chapter is divided into three sections. The first section discusses the models of the "overall" testing machine. These models, although not representing the present experimental system, give a good background to the problems that arose in trying to solve the mathematical equations numerically. A comparison is also made between the results from one of the models and those from a linearized model by Lambert and Davies [11]. The second section deals with models more closely resembling the experimental rig at its present stage of development, i.e. basically a valve situated between two long lengths of hose. The hose lengths were made large in order to increase the inertia effects of the oil. The final section describes the current experimental rig and the dynamic results obtained from it.

4.1 Hydraulic Vibration Testing Machine Models

4.1.1 Incompressible Fluid Model

Because of its apparent simplicity a simple valve-ram mechanism was originally chosen as a possible hydraulic amplifier for the vibration tester. A schematic diagram of this is shown in

figure 4.1. It is basically a four-way valve coupled to a double

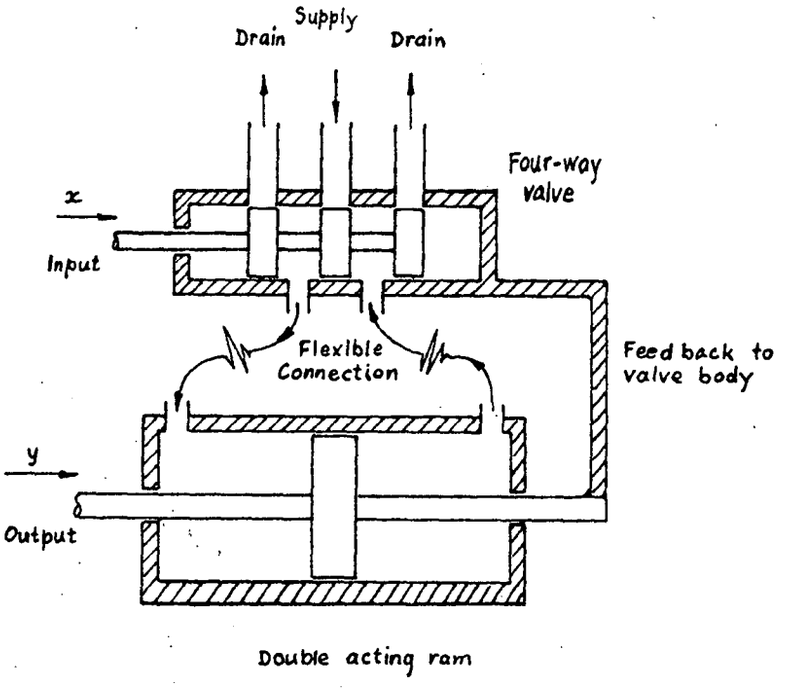

Figure 4.1

Hydraulic amplifier

acting ram, the output of which is fed back to the input in such a way as to make the output follow the input. The feedback is in fact a later addition to the basic system. However it appears to have very little effect on the numerical stability problems that arise, and as it represents a more feasable system it has been included here. Without feedback the ram would eventually move to one end or other of the cylinder due to small mean position errors of the valve spool, leakage or slight differences in the characteristics of the various orifices.

Figure 4.2 shows the system redrawn in a form more suitable for analysis. Note that p_1 and p_4 exchange numerical values as the sense of the spool displacement relative to the valve body, i.e. h, changes sign. The actual numerical values are the supply and drain pressures. The orifices also change with the sign of the relative spool displacement from O_1, O_3 to O_2, O_4 and vice versa. These variations occur as a result of the change in valve flow paths as the relative spool position changes sign. In all that follows the four orifices are

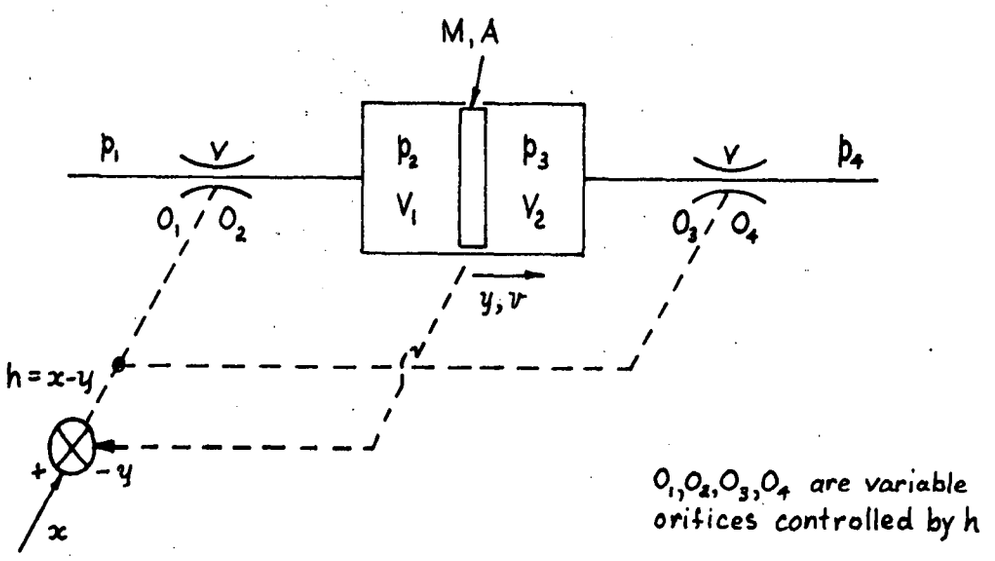

Figure 4.2

Schematic arrangement of hydraulic amplifier

assumed to be indentical in characteristics. This is not necessary; however it simplifies the equations somewhat.

The orifice flow equation (3.2) may be slightly modified to take into account possible pressure and flow reversals. This gives the oil flow into the cylinder through the left hand orifice as

$$Q_i = C_1 |h| \sqrt{|p_1 - p_2|}\ \text{sign}(p_1 - p_2) \qquad (4.1)$$

where C_1 = a constant = $C_d\ k\ w\sqrt{\frac{2}{\rho}}$ (see section 3.1)

h = relative valve spool displacement = x - y

p_1, p_2 = oil pressures as indicated in figure 4.2

$|r|$ = the absolute value of r, i.e. the unsigned value of r

$\text{sign}(r)$ = +1 or -1 depending on whether r is positive or negative

The oil flow out from the other side of the cylinder through the right hand orifice is similarly

$$Q_o = C_1 |h| \sqrt{|p_3 - p_4|}\ \text{sign}(p_3 - p_4) \qquad (4.2)$$

For the ram the equation of motion, neglecting friction terms, is

$$M \frac{dv}{dt} = A(p_2 - p_3) \tag{4.3}$$

where M = effective ram mass (allowing for the inertia of the oil in the pipes and cylinder ends)

A = "working" area of the ram

v = velocity of the ram

If the further assumption of no leakage past the ram is made then, as the oil is incompressible

$$Q_i = Q_o$$

$$= A v \tag{4.4}$$

Combining these four equations (4.1 to 4.4) and rearranging gives

$$\frac{dv}{dt} = \frac{A}{M}\left(p - \frac{2 A^2 v|v|}{C_1^2 h^2}\right) \tag{4.5}$$

$$\frac{dy}{dt} = v \tag{4.6}$$

where $p = p_1 - p_4$

$h = x - y$

The $v|v|$ term in equation 4.5 arises because of the dependence of the valve pressure drop on the direction of oil flow; it is the equivalent of the "sign" terms in equations 4.1 and 4.2. In this case, because of the assumption of incompressibility it is easily shown that $v|v|$ takes this into account correctly. Note also that p changes sign with h, as p_1 and p_4 exchange values as h changes sign.

One further piece of information is required before these equations (4.5 and 4.6) may be solved. That is the valve spool motion, x. This was assumed to be sinusoidal.

Several numerical techniques were tried in an attempt to solve these equations (4.5 and 4.6), but none were entirely satisfactory. As a result most of the studies have been done using a second order Runge-Kutta process (appendix 2). This was not because of any

superiority of this process over others, all techniques suffered from similar drawbacks, but because the second order Runge-Kutta process, while better than some of the more elementary processes, was still simple enough to be worked by hand. This enabled a good insight to be gained into the types of problems that arose and the reasons for them. It is a rather interesting result that so simple an equation (4.5) should prove extremely difficult to solve numerically!

One of the main problems with equation 4.5 is the relative spool displacement, h, which appears as a denominator in the equation. During certain periods of each cycle this must be zero, or numerically very small, and hence in a digital computer it can present very real and serious problems when the division is attempted. Intuitively of course, as a result of the "ideal" nature of the model in allowing no leakage and having an incompressible fluid, if h were zero then so also must the velocity, v, as the valve would be shut. Practically, however, the velocity is obtained numerically by a step by step approximation in time and is therefore subject to error. It is likely, and in fact observed, that as h becomes small the right hand term of equation 4.5 can become quite large. This does not infer that the velocity is significantly in error in a relative sense but only in an absolute sense. For example, suppose that for some small h the velocity is in error by, say, 1% of the maximum velocity. This would be relatively insignificant as far as the velocity waveform is concerned. However, if at this time the "true" velocity should have been only 1% of the maximum, say, then the calculated velocity would be in error by a factor of 2 at this point. This would cause the right hand term of equation 4.5 to be in error by a factor of four compared to its "true" value at this point. The result of this type of effect is that the velocity increment for that time interval tends to overcorrect the velocity. This often causes the velocity at the next time step to be even further in error but in the opposite sense. As a result, once

again the velocity is overcorrected. Consequently the calculated velocity can start to oscillate about the "true" values as h approaches zero. This oscillation also often grows very rapidly in magnitude. This is known as numerical instability. The point at which it occurs is not only dependent on the size of the time step taken but also on the constants in the equation. In fact the above statement of the problem is somewhat over-simplified, as in this case the velocity did "feed back" to modify h. However quite bad instability was often observed. Furthermore it was not only a fault of the Runge-Kutta process; all other numerical integration methods tried showed similar results. More will be said about the problem of numerical instability in section 4.2.1, where a very similar differential equation is solved.

Several methods were tried in order to overcome the problem of instability. One of the most obvious was the inclusion of leakage, both through the valve and past the ram, to "soften" the system when the valve was shut. This improved the situation slightly but did not overcome it altogether as the leakage flows were small compared to the maximum flows and consequently did not alter the equations or their solution greatly. Another technique that was tried and found moderately successful was to force the velocity of the ram to zero whenever the absolute value of h became suitably small. However the problem of just how to determine what size is meant by "suitably small" is still unsolved and practically, a trial and error process has been used. This is very unsatisfactory for the point at which instability occurs is dependent on the constants in the equation and the time step taken, and these vary whenever the system is changed, as well as with frequency. At low frequencies and/or high masses it was found that numerical instability occurred over significant sections of the cycle and made it virtually impossible to obtain a meaningful result. At high frequencies it was usually possible to obtain good results. Figure 4.3 shows a successful run, using this technique, at a frequency of 100 cps. Values of the physical

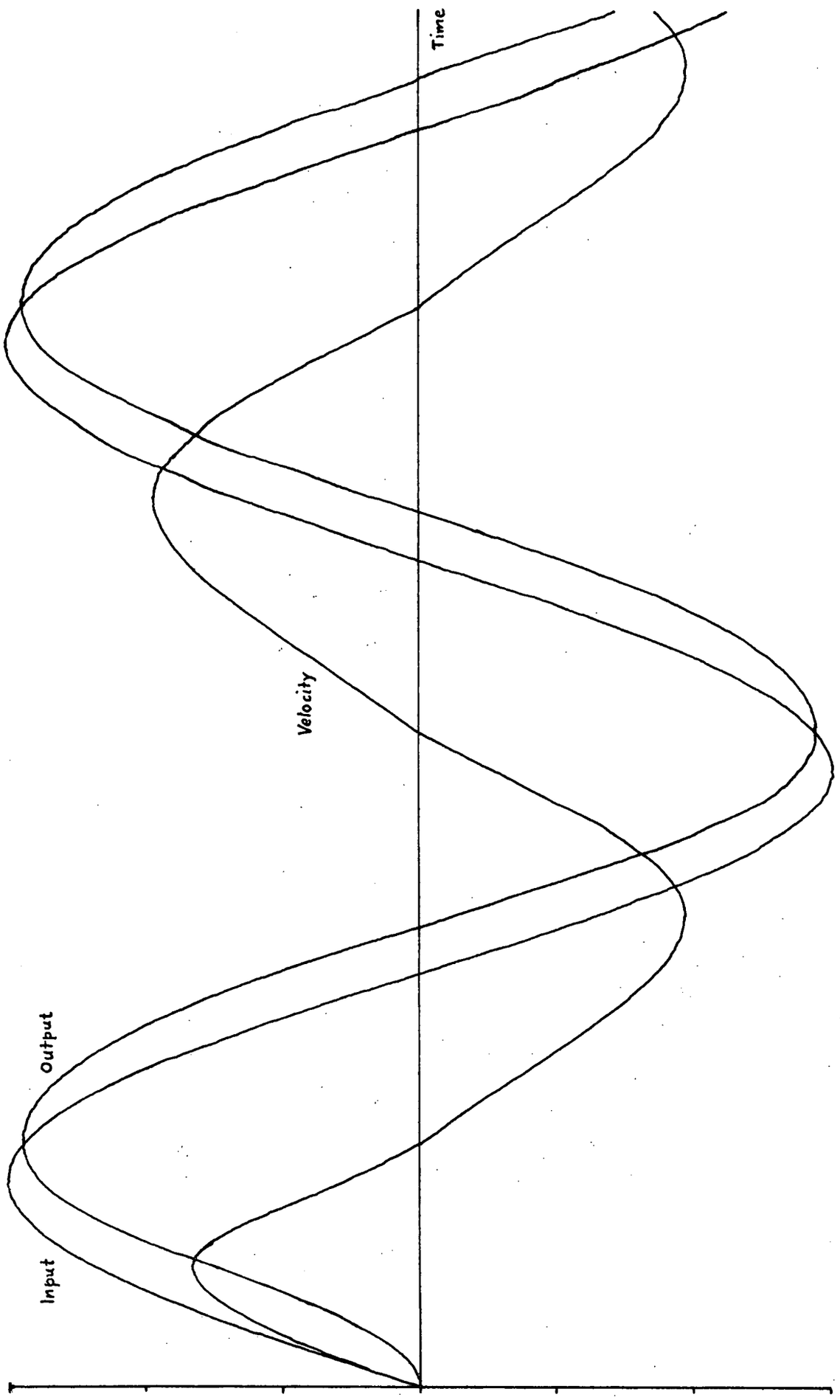

Figure 4.3
Solid slug model - 100 cps

parameters used in the equations are given in appendix 3, servo A. Several runs were made at low frequencies using different time step sizes and "cut-offs" on h, but none were very successful. Hence no low frequency results have been presented. However some of the results did suggest that compressibility was important and consequently the next model tried was one which included compressibility. This modification was also expected to overcome the problem of numerical instability.

4.1.2 Compressible Fluid Model

This model is basically that of section 4.1.1 only with a compressible fluid. Hence the volumes of oil trapped between the valve orifices and the ram are now important. Let these volumes be V_1 and V_2 as shown in figure 4.2. Suppose an oil volume, V, is subject to a pressure change, δp, resulting in a volume change, δV. Then by definition the bulk modulus of the oil, β, is

$$\beta = \frac{\delta p}{\delta V / V}$$

Rearranging this and taking derivatives with respect to time gives

$$\frac{dV}{dt} = \frac{V}{\beta} \frac{dp}{dt} \tag{4.7}$$

To overcome any argument as to the correct sign of this equation (4.7) the left hand side will be considered a fluid flow into the volume and not a change in volume. Equation 4.7 then gives the rate of pressure change expected for a given inflow of fluid.

Referring now to figure 4.2, the total oil flow into the cylinder through the left hand orifice consists of two components: the flow caused by the ram movement and that due to pressure changes within the oil in the cylinder (equation 4.7), i.e.

$$Q_i = A v + \frac{V_1}{\beta} \frac{dp_2}{dt} \tag{4.8}$$

where the symbols have the same meaning as in section 4.1.1 and figure 4.2.

Similarly the oil flow out through the right hand orifice is

$$Q_o = A v - \frac{V_2}{\beta} \frac{dp_3}{dt} \tag{4.9}$$

Once again, although it is not necessary, all the orifices are assumed to be similar in order to simplify the equations a little. As in section 4.1.1 the flows may be expressed in terms of the modified orifice flow equation, i.e.

$$Q_i = C_1 |h| \sqrt{|p_1 - p_2|}\ \text{sign}(p_1 - p_2) \tag{4.10}$$

$$Q_o = C_1 |h| \sqrt{|p_3 - p_4|}\ \text{sign}(p_3 - p_4) \tag{4.11}$$

The final equation required is the equation of motion of the ram. Neglecting friction terms this is

$$M \frac{dv}{dt} = A (p_2 - p_3) \tag{4.12}$$

Unless further arbitrary assumptions are made which can only be justified under certain circumstances, it is difficult to combine these last five equations (4.8 to 4.12) to give a differential equation in just one dependent variable. The problem was therefore solved in terms of the pressures by using the Runge-Kutta process on the following equations:

$$\frac{dp_2}{dt} = \frac{\beta}{V_1} \left(C_1 |h| \sqrt{|p_1 - p_2|}\ \text{sign}(p_1 - p_2) - A v \right) \tag{4.13}$$

$$\frac{dp_3}{dt} = \frac{\beta}{V_2} \left(A v - C_1 |h| \sqrt{|p_3 - p_4|}\ \text{sign}(p_3 - p_4) \right) \tag{4.14}$$

$$\frac{dv}{dt} = \frac{A}{M} (p_2 - p_3) \tag{4.15}$$

$$\frac{dy}{dt} = v \tag{4.16}$$

Before these equations were actually solved a further assumption was made. This was, the oil volumes either side of the ram are constant and equal. This assumption is in fact not necessary for the numerical process can easily handle variations in the volumes. However it does simplify the equations slightly and, initially anyway, it should prove

reasonable as the ram ought to be maintained near the centre of its stroke and the stroke amplitude should be small.

Setting the equations up as above also has the advantage that oil leakage both through the valve and past the ram, and friction terms can easily be included in the equations. However, so far the majority of computer runs have been made without these added effects. The assumed input motion was once again sinusoidal.

As mentioned in the previous section, it was thought that the inclusion of compressibility in this model would overcome the numerical stability problems. This has in fact proved unfounded. The solutions still often show instability. However in this case the occurence of numerical instability is much more readily controlled by a suitable choice of time step size. From experience it appears that, provided the time step chosen does not result in a pressure increment, during any time interval, exceeding about 10% of the supply pressure the solution will be stable. Admittedly this is a fairly unsatisfactory criterion to use with most standard integration procedures using fixed time steps, for it requires at least some idea of the likely pressure response in order to estimate the time step. Nevertheless it is usually possible to make a reasonable estimate of the time step, and this can then be tried and modified if necessary. At high frequencies this criterion generally results in a reasonable number of steps per cycle. However at low frequencies the number of steps can become prohibitive, particularly if the valve "gain" is high and the oil volumes small. This combination often results in very rapid pressure variations in relation to the speed of the input. This necessitates a very large number of steps per cycle, and consequently round-off errors and computation times may become excessive. In these circumstances it should be possible to devise a variable step size numerical integration procedure which would reduce the step size during rapid pressure variations, and hence reliably follow the change, and yet during slow variations increase the step size so as to keep the total number of steps per cycle to a reasonable number. Initial studies of this, in relation to the second-order

Runge-Kutta process have shown that it is feasable, although as yet no work has been done to modify the procedure as the systems studied to date have had relatively large oil volumes and hence reasonably slow pressure responses.

Figures 4.4 to 4.9 show some typical computer results for two different servomechanisms with varying input amplitudes and frequencies. The physical parameters used for the two servomechanisms are specified in appendix 3. The basic difference between them is that servo A has a slightly larger, heavier ram than servo B and a very much higher valve "gain"; it is some fifteen times larger. However servo B more closely represents the components from which it is anticipated the prototype vibration tester will be built. The input amplitude has been decreased at the higher frequencies in order to simulate the behaviour expected from an electromechanical valve spool excitation. Generally the peak force available from such an exciter is relatively small and consequently a constant displacement amplitude can only be maintained up to a certain frequency. Beyond this frequency the displacement amplitude falls with increasing frequency as the acceleration amplitude is the variable which then remains constant.

It is of interest to compare the form of output from each of these servomechanisms. With servo A, figures 4.4 and 4.5, the output although exhibiting a considerable amount of "bounce", follows the input reasonably well. On the other hand the output of servo B, figures 4.6 to 4.9, exhibits almost no "bounce". But at 100 cps it fails to "lock" onto the input, even after the input amplitude is increased (compare figure 4.7 with 4.8). These two cases have been traced over many more cycles than those presented here, and there is no apparent change; the output appears to be freely oscillating at a frequency of about 147 cps. The only apparent effect of the input is to modulate the amplitude of the oscillation. It is in fact interesting to compare this frequency with the natural frequency of the ram and oil volumes considered as a mass-spring combination. The natural frequency of this is 148 cps - very close to the 147 cps observed in

I was wondering when this would occur

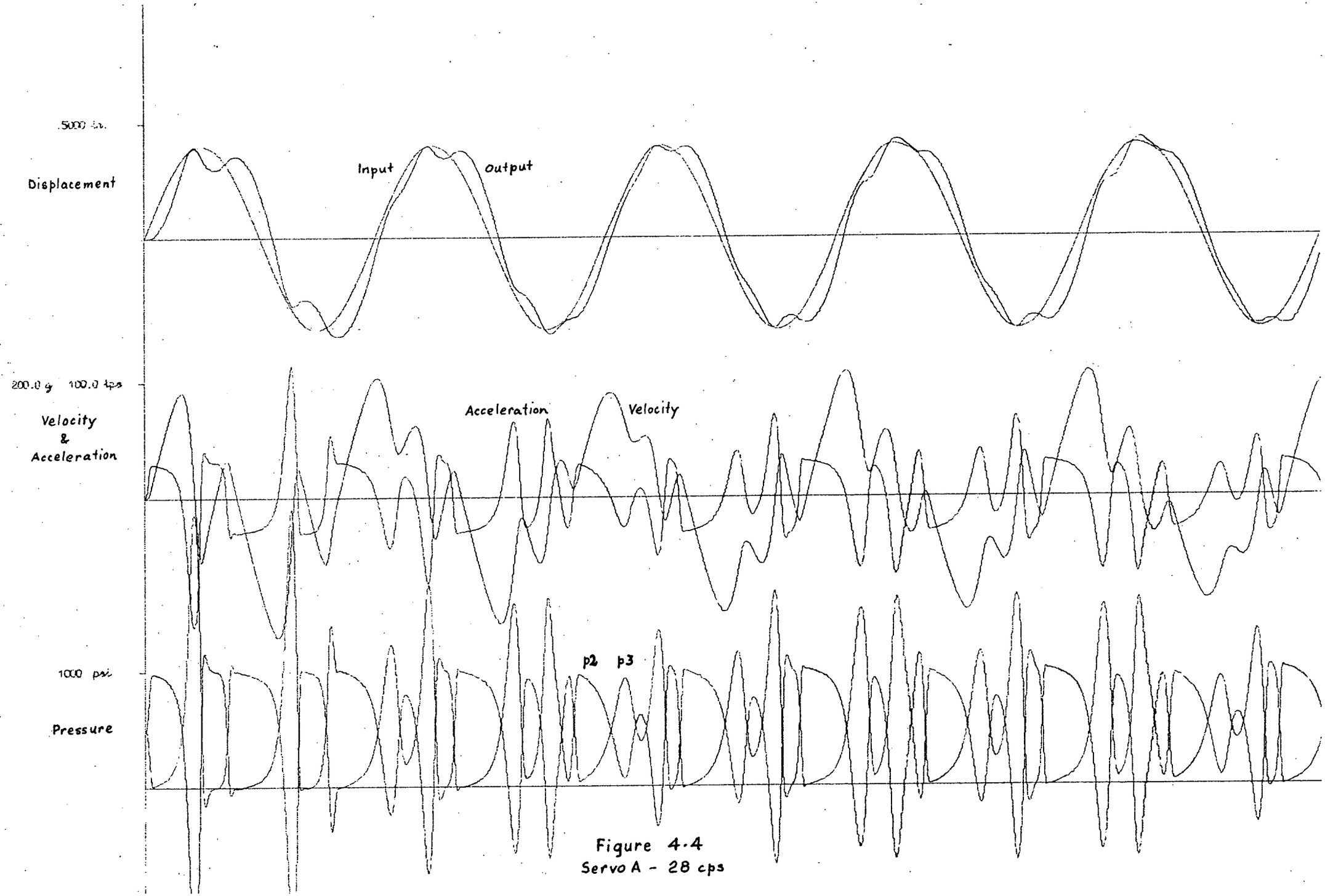

Figure 4.4
Servo A - 28 cps

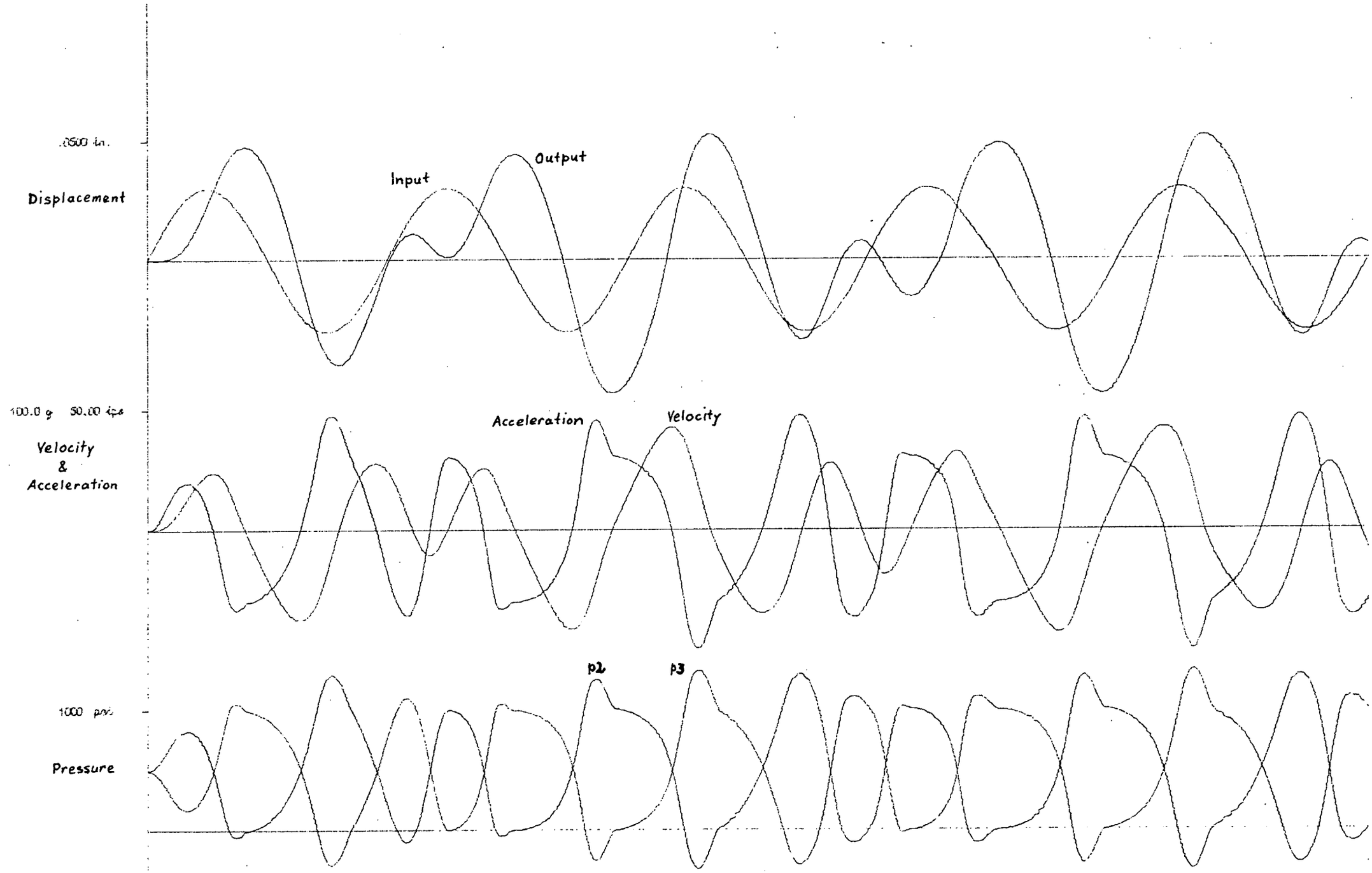

Figure 4.5
Servo A – 100 cps

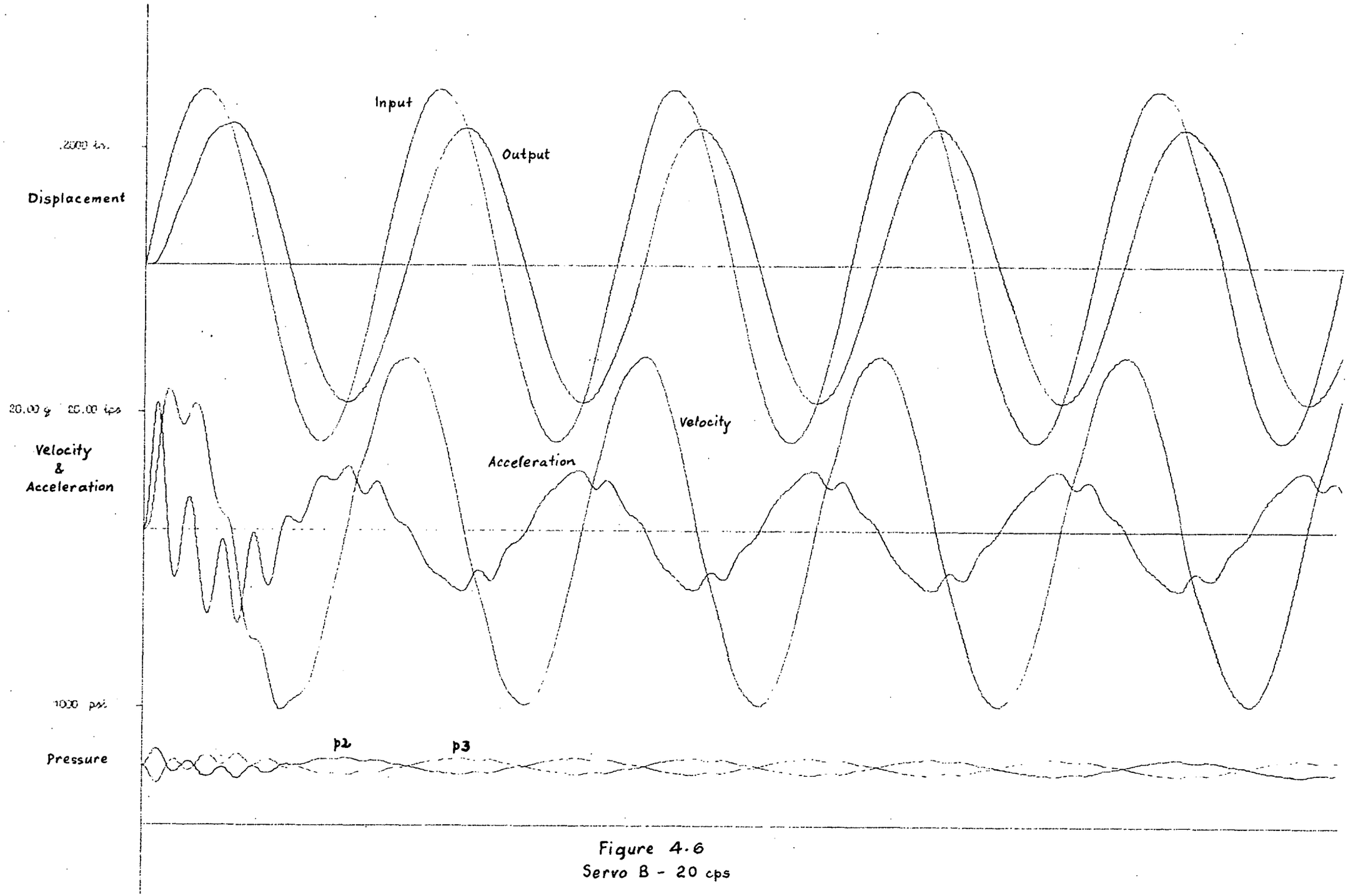

Figure 4.6
Servo B - 20 cps

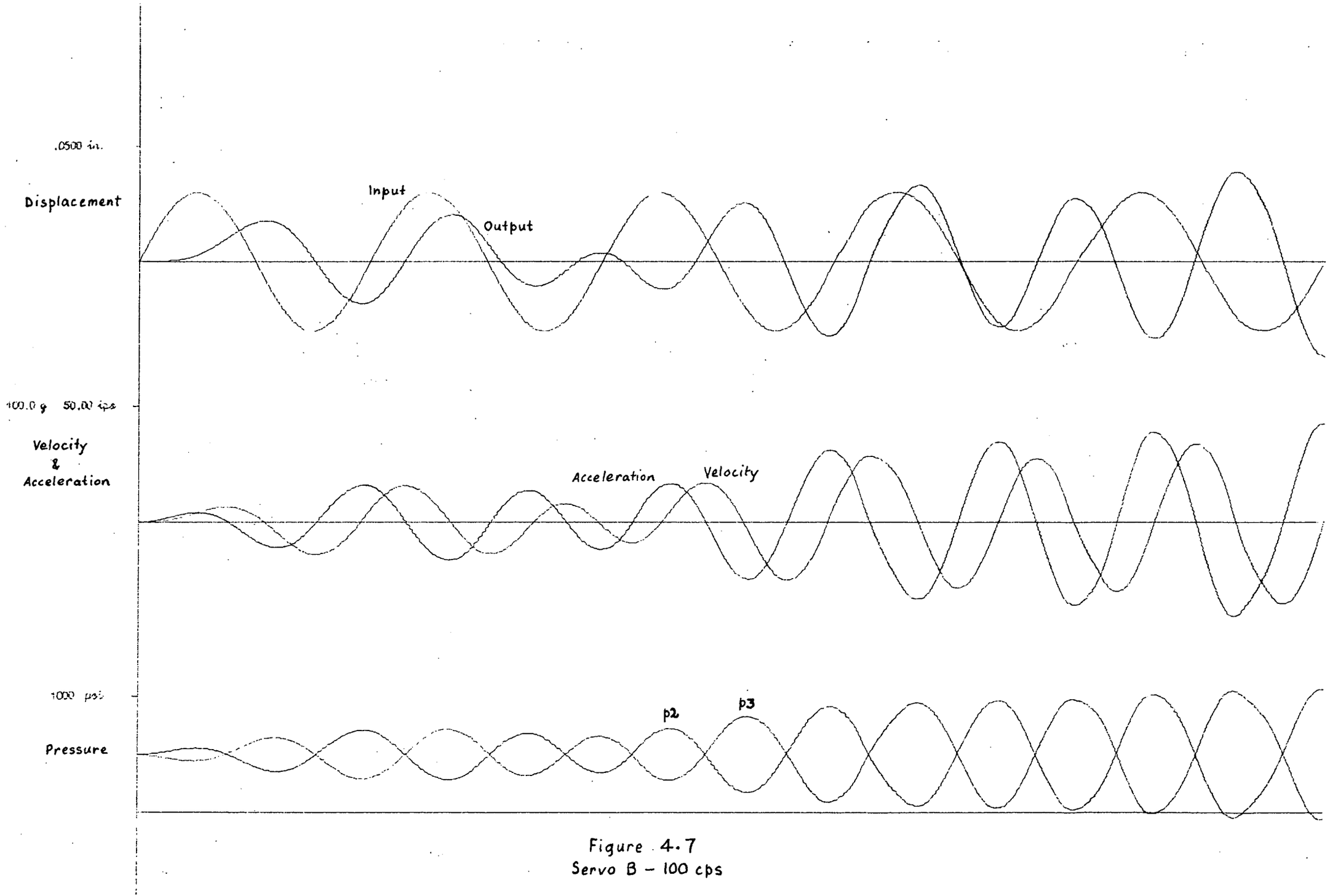

Figure 4.7
Servo B – 100 cps

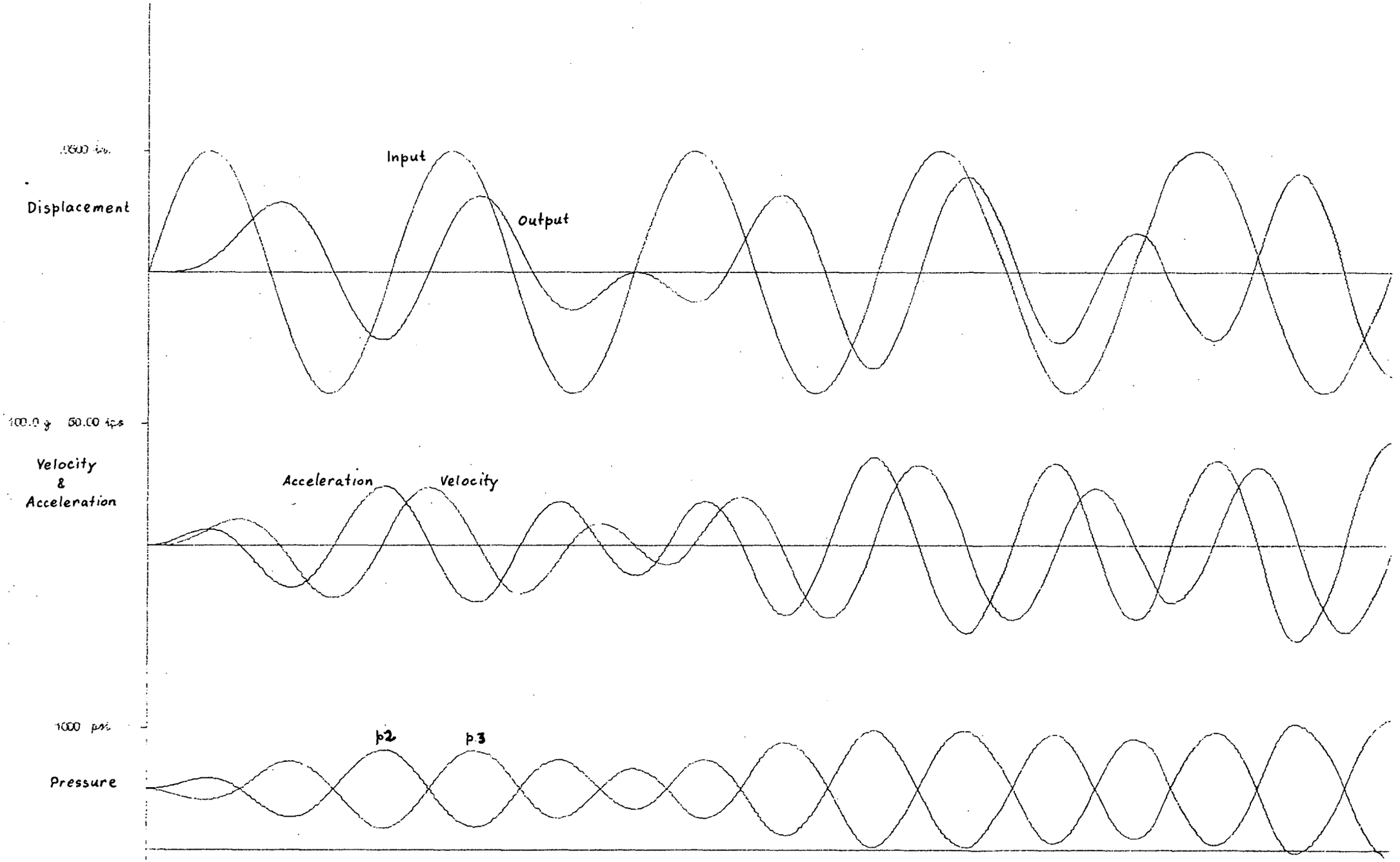

Figure 4.8
Servo B - 100 cps

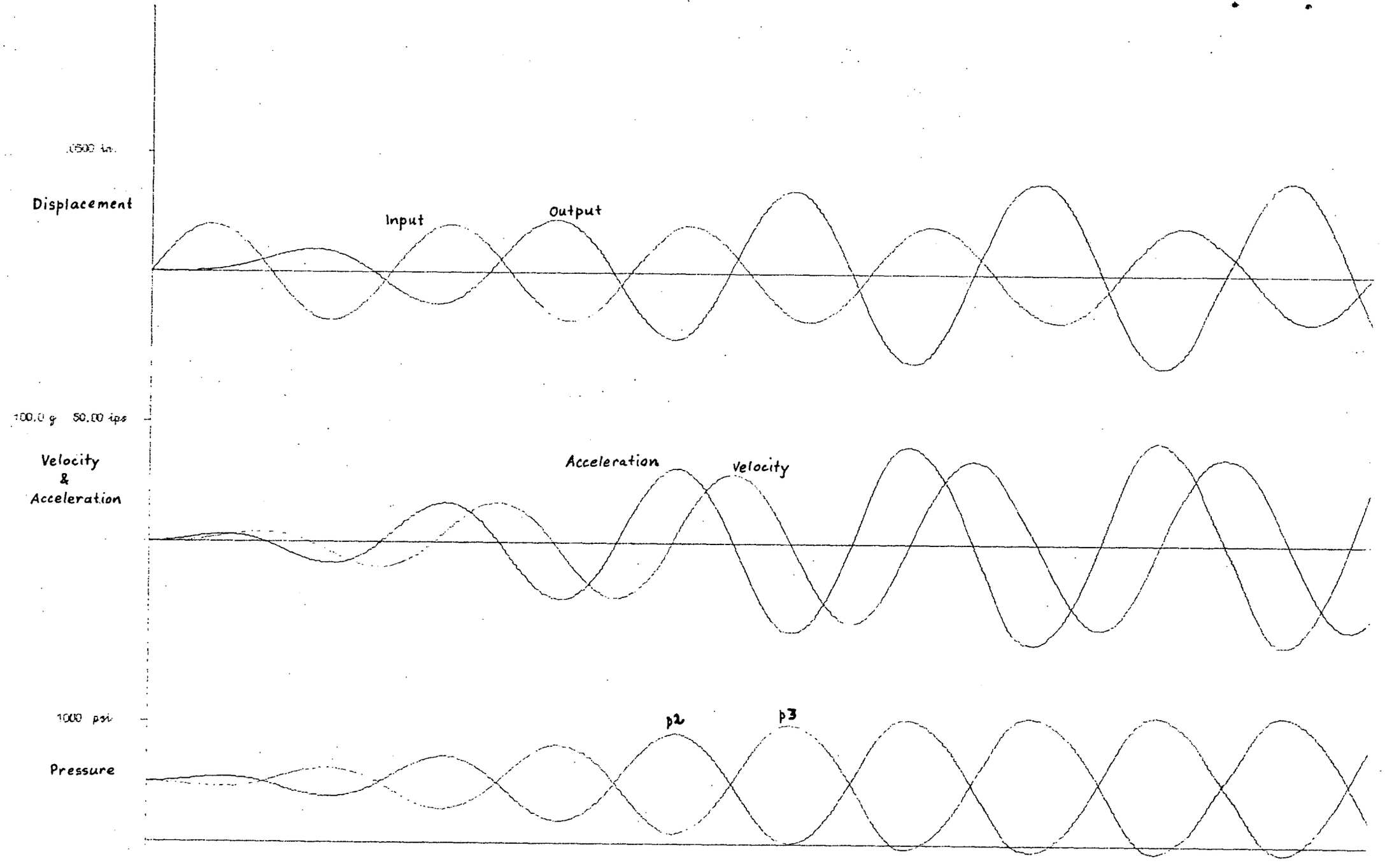

Figure 4.9
Servo B - 145 cps

figures 4.7 and 4.8! Even so, results obtained at frequencies near the natural frequency, viz 145, 150 and 155 cps, all settle down and "lock" onto the input reasonably quickly. It has even been possible to plot the phase of the output relative to the input near the natural frequency. This has shown the phase shift at the natural frequency to be 180°.

It is also of interest to compare the results from this non-linear model with those from some of the linearized models presented in many of the papers on this topic. A fairly recent linearized model describing virtually the same servomechanism is that of Lambert and Davies [11]. The linearized transfer function derived by them, using the same notation as used in this section, is

$$\frac{x}{y} = \frac{1}{1 + \frac{2A}{k\sqrt{2p}} D + FD^2 + \frac{VM}{\beta k A \sqrt{2p}} D^3}$$

where D = differential operator

k = valve "gain" = C_1 of this section

F = friction and leakage factor

p = supply pressure

Since no friction or leakage has been assumed the damping factor F reduces to zero. Therefore, as the condition for stability with this model is

$$F > \frac{VM}{2A^2\beta}$$

the linearized system is unstable. This points up one of the most desireable aspects of the non-linear analysis presented in this section. The non-linearities tend to stabilize the output, as can be seen in figures 4.4 to 4.9. Even the case of servo B at 100 cps is only quasi unstable. The output amplitude does not grow indefinitely as predicted by the linearized model. Nevertheless it is still of interest to compare the results of the linearized and non-linear models to see if any similarity at all exists. Figures 4.10 and 4.11 show the results of the two models superimposed. The linearized model was solved by the

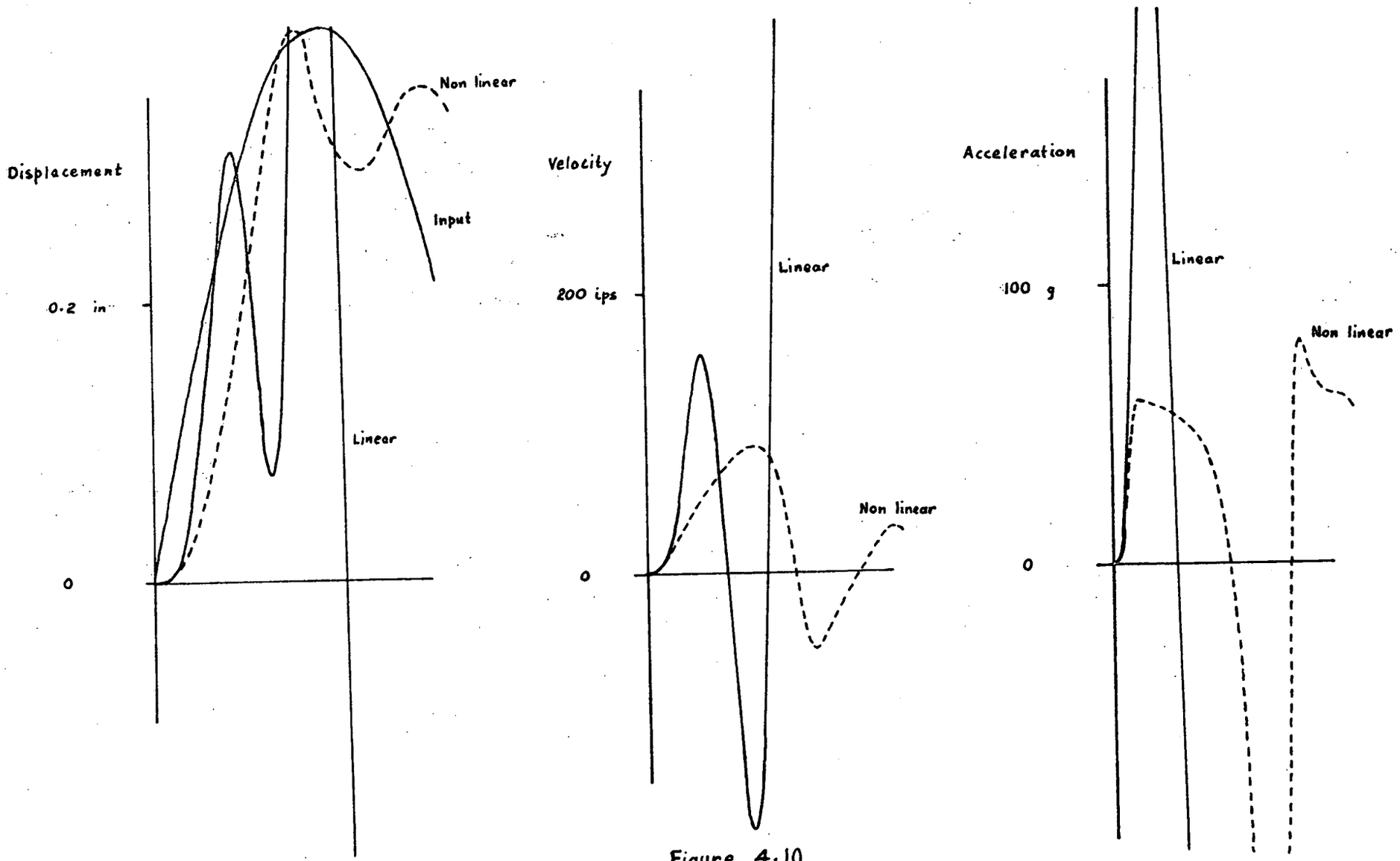

Figure 4.10
Servo A - 28 cps

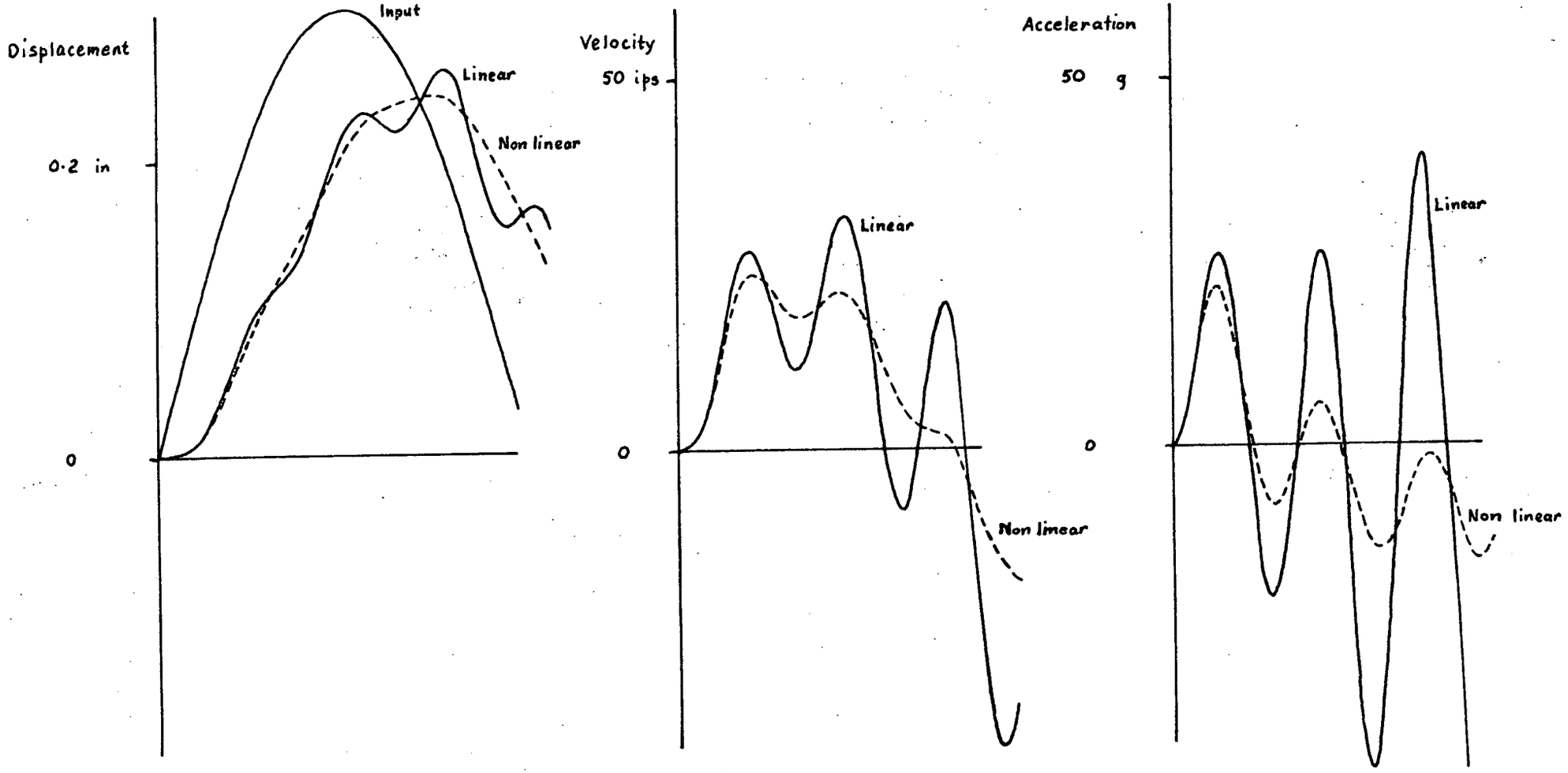

Figure 4.11
Servo B - 20 cps

analytic matrix method of Bellman [13]. In the case of servo A, figure 4.10, the instability in the linearized model grows so rapidly that there is virtually no similarity whatsoever. However with the much lower valve "gain" of servo B the two results show a marked similarity, figure 4.11, although the linearized model of course maintains a steady growth in amplitude.

The instability predicted by the linearized model also suggests one further case that might be considered; that is the case of the input removed and the output given a slight initial displacement. The linearized model predicts an exponentially growing oscillation of the output. The results obtained from the non-linear model of this section are shown in figures 4.12 and 4.13. These results are most encouraging. The oscillation initially grows, and with extreme rapidity, but then stabilizes due to the non-linearity. Further more, results at other valve "gains" show that the final amplitude is almost independent of valve "gain"; it appears mainly dependent on the supply pressure, provided the ram "working" area and mass are taken to be constant. The frequency of oscillation of the output is also close to that predicted by considering the natural oscillation of the ram against the compressible oil volumes, i.e. taking the ram and oil volumes as a mass-spring system. For servo A the frequency observed in figure 4.12 is 178 cps compared with 187 cps predicted by the mass-spring system. The servo B results are "identical" at 148 cps. Presumably the greater non-linearities in the servo A results cause the discrepancy in frequency. Figure 4.14 compares the "free" oscillation results of the linearized and non-linear models for servo B. Once again, although the linearized results grow in amplitude, there is a reasonable similarity.

A word of caution should perhaps be mentioned with respect to the interpretation of the results of the non-linear analysis so far presented. They should not be taken as representing a physical system as yet, as no account has been taken of friction or leakage. These would no doubt considerably alter the output, particularly with regard to the instabilities observed. Furthermore the pressures in many cases fall

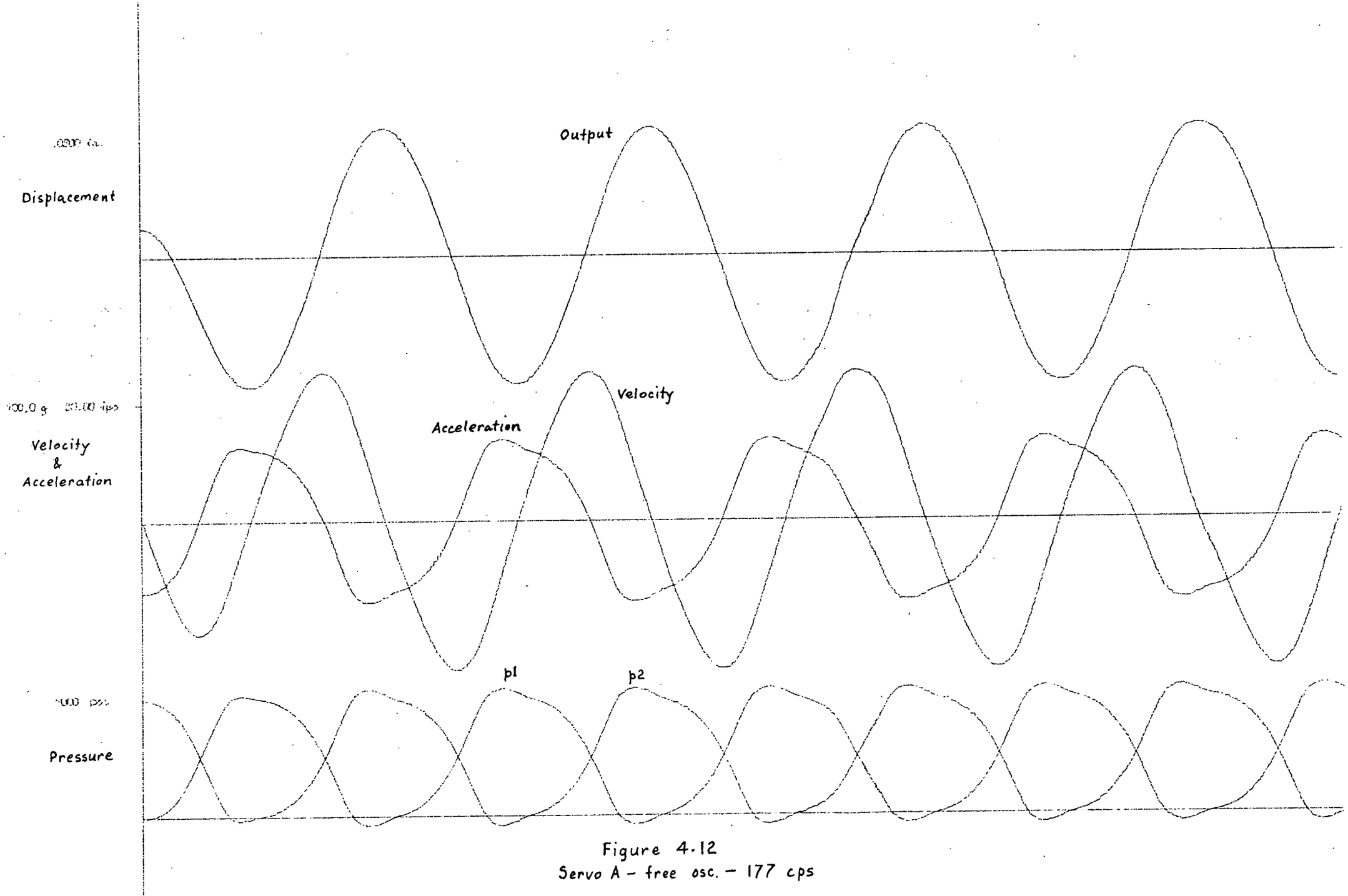

Figure 4.12
Servo A – free osc. – 177 cps

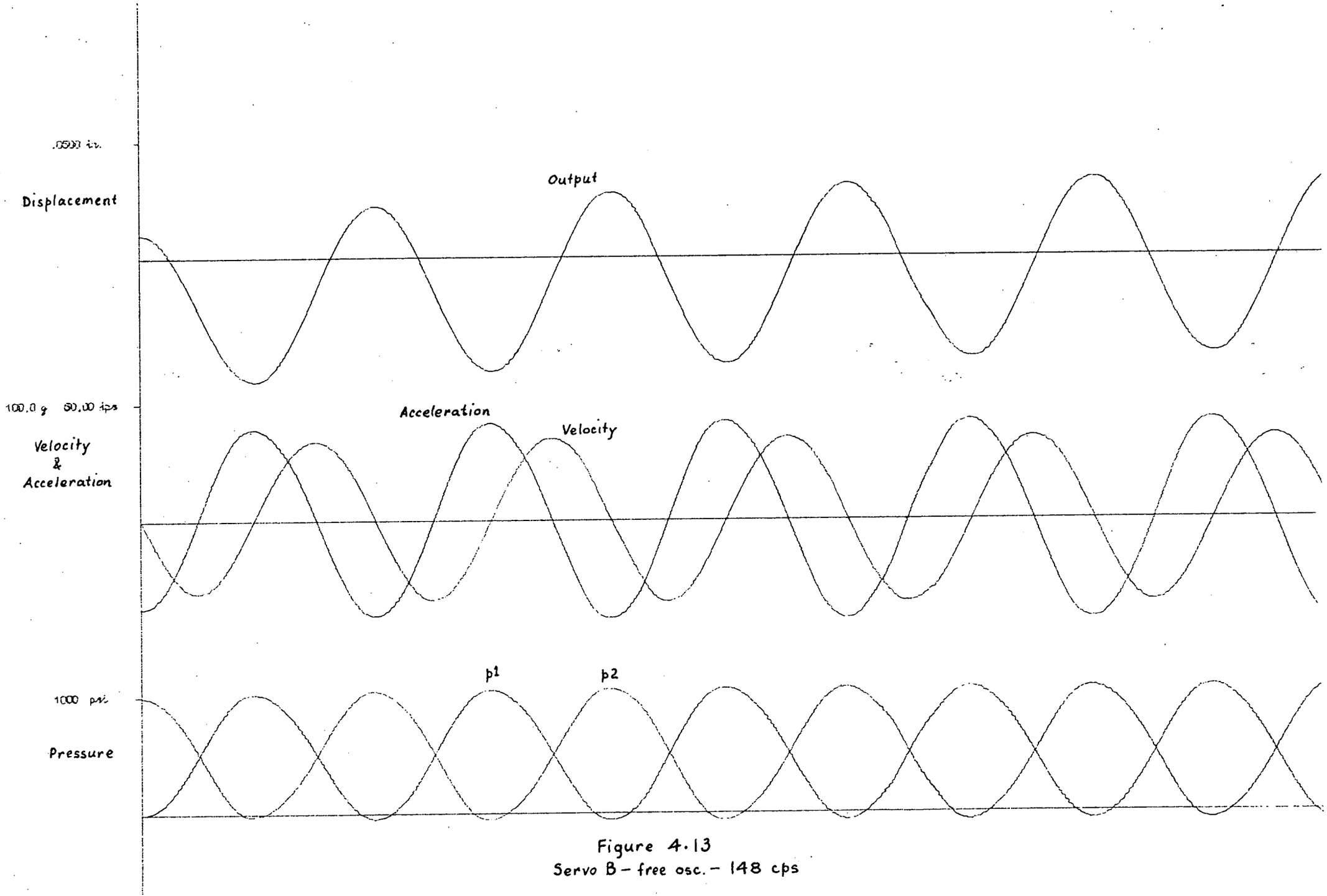

Figure 4.13
Servo B – free osc. – 148 cps

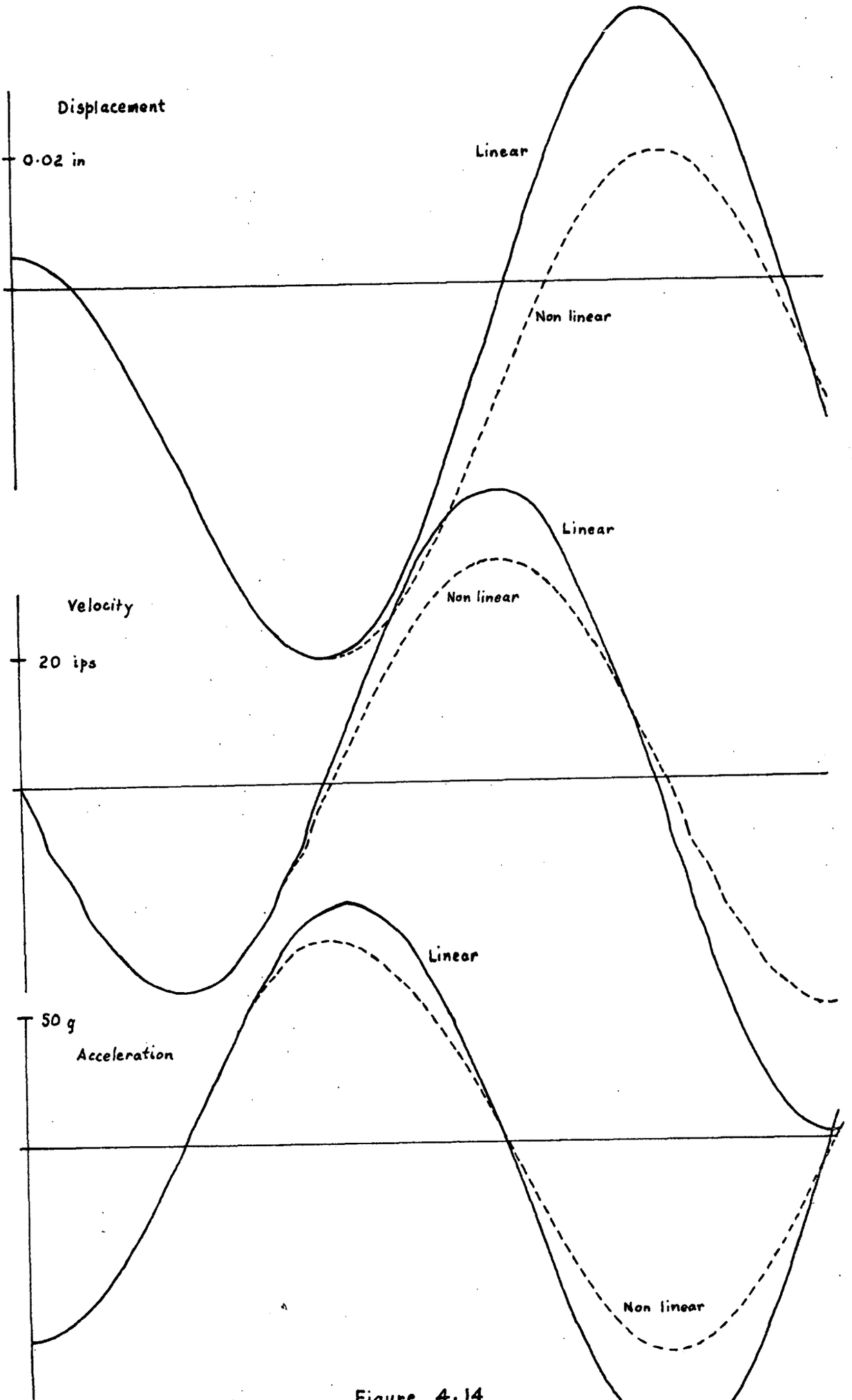

Figure 4.14
Servo B – free osc – 148 cps

considerably below zero and as such, in any physical system, would cause cavitation within the oil. Cavitation has not been included in this model yet. However studies have shown that it should be possible for this to be fairly readily incorporated in the computer program. Of course eventually it would be hoped to modify the system in such a way as to eliminate cavitation, as in general it has many undesirable effects. Nevertheless it would be pleasing, and should be possible, to predict the effect of cavitation should it occur. Flow reaction forces, both static and dynamic [12], could also seriously effect the assumed input and it might be necessary to include this effect at some stage.

Even with all the restrictions and faults that have been mentioned, the results from this non-linear model (equations 4.13 to 4.16) are most encouraging. With the equations modified to remove some of the restrictions the results should prove even more exciting. It is also hoped to "patch up" the modified equations on an analogue computer, provided one of suitable size and complexity becomes readily accessible.

4.2 Models of the Experimental Rig

4.2.1 Solid Slug Model

For a detailed description of the experimental arrangement used to study the dynamic behaviour of the valve, and the reasons for it, the reader is referred to section 4.3. Basically it consisted of the four-way valve connected on the upstream side to the high pressure oil supply. Downstream two long lengths of flexible hose were used to connect one valve port to the measuring tank and the other to the drain line. The hose lengths were made large in order to increase the inertia effects of the oil within them. The valve spool was oscillated with a sinusoidal motion of various amplitudes and frequencies. The arrangement may therefore be considered, during any half-cycle of the spool motion, as equivalent to a variable area orifice mounted between two lengths of hose, as illustrated in figure 4.15. The difference between any two successive half-cycles is that the oil flow is through different downstream hoses in each.

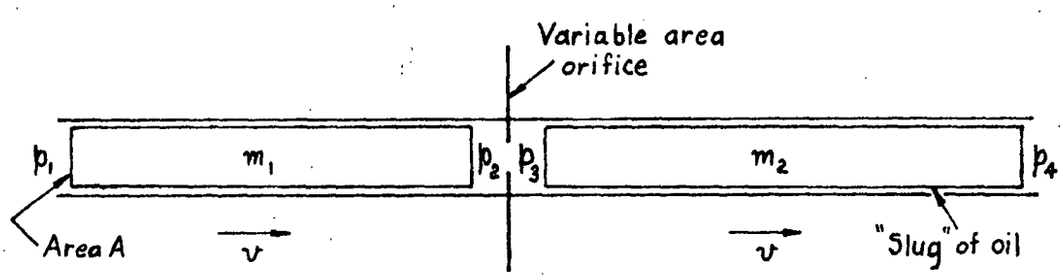

Figure 4.15

The solid slug model

As a first approximation consider the oil within the hoses to behave as a solid slug of appropriate mass, acted on by pressures at each end. This approach is often referred to as a "lumped parameter" model [12], for with it the various parameters describing the oil lines can be considered concentrated at single points and their interactions can be assumed negligible. In this particular case friction effects will be ignored. Of course strictly speaking, if the pressure or flow is too rapidly changed the compressibility of the oil becomes important and the oil column can no longer be considered a solid slug, as the flow rate will not be uniform throughout the line. Under these circumstances the results are likely to be considerably in error and another technique, such as the method of characteristics, section 4.2.2, has to be used.

For the oil column to the left of the valve, figure 4.15, the equation of motion, considering it as a solid slug of mass m_1 and velocity v, is

$$A(p_1 - p_2) = m_1 \frac{dv}{dt}$$

where A = cross-sectional area of the oil column

p_1, p_2 = pressures as shown in figure 4.15

As

$$v = \frac{Q}{A}$$

where Q = oil flow rate,

$$p_1 - p_2 = \frac{m_1}{A^2} \frac{dQ}{dt} \tag{4.17}$$

Similarly for the right hand oil column of mass m_2

$$p_3 - p_4 = \frac{m_2}{A^2} \frac{dQ}{dt} \tag{4.18}$$

The orifice flow equation, allowing for the slight underlap of the valve (see section 3.3.1), is equation 3.4, i.e.

$$Q = C_1 (x + x_o) \sqrt{p_2 - p_3} \tag{4.19}$$

where C_1 = constant = $C_d \, k \, w \sqrt{\frac{2}{\rho}}$ (see section 3.3.1)

x = valve displacement from centre

x_o = "equivalent" valve underlap (see section 3.3.1)

No allowance has been made in equation 4.19 for reverse flows as only positive flows are considered, as will be explained presently. Eliminating p_2 and p_3 from these equations (4.17 to 4.19), and rearranging gives

$$\frac{dQ}{dt} = \frac{A^2}{(m_1 + m_2)} \left(p_1 - \frac{Q^2}{C_1^2 (x + x_o)^2} \right) \tag{4.20}$$

where p_4 has been set zero

This is basically the same equation as that derived in section 4.1.1 for the incompressible fluid model of the vibration tester, i.e. equation 4.5. However in this case only the transient flow occuring during one half cycle of the valve spool motion is considered. The justification for this downstream of the valve is as follows. During one complete valve spool cycle each downstream hose only carries the oil flow for one half cycle. If it is assumed that during the "dead" half cycle any disturbance in the hose dies away, then the valve opens at the commencement of the next half cycle with a relatively still oil column downstream. This is equivalent to the transient response that

results from the valve moving through only one half cycle. Unfortunately this assumption is not justified upstream of the valve as only one hose carries the oil flow during both half cycles. If the valve were "ideal", i.e. had no underlap it could be argued that, because of the implied assumption of incompressibility the oil column must come to rest as the valve spool passed through its closed position. However the valve is not "ideal" and consequently the oil column can have large decelerations and hence pressures as the valve passes through centre. Nevertheless this effect has been neglected as the upstream hose was considerably shorter than the downstream hoses, and in any case, the model was expected to be approximate at best.

Once again a second-order Runge-Kutta procedure (see appendix 2) was used in attempting to solve equation 5.6. However even with the "softening" of the system afforded by the valve underlap the difference equations still proved unstable at small openings and low frequencies. That the instability should be so dependent on frequency is perhaps not obvious. It arises mainly because of the manner in which the time step is chosen. The valve spool cycle is divided into a given number of steps per cycle and this then sets the time step size. Consequently if the number of steps per cycle is kept constant with decreasing frequency the time step size increases and instability might be expected at the lower frequencies. On the other hand this suggests that provided the time step is held constant as the frequency is decreased the equations might remain stable, for they are certainly stable at the higher frequencies. Unfortunately the problem is found to be somewhat more subtle than this, for, although the time step is constant the increments in the spool displacement at each step decrease at the lower frequences and they can become quite small compared with the "effective" underlap. Consequently the difference equations do not remain similar as the frequency is decreased, even though the time step is held constant. In fact it has been observed that, although the high frequency results are stable, the low frequency results with the same time step, are often violently unstable. Even

decreasing the time step further does not always help. For instance at 5 cps the solution was still found to be quite unstable with as many as 5000 steps per cycle. Furthermore, even if the solution is stabilized by decreasing the step size to this extent, with so large a number of steps the round-off errors can become quite appreciable. This could lead to the type of instability discussed in section 4.1.1, as the valve closes. The computation time may also become excessive with such large numbers of steps per cycle.

In many respects the instability observed in this case appears very similar to that encountered in the numerical analysis of many chemical processes, e.g. the analysis of distillation columns. Rosenbrock and Storey in their book "Computational Techniques for Chemical Engineers" (14) give quite a reasonable account of how numerical instability can arise. They investigate by way of examples the stability of the difference equations used to replace several linear differential equations. In general the investigation of non-linear differential equations is impractical because of analytical difficulties. It is, in fact, not intended here to delve too deeply into numerical stability; however some of the observations of the authors just mentioned are of interest. Firstly, instability of the difference equations should be distinguished from instability of the differential equations. There is no reason to suspect that the differential equations are unstable just because the difference equations are. In fact the reverse is often true, i.e. the very high stability of many differential equations tend to make the difference equations, used to replace them, unstable. Also the restrictions on the step size that can be used in the difference equations in order to give stability are often very much more severe than would be expected if the truncation error were the only criterion on step size. That is an estimate of the step size based on a maximum allowable truncation error may have very little bearing on the step size actually required to ensure stability. Furthermore, the problems of stability are shared by most explicit methods of solution; if one explicit method shows

instability then in general other explicit methods will also show similar instability. By explicit processes is meant those processes which compute the value of the dependent variable at some time step directly in terms of its values at preceeding time steps. Most well-known, standard methods are of this type, e.g. Euler's method and the Runge-Kutta techniques. Finally if results are not to be output at each time step then the output should be made at odd time steps. The reason for this is that the unstable results tend to oscillate about the "true" solution at each successive time step. Hence if even time steps are chosen for the output it is possible to obtain quite "smooth" results even though violent instability may be present. It is interesting to note that the effects mentioned have been observed in this case. In fact with regard to stability it has been found that the fourth-order Runge-Kutta process suffers just as badly from instability as the second-order process, even though in other respects, e.g. truncation error, it is far superior.

Many techniques were tried in an attempt to overcome the problem of instability. Most involved placing restrictions on the maximum size the flow increment could take at any time step while the valve displacement was small. Some transformation techniques were also examined. None of these proved very satisfactory. However one technique did at least allow the solution to progress through the unstable region corresponding to the valve just opening. Once the valve opened far enough the solution usually stabilized. This technique relied on the fact that there is a maximum possible acceleration of the oil slugs. This maximum occurs when the oil slugs have no inertia. Under these conditions the flow is completely determined by the valve motion, which is known to be sinusoidal. Consequently, as any slug with inertia must have this as a maximum acceleration limit, the maximum possible pressure difference across the slug, during accelerating conditions, can be determined. In fact the upper limit on this was increased a further 50% in the computer program to allow the numerical process slightly more freedom. This resulted in the flow being slightly underestimated within the unstable region.

Figures 4.16 to 4.20 show the flow and pressures just upstream and downstream of the valve that resulted from this model at various frequencies. The flow corresponding to an "inertialess" case is also plotted for comparison. The maximum flow decreases at the higher frequencies because of the assumed variation in valve spool displacement amplitude. This was constant at 0.1 in. up to 54.2 cps after which it decreased due to the acceleration amplitude being maintained constant at 30 g. The values of the parameters used in the equations are given in appendix 3. The unstable region in the 5 cps results, figure 4.16, is clearly indicated by the small "flats" in the pressure plots caused by the restriction discussed above. It is also interesting to note at this frequency that the solution has become unstable again as the valve closes, although this has been partially overcome by not allowing negative flows. The pressures downstream of the valve also become very large in a negative, i.e. suction, sense as the valve closes. This is to be expected for it is the only means of decelerating the downstream slug in the absence of friction. Of course, in reality these pressures could not be achieved as the oil would cavitate, unless the system were operated under some large positive pressure throughout. It is possible in many models to allow for cavitation by assuming a cavity of constant pressure forms. However in this case cavitation has not been included as there are several problems associated with the collapse of the cavity under the assumption of incompressibility. Fortunately the likely error introduced into the average flow for the half cycle by not including cavitation is only a few percent of the average flow calculated from this model. Also the inclusion of friction within the hoses would no doubt improve the situation. By assuming a leakage flow during the "dead" half cycle of the valve motion the average flow over a complete cycle can be computed. These average flow results at different frequencies are presented and discussed with the experimental results in section 4.3.

One modification to this model which has proved reasonably successful is a quasi linearization of the orifice flow equation. It is quasi

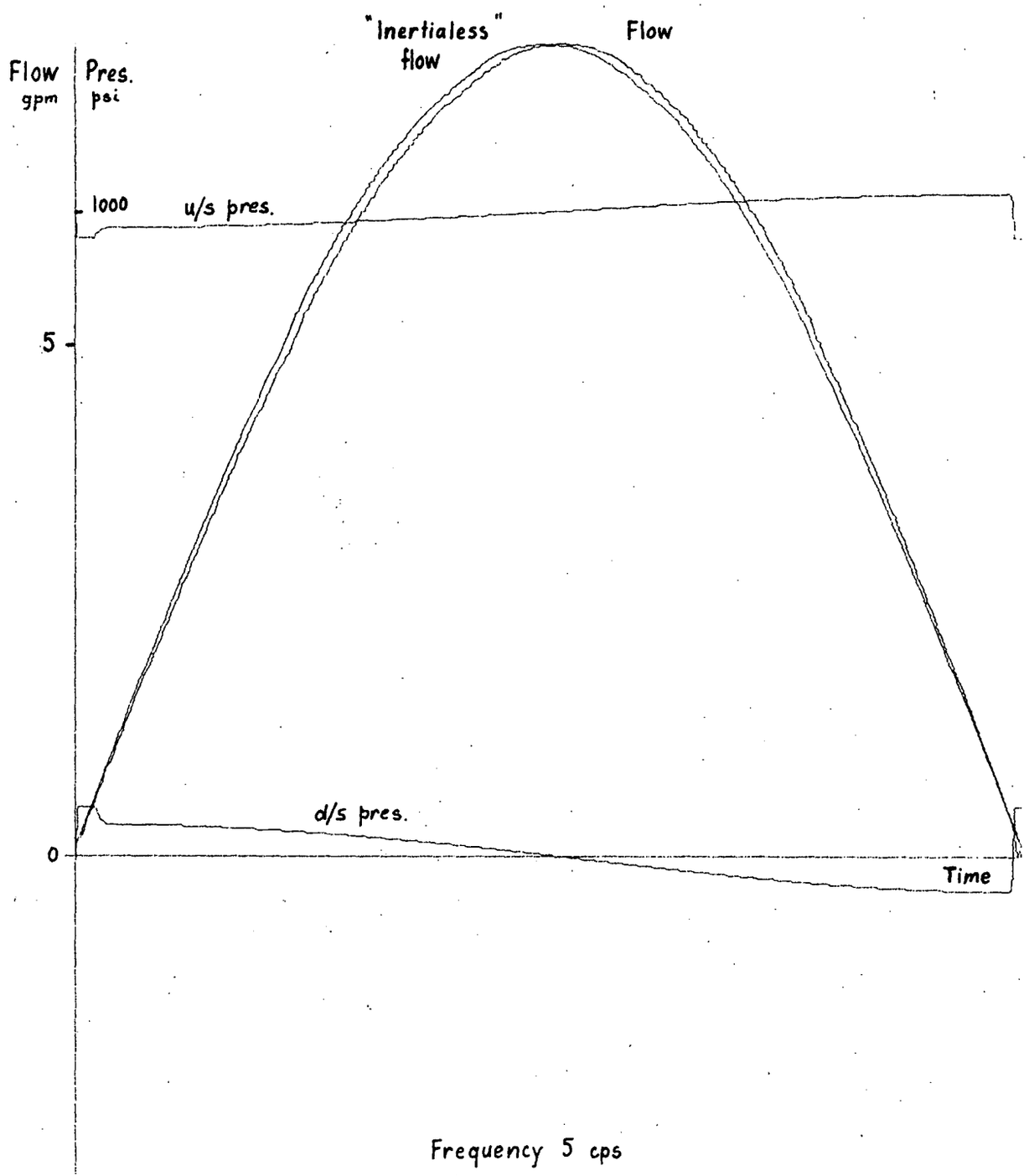

Frequency 5 cps

Figure 4.16

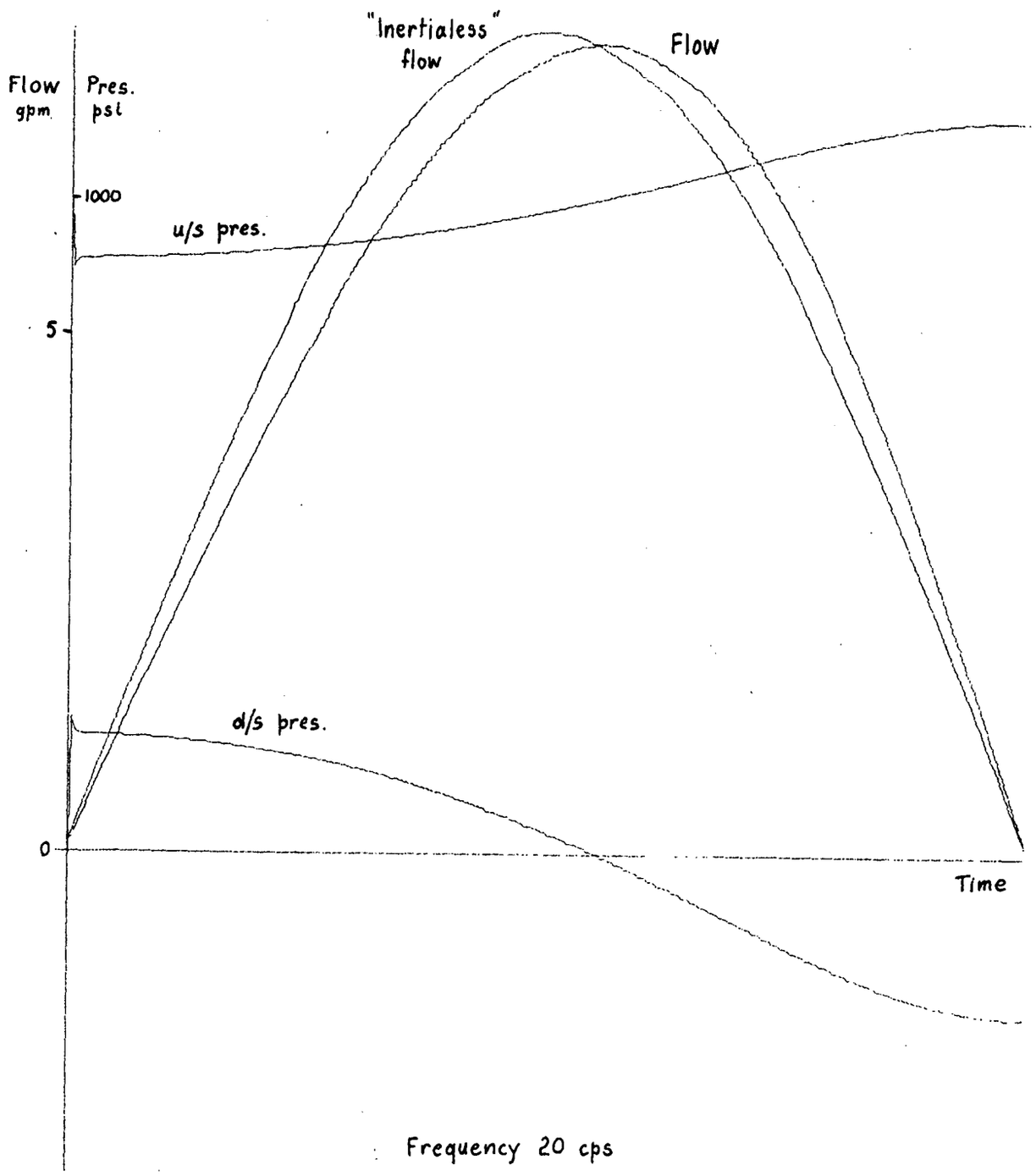

Frequency 20 cps

Figure 4.17

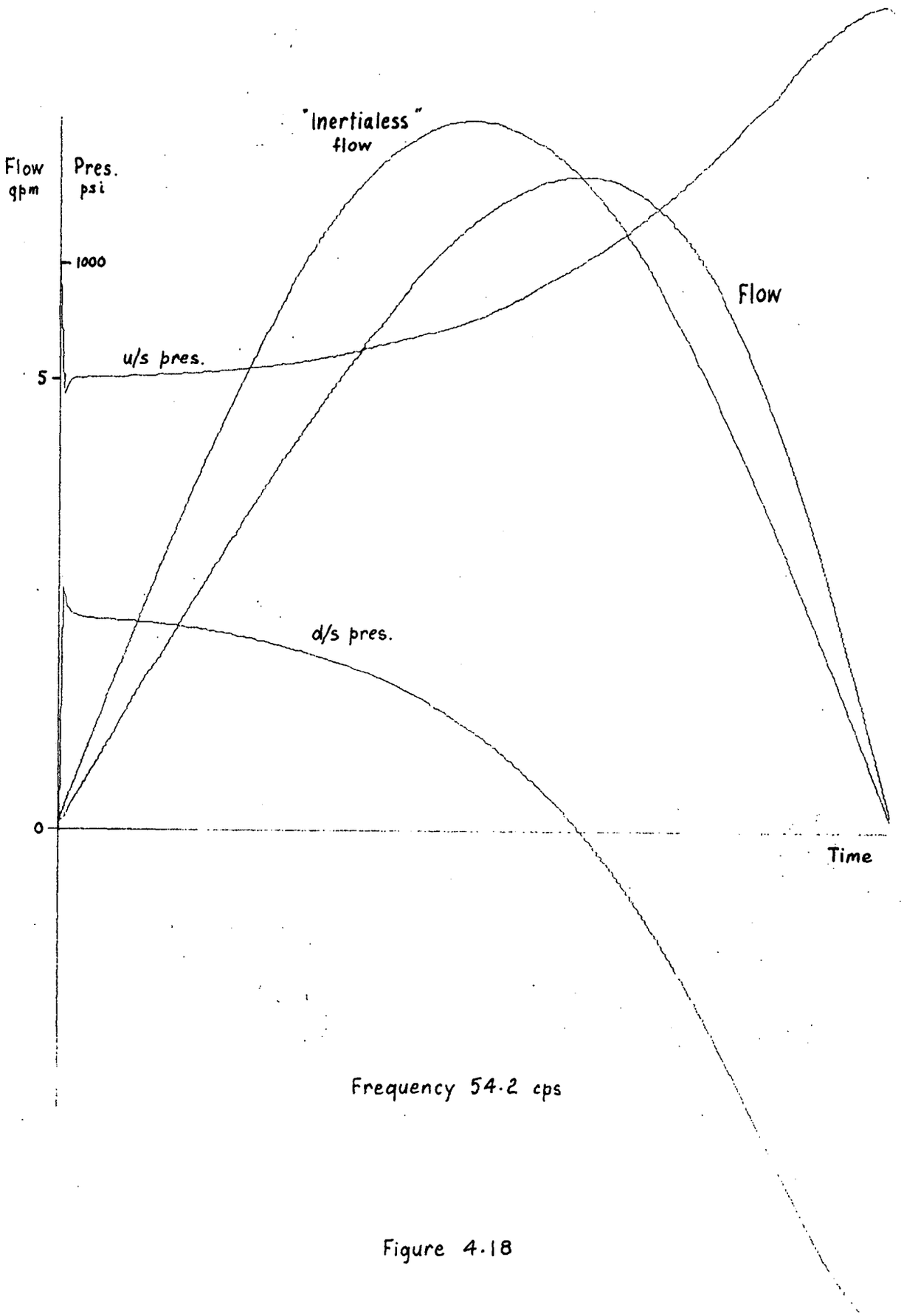

Frequency 54.2 cps

Figure 4.18

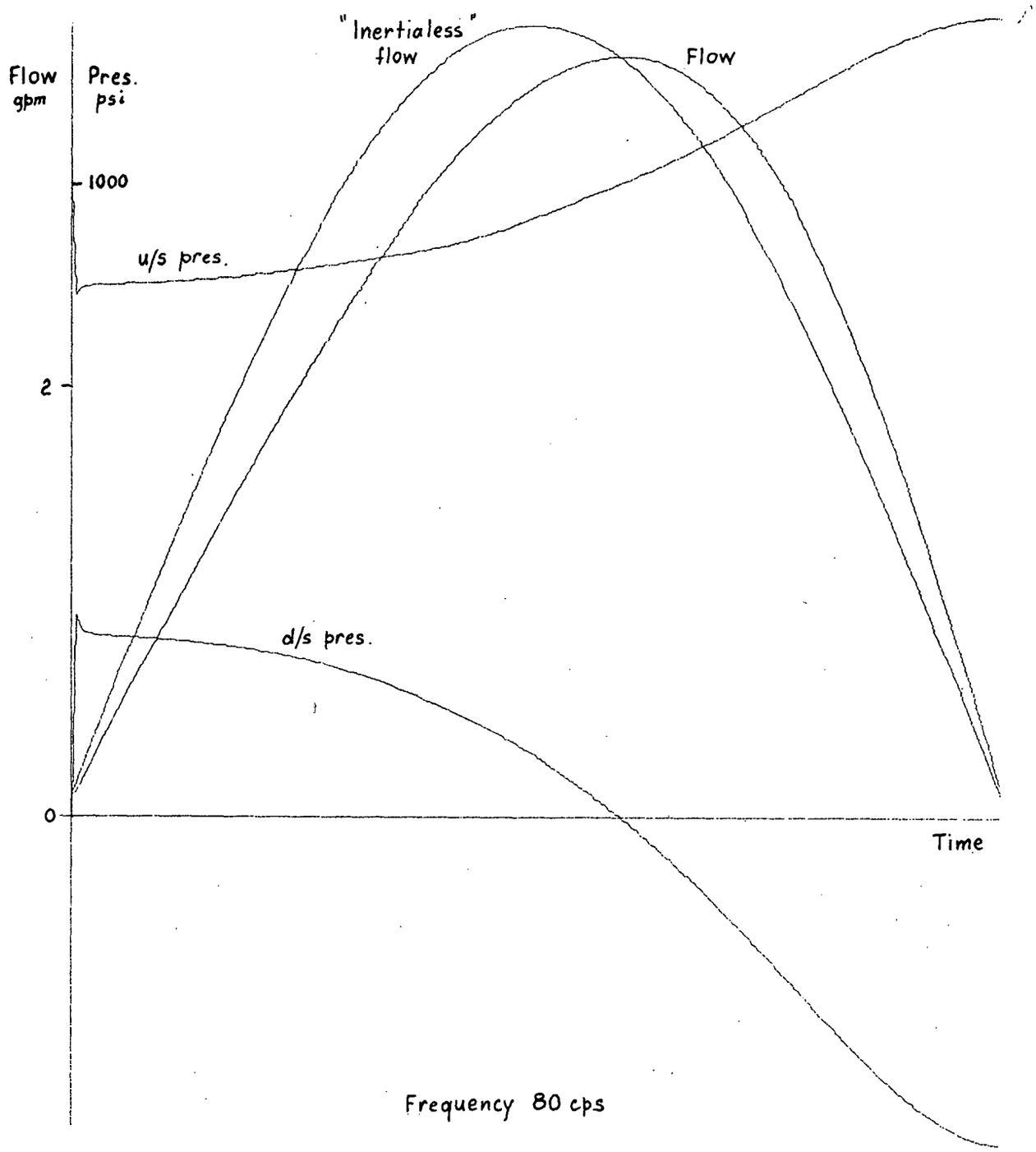
"Inertialess" flow
Flow
Flow gpm
Pres. psi
1000
u/s pres.
2
d/s pres.
0
Time
Frequency 80 cps

Figure 4.19

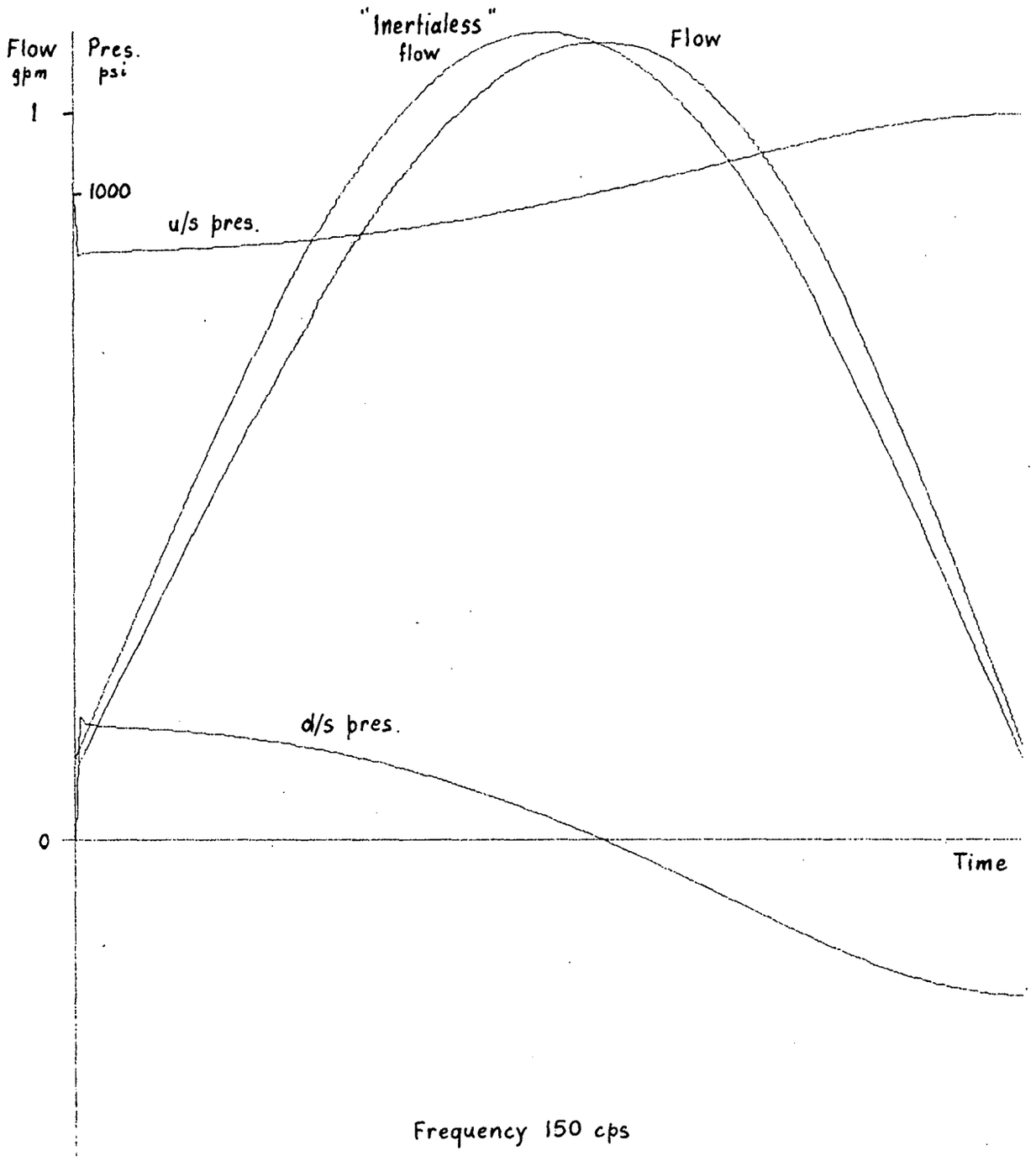

Frequency 150 cps

Figure 4.20

linear in that a linear approximation is made at each time step, whereas "true" linearization is generally associated with only one linear approximation made to cover the complete solution range. In this modified model the orifice flow equation (4.19) is approximated at each time step by the tangent to the pressure-flow curve through the then current pressure-flow point. Solving the resultant equation with the other equations for the solid slug model yields a differential equation which can be integrated analytically. The solution of this gives the approximate flow and pressure at the end of the time step. The process is then repeated for successive time steps. An advantage of the modified model is that it has shown no tendency to instability, and the results obtained from it are almost identical with those from the non-linear model. The resultant flow is certainly very close. On the other hand the pressure results, although corresponding over most of the half cycle, have a "smoother" rise and fall at the start of the cycle and a tendency to return to their static values towards the end of the cycle. The correspondence improves as the step size is reduced. However as the steps become smaller the improvement with each successive reduction in step size becomes less, and it is doubtful if the results will eventually correspond, unless perhaps an excessive number of steps per cycle is used. Furthermore the pressure results obtained by the method of characteristics (section 4.2.2), which should be quite realistic, although differing both in absolute magnitude and in other minor ways from these results, show more similarity to the non-linear rather than modified, model results. This throws some doubt onto the reliability of the linearized model, with regard to the pressure response anyway, if a reasonable step size is used.

For this type of problem in general, i.e. one in which "pipe flow" effects are significant, there is no doubt that the method of characteristics is probably one of the easiest, most realistic and reliable techniques available.

4.2.2 Method of Characteristics

In this method it is first necessary to derive the partial differential equations of motion and continuity for unsteady flow. The partial differential equations derived are then converted into four ordinary differential equations which are readily solved by finite difference techniques. It should be mentioned at this stage that it is not intended the following should be a completely rigorous account of the method of characteristics. References [15] and [16] have been included in the list of references for those requiring more information.

Equation of Motion

Consider the forces acting on a small element of fluid, length δx, within a conduit as shown in figure 4.2.1. In this analysis gravitational and friction effects will be neglected. The omission of

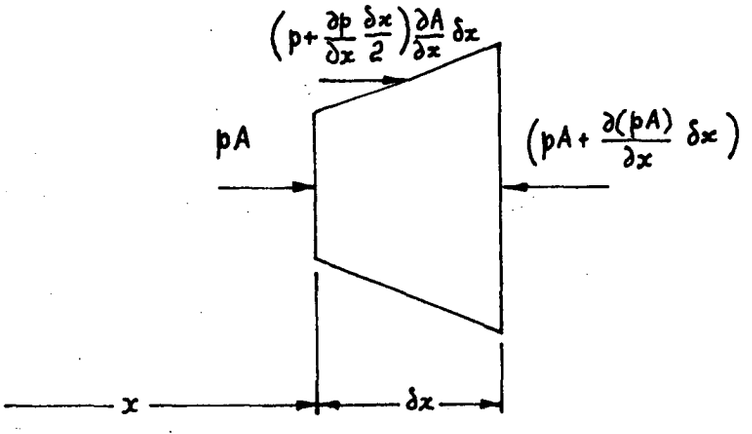

Figure 4.21

Forces on element of fluid in a conduit

gravitational effects is quite justified as the pressures caused by elevation changes are extremely small compared with the system pressures. However the omission of friction is not readily justified. In fact one of the great advantages of the method of characteristics is the relative ease with which friction effects can be accommodated. Nevertheless for comparison with previous models it is ignored in this case. Hence the

only resulting forces on the element are pressure forces and the equation of motion becomes

$$\left(p + \frac{\partial p}{\partial x}\frac{\delta x}{2}\right)\frac{\partial A}{\partial x}\,\delta x - \frac{\partial (pA)}{\partial x}\,\delta x = \rho\left(A + \frac{\partial A}{\partial x}\frac{\delta x}{2}\right)\delta x\,\frac{dv}{dt}$$

where p = fluid pressure

v = velocity of element

ρ = density of the fluid

Ignoring higher powers of δx and expanding dv/dt, observing that

$$\frac{dx}{dt} = v$$

finally gives the equation of motion

$$\frac{1}{\rho}\frac{\partial p}{\partial x} + \frac{\partial v}{\partial t} + v\frac{\partial v}{\partial x} = 0 \qquad (4.21)$$

Continuity Equation

Figure 4.22 shows a small element of the conduit with fluid flowing through it. By the conservation of mass the net inflow mass of fluid

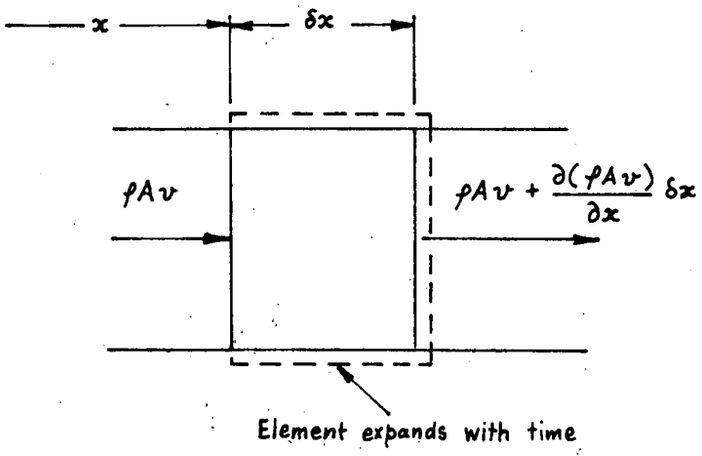

Figure 4.22

Notation for continuity equation

must equal the time rate of increase of mass within the volume, i.e.

$$\frac{\partial}{\partial x}(\rho A v)\,\delta x = -\frac{\partial}{\partial t}(\rho A\,\delta x)$$

where δx = length of conduit element

A = cross-sectional area

v = fluid velocity

It should be noted that δx is also a variable as the conduit may elongate. Assuming density changes are small compared with the density proper and expanding the derivatives, gives

$$\frac{1}{\rho}\left(\frac{\partial \rho}{\partial t} + v\frac{\partial \rho}{\partial x}\right) + \frac{1}{A}\left(\frac{\partial A}{\partial t} + v\frac{\partial A}{\partial x}\right) + \frac{1}{\delta x}\frac{\partial(\delta x)}{\partial t} + \frac{\partial v}{\partial x} = 0 \qquad (4.22)$$

As the total derivates $d\rho/dt$ and dA/dt following the motion of the fluid, i.e. with $dx/dt = v$, are

$$\frac{d\rho}{dt} = \frac{\partial \rho}{\partial t} + v\frac{\partial \rho}{\partial x}$$

and

$$\frac{dA}{dt} = \frac{\partial A}{\partial t} + v\frac{\partial A}{\partial x}$$

and δx is a function of time only, equation 4.22 reduces to

$$\frac{1}{\rho}\frac{d\rho}{dt} + \frac{1}{A}\frac{dA}{dt} + \frac{1}{\delta x}\frac{d(\delta x)}{dt} + \frac{\partial v}{\partial x} = 0 \qquad (4.23)$$

The equation in this form is not of much use. However by recognising that the first three terms represent compressibility and conduit expansion it is possible to replace them by pressure terms. The equation for the bulk modulus of the fluid (see section 4.1.2) may be written in terms of the densities as

$$\beta = \frac{\delta p}{\delta \rho / \rho}$$

where δp and $\delta \rho$ are small changes in the pressure and density. Differentiating and rearranging gives

$$\frac{1}{\rho}\frac{d\rho}{dt} = \frac{1}{\beta}\frac{dp}{dt} \qquad (4.24)$$

For the second and third terms of equation 4.23, it can be shown that for thin walled, elastic conduits the strain is proportional to the pressure, and hence

$$\frac{1}{A}\frac{dA}{dt} = k_1\frac{dp}{dt} \qquad (4.25)$$

and

$$\frac{1}{\delta x}\frac{d(\delta x)}{dt} = k_2 \frac{dp}{dt} \tag{4.26}$$

where k_1 and k_2 are constants.

In fact the hoses used in this experiment were neither thin walled nor elastic. However the assumption will be made as an approximation to the actual behaviour. Therefore substituting equations 4.24 and 4.26 into equation 4.23 gives

$$\frac{1}{\beta}\left[1+\beta(k_1+k_2)\right]\frac{dp}{dt} + \frac{\partial v}{\partial x} = 0$$

Or by defining an effective bulk modulus, β_e, as

$$\beta_e = \frac{\beta}{1+\beta(k_1+k_2)}$$

and expanding dp/dt following the motion of the fluid finally yields for the continuity equation

$$\frac{1}{\beta_e}\frac{\partial p}{\partial t} + \frac{v}{\beta_e}\frac{\partial p}{\partial x} + \frac{\partial v}{\partial x} = 0 \tag{4.27}$$

Small Wave Velocity

Before proceeding with the method of characteristics it is of interest to derive the "small wave" velocity within the conduit. This velocity is used in the method to simplify the equations and their visualization. If only small perturbations and velocities are considered the equations of motion and continuity (4.21 and 4.27) may be reduced to

$$\frac{1}{\rho}\frac{\partial p}{\partial x} + \frac{\partial v}{\partial t} = 0 \tag{4.28}$$

and

$$\frac{1}{\beta_e}\frac{\partial p}{\partial t} + \frac{\partial v}{\partial x} = 0 \tag{4.29}$$

Taking the partial derivatives of equations 4.28 and 4.29 with respect to x and t respectively, and eliminating v from the resulting equations, gives

$$\frac{\partial^2 p}{\partial t^2} = \frac{\beta_e}{\rho}\frac{\partial^2 p}{\partial x^2} \tag{4.30}$$

Equation 4.30 is known as the wave equation and the general solution for the pressure may be shown to be

$$p - p_o = F\left(t + \frac{x}{a}\right) + f\left(t - \frac{x}{a}\right)$$

$$\text{where} \quad a = \sqrt{\frac{\beta_e}{\rho}} \tag{4.31}$$

The functions $F(t + \frac{x}{a})$ and $f(t - \frac{x}{a})$ are chosen so as to satisfy the conditions at the end of the conduit. They may be thought of as waves moving in the -x and +x directions with speed a, defined by equation 4.31. That is disturbances are propogated through the fluid with speed a.

We will now return to the method of characteristics. The equations of motion and continuity may be combined with an arbitrary and, as yet, unknown multiplier λ, i.e.,

$$\frac{1}{\rho}\frac{\partial p}{\partial x} + \frac{\partial v}{\partial t} + v\frac{\partial v}{\partial x} + \lambda\left(\frac{1}{\beta_e}\frac{\partial p}{\partial t} + \frac{v}{\beta_e}\frac{\partial p}{\partial x} + \frac{\partial v}{\partial x}\right) = 0$$

Rearranging this and grouping terms gives

$$\frac{\lambda}{\beta_e}\left[\frac{\partial p}{\partial t} + \frac{\partial p}{\partial x}\left(v + \frac{\beta_e}{\lambda\rho}\right)\right] + \left[\frac{\partial v}{\partial t} + \frac{\partial v}{\partial x}\left(v + \lambda\right)\right] = 0 \tag{4.32}$$

By inspection, equation 4.32 is almost in ordinary differential form, for

$$\frac{dp}{dt} = \frac{\partial p}{\partial t} + \frac{\partial p}{\partial x}\frac{dx}{dt}$$

and

$$\frac{dv}{dt} = \frac{\partial v}{\partial t} + \frac{\partial v}{\partial x}\frac{dx}{dt}$$

Therefore, provided it is possible to make

$$\frac{dx}{dt} = v + \frac{\beta_e}{\lambda\rho} = v + \lambda \tag{4.33}$$

equation 4.32 becomes the ordinary differential equation

$$\frac{\lambda}{\beta_e}\frac{dp}{dt} + \frac{dv}{dt} = 0 \qquad (4.34)$$

Solving equation 4.33, and substituting from equation 4.31, gives the two possible solutions for λ as

$$\lambda = \pm a$$

Therefore the condition that must be satisfied by dx/dt for the ordinary differential equation 4.34 to be valid, is

$$\frac{dx}{dt} = v \pm a \qquad (4.35)$$

Often the fluid velocity, v, is very much smaller than the wave speed, a, and equation 4.35 may be written

$$\frac{dx}{dt} = \pm a \qquad (4.36)$$

This simplification is justified in this case, as the maximum oil velocity within the hoses is less than 1% of the wave velocity.

The significance of equations 4.34 and 4.36 is best illustrated by reference to the x-t plane (see figure 4.23).

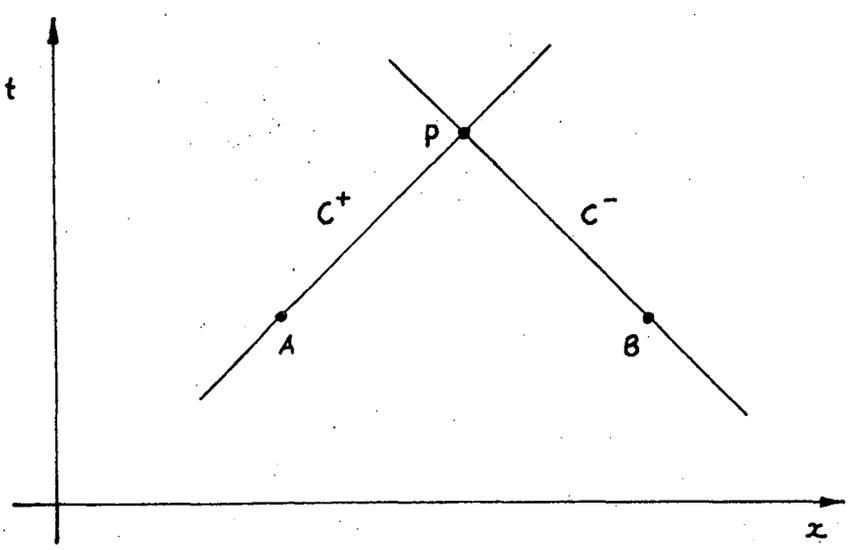

Figure 4.23

Characteristics in the x-t plane

Equation 4.36 describes straight lines in the x-t plane. There is no restriction on where these lines may be situated. The only restriction imposed on them is they must have a slope of $\pm$ 1/a. These lines are called "characteristic" lines, and are identified as C^+ and C^- depending on which slope they have. Along them the ordinary differential equations (4.34 with the appropriate value of λ, i.e. +a on C^+ or -a on C^-) define the relationship between the pressure and velocity. Consequently, provided the pressures and velocities are known at two points, A and B, the pressure and velocity at another point P, the intersection of the "characteristics" through A and B, may be determined by solving the resultant equations along C^+ and C^-. This is normally done using finite difference approximations to the equations (4.34 and 4.36). Inserting the appropriate values of λ in equation 4.34 and substituting from equation 4.31, these become:

along C^+

$$\delta x = + a\, \delta t \qquad (4.37)$$

$$\delta p = - \rho a\, \delta v \qquad (4.38)$$

and along C^-

$$\delta x = - a\, \delta t \qquad (4.39)$$

$$\delta p = + \rho a\, \delta v \qquad (4.40)$$

By setting up an appropriate grid of "characteristics" in the x-t plane, the pressure and velocity solutions, consistent with given initial and boundary conditions, may be followed as they progress up the intersections on the grid of "characteristics". Often the variables in the difference equations (4.37 to 4.40) are non-dimensionalized by dividing them by appropriate quantities. However, in this case it has been found convenient to use the dimensional quantities, with the exception of the pressure. This has been converted to a pseudo pressure p^* by dividing by ρa, i.e.

$$p^* = \frac{p}{\rho a}$$

The difference equations then simplify to:

along C^+

$$\delta x = + a\, \delta t \tag{4.41}$$

$$\delta p^* = - \delta v \tag{4.42}$$

and

along C^-

$$\delta x = - a\, \delta t \tag{4.43}$$

$$\delta p^* = + \delta v \tag{4.44}$$

It is now possible to analyse the problem formulated in the last section, i.e. a valve situated between two lengths of hose. This may be visualized in the x-t plane as in figure 4.24. For convenience the cross-sectional areas and wave velocities in each hose are assumed the same. It will be noted that the time

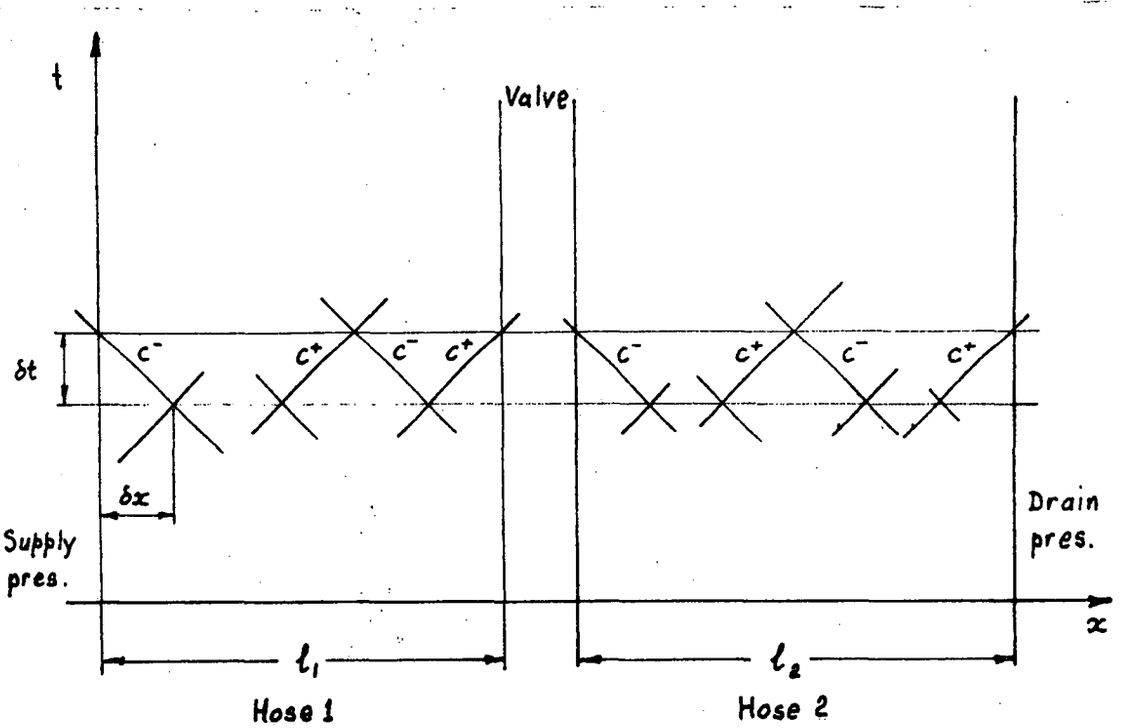

Figure 4.24

Experimental model visualized in the x-t plane

increments have also been made constant throughout the system. This is known as the method of specified time intervals. It allows a very orderly solution of the equations in a digital computer. However as there are two hoses in this problem and each has to be divided into an integral number of divisions, this method leads to the rather awkward

condition

$$t = \frac{l_1}{na} = \frac{l_2}{ma} \qquad (4.45)$$

where n and m are integers

This equation is difficult to satisfy exactly with reasonable values for n and m. This has been partially overcome by first choosing reasonable values for n and m, and then allowing the second hose length to be slightly in error in order to satisfy equation 4.45. The appropriate difference equations for the various hose sections and boundaries are derived below.

Hose Section Equations

Figure 4.25 shows a section of the "characteristics" grid in the x-t plane away from the boudaries. The "pressures" and velocities at

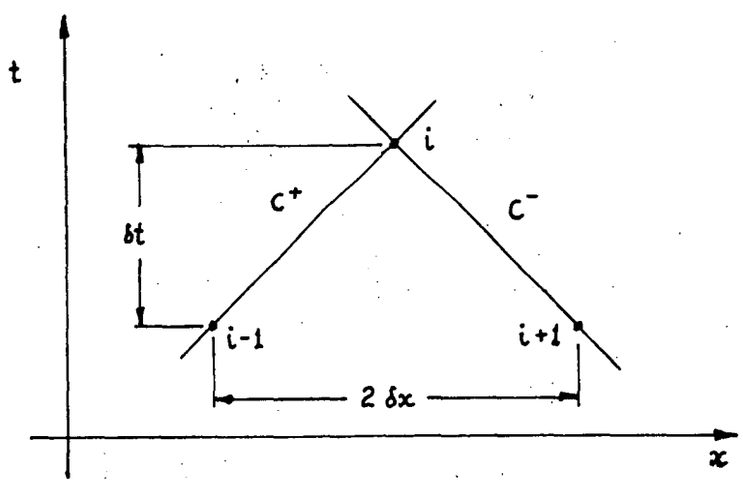

Figure 4.25

"Characteristics" in the x-t plane

away from boundaries

the points i-1 and i+1 are assumed known and are p^*_{i-1}, v_{i-1} and p^*_{i+1}, v_{i+1}. The unknown "pressure" and velocity at the point i, the intersection of the characteristics through i-1 and i+1, is p^*_i and v_i. Applying equations 4.42 and 4.44 along C^+ and C^- respectively gives

$$p^*_i - p^*_{i-1} = -(v_i - v_{i-1})$$

and

$$p^*_i - p^*_{i+1} = v_i - v_{i+1}$$

Solving these two equations for the two unknowns p_i^* and v_i gives

$$v_i = 0.5(p^*_{i-1} - p^*_{i+1}) + 0.5(v_{i-1} + v_{i+1}) \qquad (4.46)$$

and

$$p_i^* = p^*_{i-1} + v_{i-1} - v_i \qquad (4.47)$$

Left and Right Boundary Conditions

Figure 4.26 shows the appropriate sections of the "characteristics" grid. Consider the left boundary first. At the boundary the "pressure"

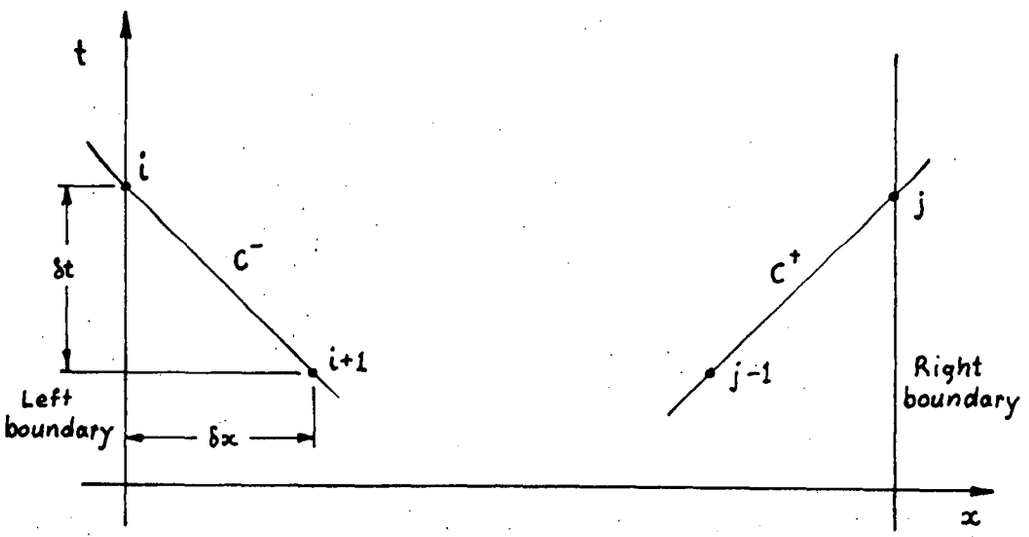

Figure 4.26

"Characteristics" grid

at the left and right boundaries

must be the supply "pressure". As before p^*_{i+1} and v_{i+1}, are the "pressure" and velocity at point i+1. Applying equation 4.44 along C^- through i+1 gives

$$v_i = p^*_s - p^*_{i+1} + v_{i+1} \qquad (4.48)$$

as

$$p_i^* = p_s^* \qquad (4.49)$$

where p_s^* is the supply "pressure"

Similarly for the right hand boundary, applying equation 4.22 along C^+ through j-1 gives

$$v_j = p_{j-1} - p^*_D + v_{j-1} \qquad (4.50)$$

as
$$p_j^* = p_D^* \tag{4.51}$$

where p_D^* is the drain "pressure".

Valve Boundary Conditions

For the valve the orifice equation, including the effective underlap, may be written in terms of pseudo pressures and hose velocities as

$$v = B\sqrt{p^*} \tag{4.52}$$

where $B = \frac{C_1(x + x_o)}{A}\sqrt{\rho a}$ = function of time

and A = hose cross-sectional area

Figure 4.27 shows the "characteristics" grid around the valve boundaries. As previously it is assumed the "pressures" and velocities are known at

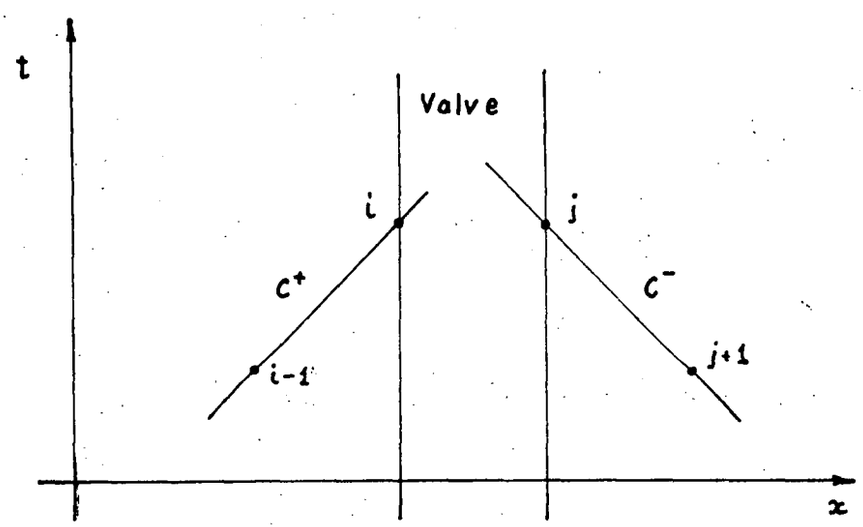

Figure 4.27
"Characteristics" at valve boundaries

the points i-1 and j+1. As there must be continuity of flow through the valve by equation 4.52

$$v = v_i = v_j = B\sqrt{p_i^* - p_j^*} \qquad v \geqslant 0 \tag{4.53}$$

$$= -B\sqrt{p_j^* - p_i^*} \qquad v < 0 \tag{4.54}$$

Applying equation 4.42 along C^+ to the left of the valve gives

$$p_i^* - p_{i-1}^* = -(v_i - v_{i-1}) \tag{4.55}$$

and applying equation 4.44 along C^- to the right of the valve gives

$$p_j^* - p_{j+1}^* = v_j - v_{j+1} \tag{4.56}$$

Subtracting equation 4.56 from 4.55 and rearranging gives

$$(p_i^* - p_j^*) = (p_{i-1} - p_{j+1}) + (v_{i-1} + v_{j+1}) - 2v \tag{4.57}$$

$$= \Delta - 2v$$

where $\Delta = p_{i-1} - p_{j+1} + v_{i-1} + v_{j+1}$

The two cases of v positive and v negative will be considered separately. For v positive, equations 4.53 and 4.57 may be solved to yield

$$v = -B^2 \pm \sqrt{B^2(B^2 + \Delta)}$$

and the negative solution may be immediately ignored as v has been assumed positive, i.e.

$$v = -B^2 + \sqrt{B^2(B^2 + \Delta)} \qquad (4.58)$$

For v negative, equations 4.54 and 4.57 may be solved to yield

$$v = B^2 \pm \sqrt{B^2(B^2 - \Delta)}$$

and the positive solution may be ignored as v was assumed negative, i.e.

$$v = B^2 - \sqrt{B^2(B^2 - \Delta)} \qquad (4.59)$$

It is unfortunate at this stage, that to solve the appropriate equation (4.58 or 4.59) for v requires a prior knowledge of the sign of v! However it can be shown that unless Δ is positive in equation 4.58 or negative in equation 4.59, a contradiction results. Hence the sign of Δ may be used to determine which equation has to be solved for v, i.e.

$$v = -B^2 + \sqrt{B^2(B^2 + \Delta)} \qquad \text{for } \Delta \geq 0 \qquad (4.60)$$

$$= B^2 - \sqrt{B^2(B^2 - \Delta)} \qquad \text{for } \Delta < 0 \qquad (4.61)$$

$$\text{where } \Delta = p_{i-1} - p_{j+1} + v_{i-1} + v_{j+1} \qquad (4.62)$$

From equations 4.55 and 4.56

$$p_i^* = p_{i-1}^* + v_{i-1} - v \qquad (4.63)$$

and

$$p_j^* = p_{j+1} - v_{j+1} + v \qquad (4.64)$$

Equations 4.46 through 4.64, together with the initial boundary conditions are sufficient to solve the problem. For the boundary conditions the steady state pressures and velocities along each hose, with the valve closed, were chosen.

Usually the solution is obtained at successive times in the x-t plane starting with the initial conditions at the grid points at time zero, by advancing in equal time increments from one row of grid points to the next. However, in this particular case, as any disturbance originating at the valve must travel along a characteristic in the x-t plane, it was more convenient to set the intial conditions along the

characteristics from the valve and advance the solution from characteristic to characteristic as sketched in figure 4.28. This meant that at

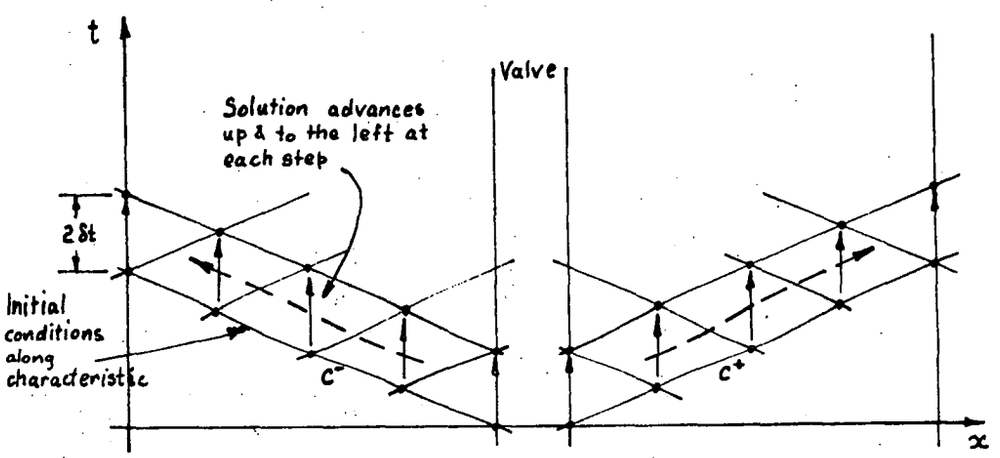

Figure 4.28

Solution advanced "by characteristics"

any step in the procedure the solutions at different points along the hoses corresponded to different times not the same time. The sinusoidal input valve motion was approximated in a stepwise fashion. In fact at the higher frequencies the number of grid points along each hose was determined by the time increment required to allow a reasonable stepwise approximation to the valve motion rather than by the error in hose length.

Figures 4.29 to 4.33 show some of the results obtained by this method. As previously the amplitude of the valve motion was decreased at the higher frequencies. The values of the parameters used in this model are included in Appendix 3.

The pressure disturbances initiated by the valve motion, and at the lower frequencies, their subsequent damping due to the non-linear valve behaviour, can be clearly seen. However even with these disturbances it is interesting to note the very good agreement between the "average" pressures and those obtained from the "solid slug model" presented in section 4.2.1. The flows on the other hand are somewhat smaller than those of the solid slug model, due mainly to the effect of these disturbances. The large negative, i.e. suction, pressures are

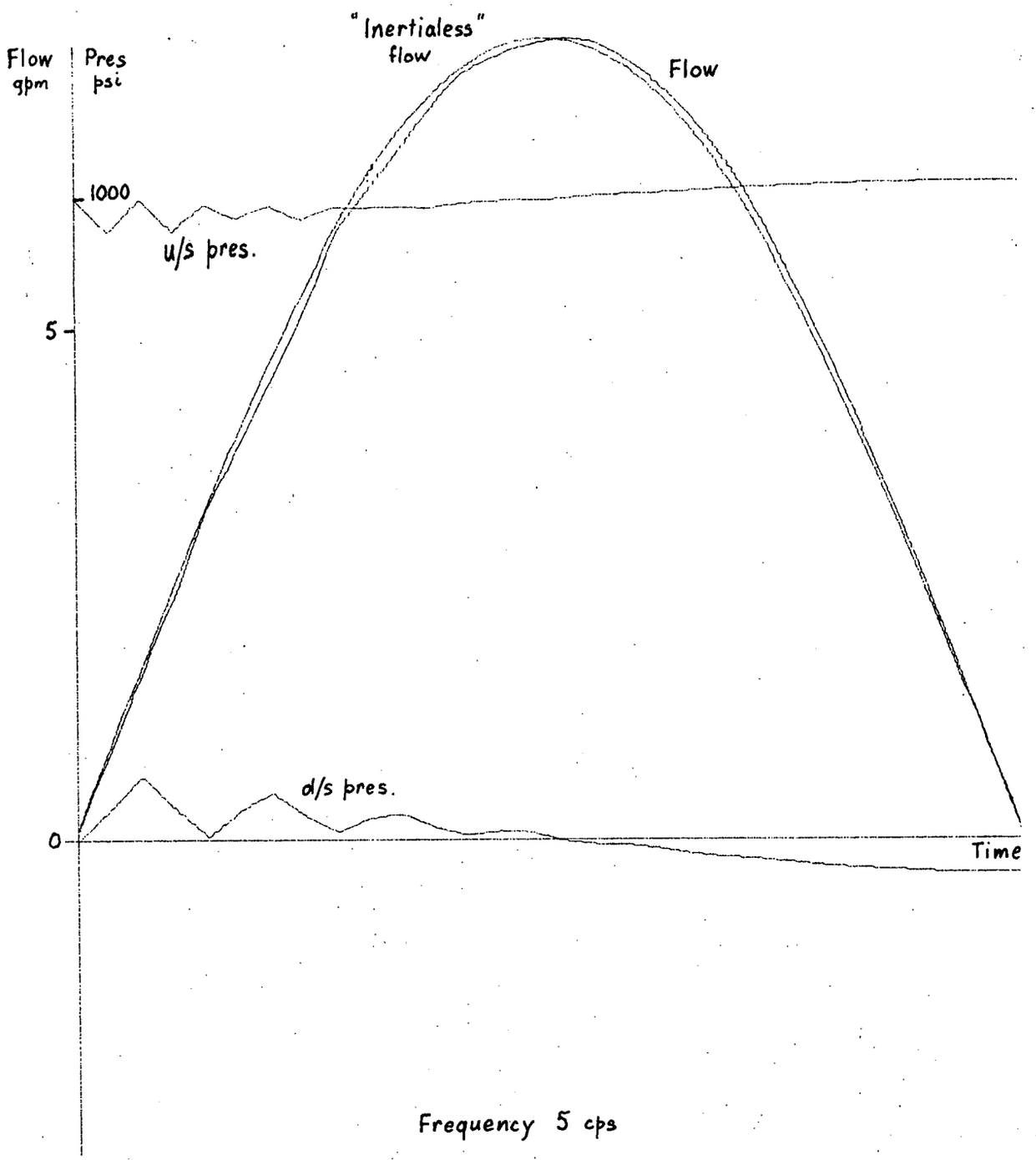

Frequency 5 cps

Figure 4.29

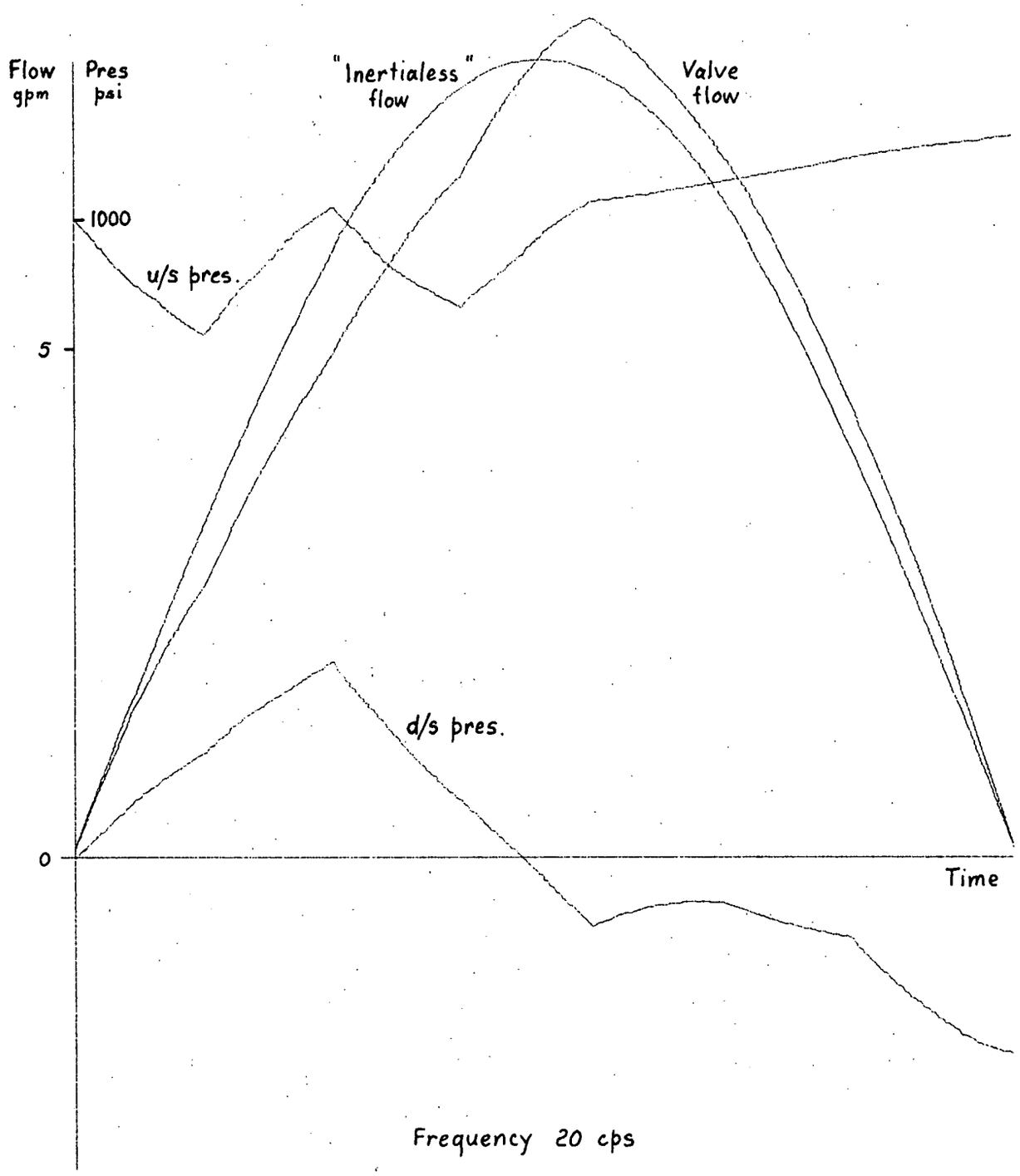

Frequency 20 cps

Figure 4.30

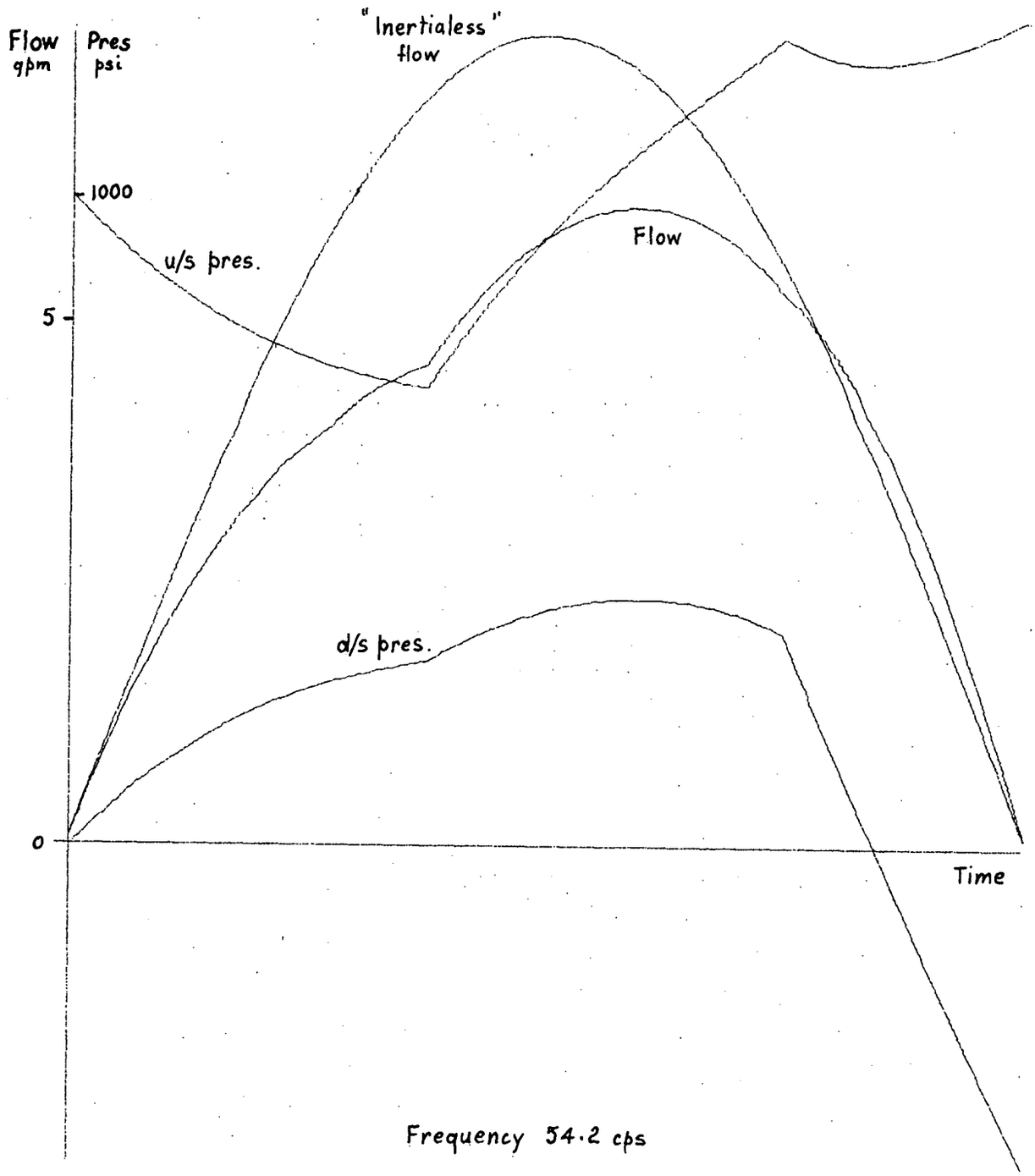
Flow
gpm
Pres
psi
"Inertialess"
flow
1000
u/s pres.
Flow
5
d/s pres.
0
Time
Frequency 54.2 cps

Figure 4.31

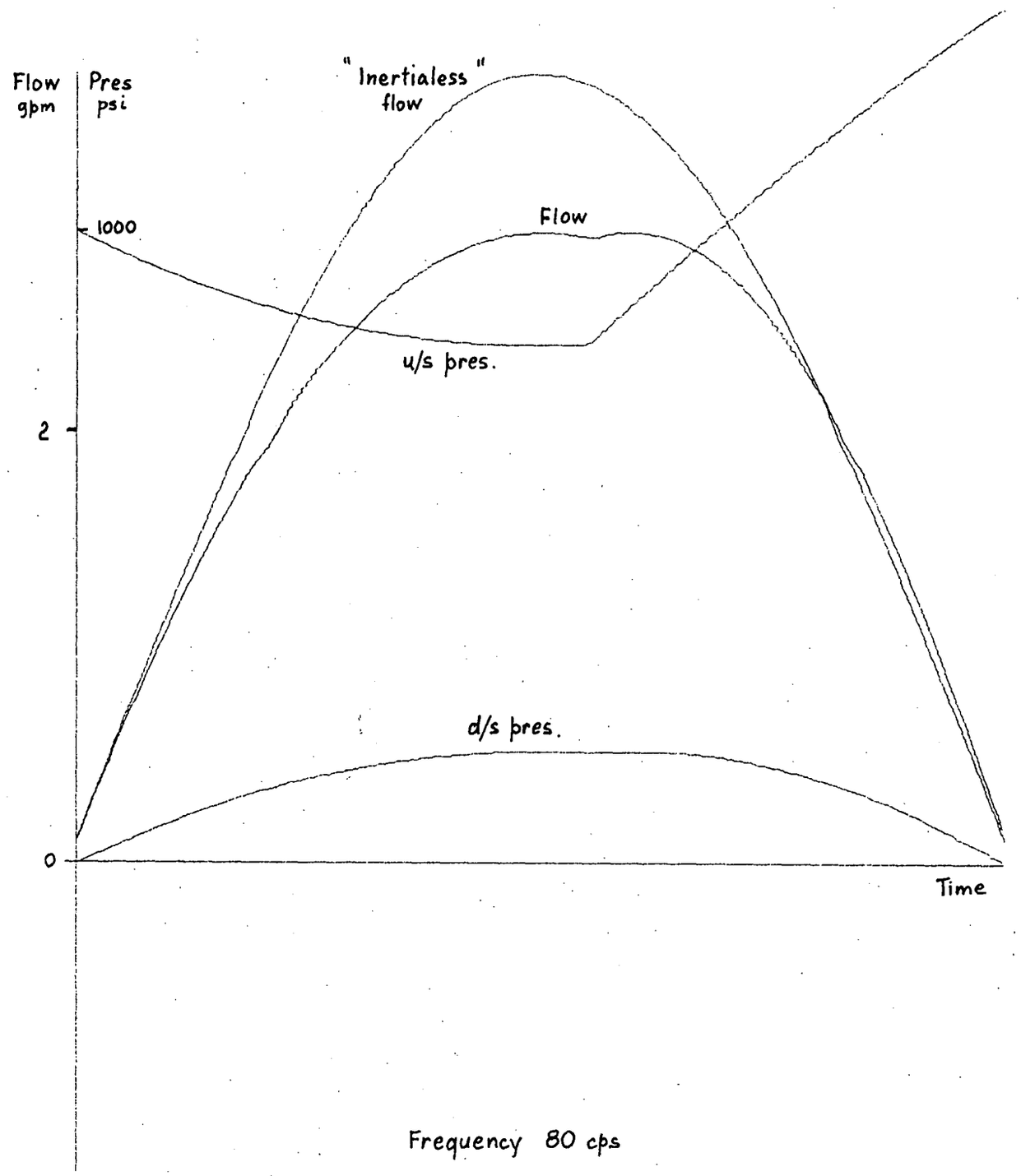

Frequency 80 cps

Figure 4.32

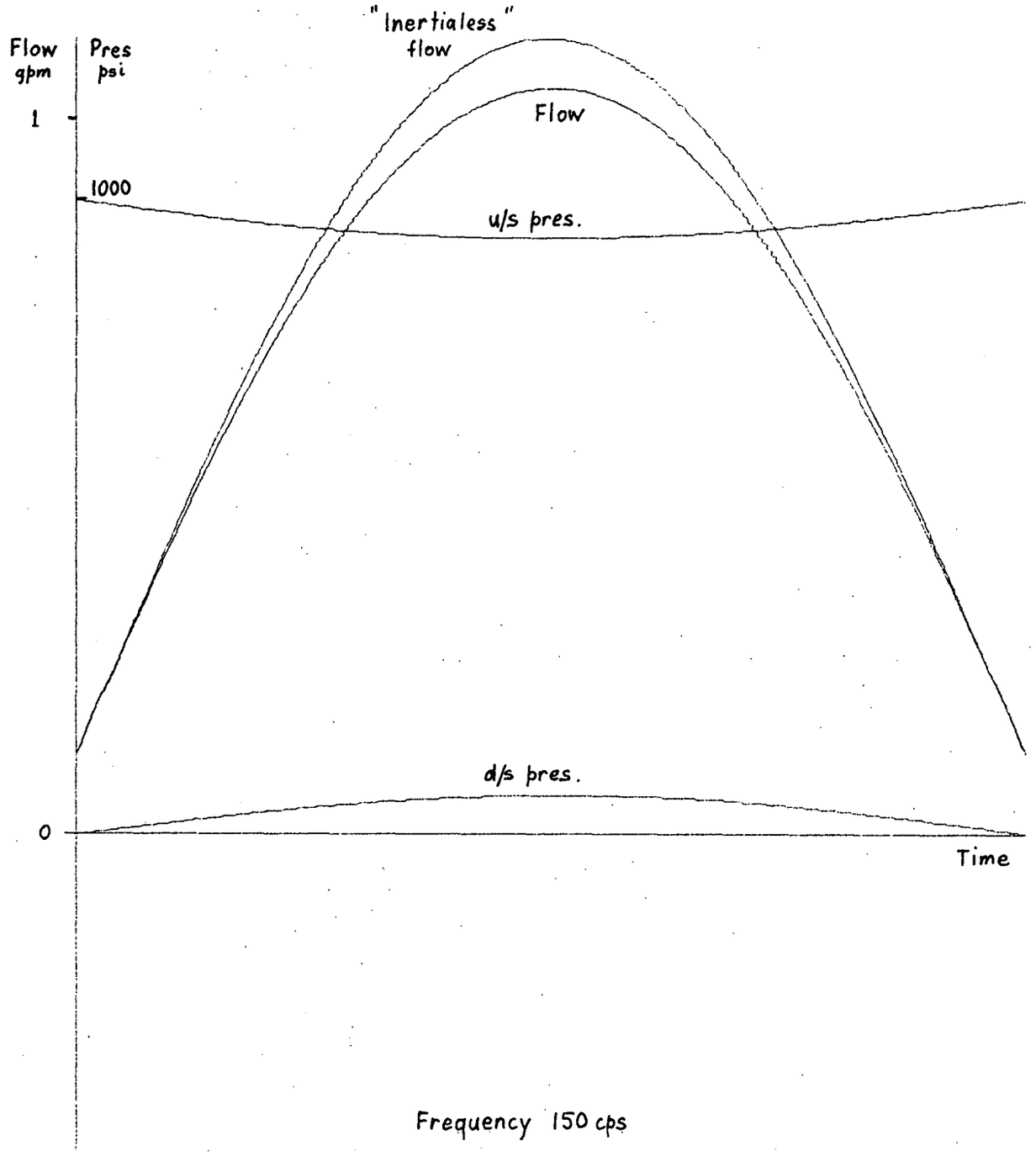

Frequency 150 cps

Figure 4.33

once again a result of the mathematical model. In reality the oil would cavitate. This effect can readily be taken into account with this model, although the moving boundary of the cavity does complicate the organisation of the problem within the computer somewhat. In any case it would be preferrable before introducing the effects of cavitation to include friction within the hoses. Although this has not been done it can be very easily incorporated in the method. As in previous models an average oil flow was calculated at each frequency, by assuming a leakage flow during each "dead" half cycle. These results are presented with the experimental results in section 4.3.

An interesting modification to this model was the inclusion of a fixed orifice in the downstream hose. In the discussion of the static valve characteristics, section 3.3.1, reference was made to the pressure drop downstream of the valve. A large portion of this can be attributed to the "back-pressure" needle valve. An equivalent orifice type restriction was therefore calculated and placed near the centre of the downstream hose, as shown schematically in figure 4.34. The method of analysis was as in the previous case. This in fact shows the versatility of the method of characteristics, for the complexity of the system can

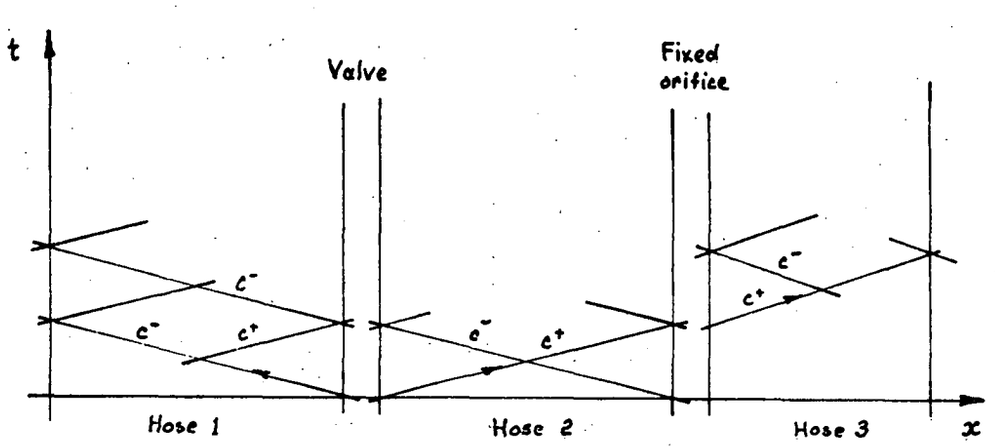

Figure 4.34

Modified method of characteristics model

be increased quite substantially by the addition of extra pipes or orifices and yet the basic analysis remains the same. The only difficulty that does arise is in satisfying the extra constraints imposed on the system. For example with the extra hose a further

condition on the hose division, similar to equation 4.45, has to be satisfied.

Figures 4.35 to 4.39 show some of the results from the modified model. The parameters used are given in Appendix 3. Included at the bottom of each figure, are the plots of the pressures just upstream and donwstream of the fixed orifice. These have been displaced in time for convenience in plotting; the displacement in each case is shown. It is interesting to note that the inclusion of this extra orifice has not greatly altered the response of the system. This is presumably because the fixed orifice is relatively large and hence has little effect. No doubt friction within the hoses would have a more marked effect.

As with the other models, average flows were calculated and are included in the next section dealing with the experimental results.

4.3 Experimental Results

As no ram was available to couple to the valve at the time the dynamic tests were conducted, an attempt was made to use the inertia of the oil within the hoses as a substitute. To do this the hose lengths downstream of the valve were made as long as possible.

Once again, as in the static tests of the valve, the limitations of the two land valve configuration made a satisfactory hose connection scheme difficult. The most satisfactory arrangement is shown in figure 4.40. This was far from ideal, as will be shown presently, for any pressure pulses travelling down the hoses into the drain line were communicated back to the valve end chamber. This caused a sudden extra force on the valve spool which badly distorted the waveshape in many instances. Furthermore there was a pumping action by the valve spool on the oil in these end chambers which limited the valve stroke at the higher frequencies due to the large amount of power absorbed.

As described in Chapter 1, the valve was driven by an electro-mechanical vibrator and power amplifier. The signal for these came from what was basically a signal generator with a feedback controlled amplitude.

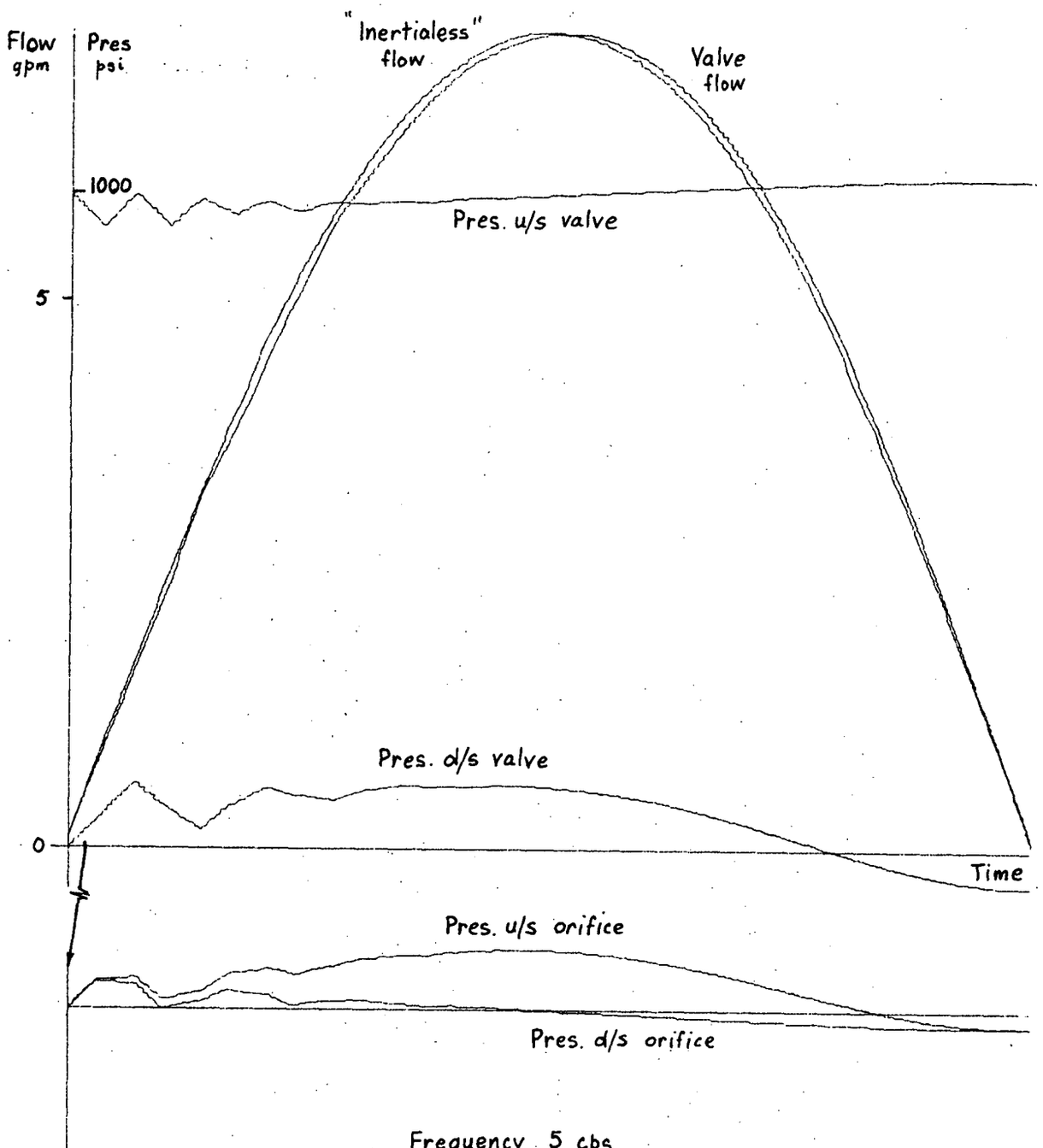
Flow
gpm
Pres
psi
"Inertialess"
flow
Valve
flow
1000
Pres. u/s valve
5
Pres. d/s valve
0
Time
Pres. u/s orifice
Pres. d/s orifice
Frequency 5 cps

Figure 4.35

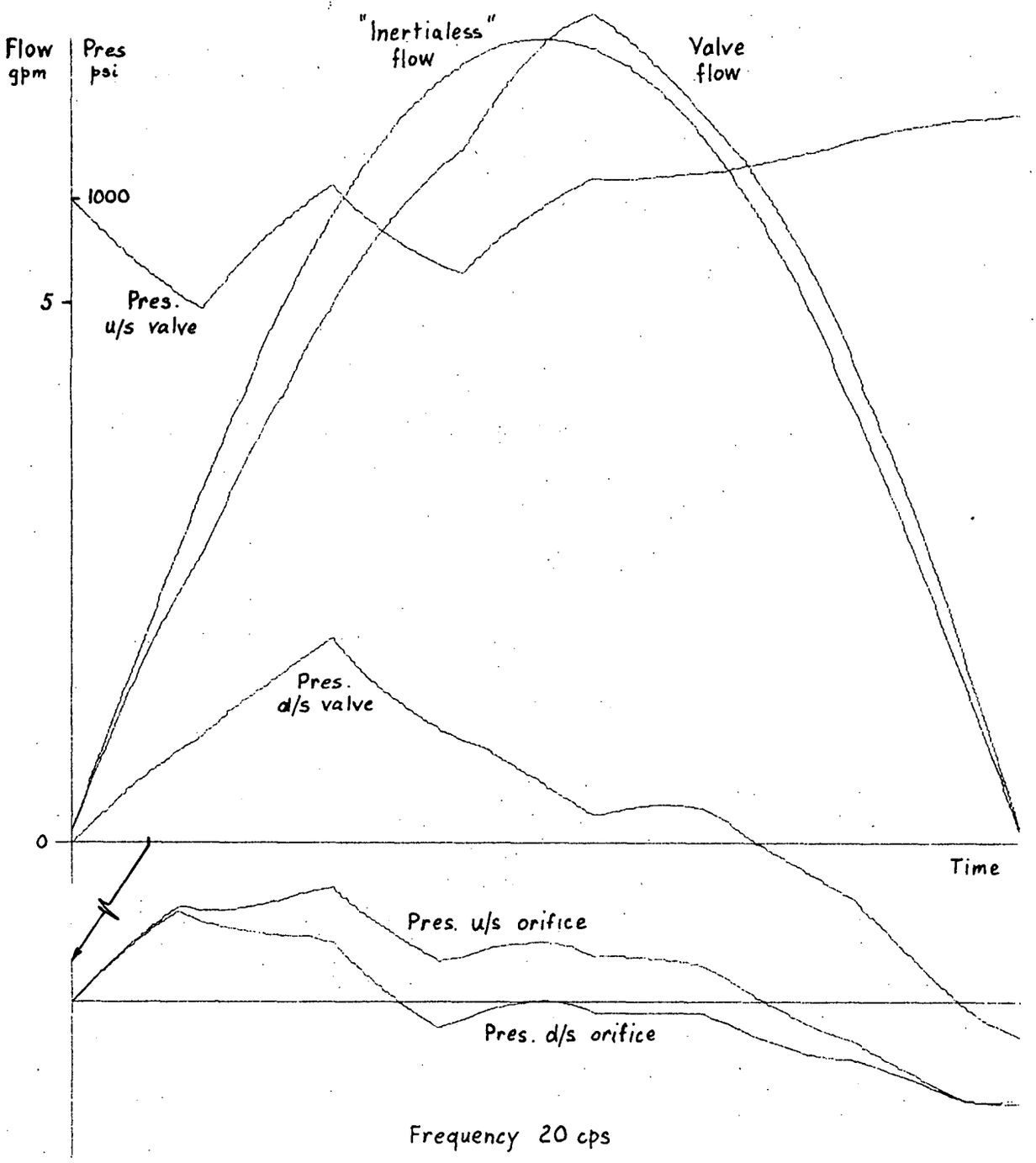
Flow
gpm
Pres
psi
"Inertialess"
flow
Valve
flow
1000
5
Pres.
u/s valve
Pres.
d/s valve
0
Time
Pres. u/s orifice
Pres. d/s orifice
Frequency 20 cps

Figure 4.36

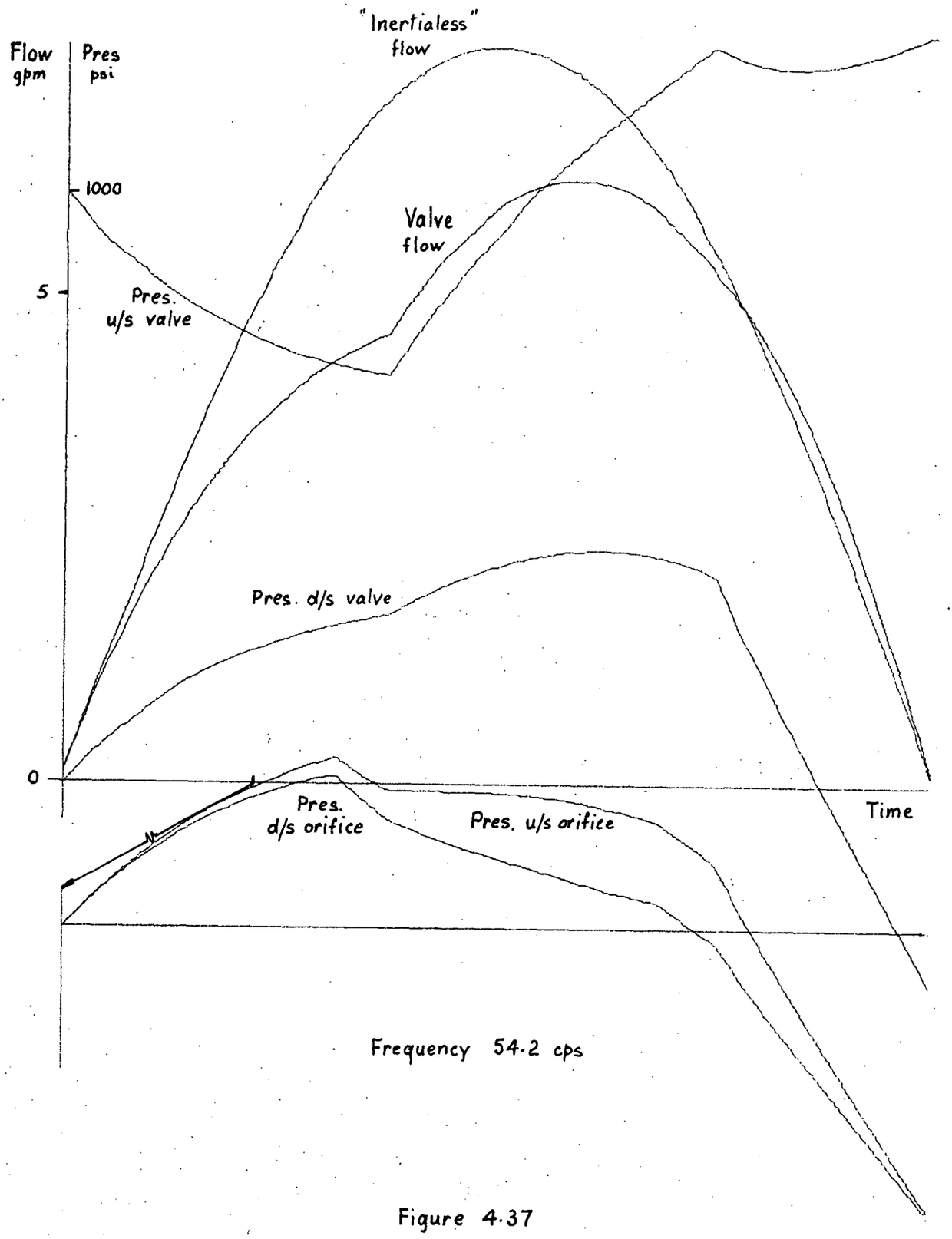
Flow
gpm
Pres
psi
"Inertialess"
flow
1000
Valve
flow
5
Pres.
u/s valve
Pres. d/s valve
0
Pres.
d/s orifice
Pres. u/s orifice
Time
Frequency 54.2 cps

Figure 4.37

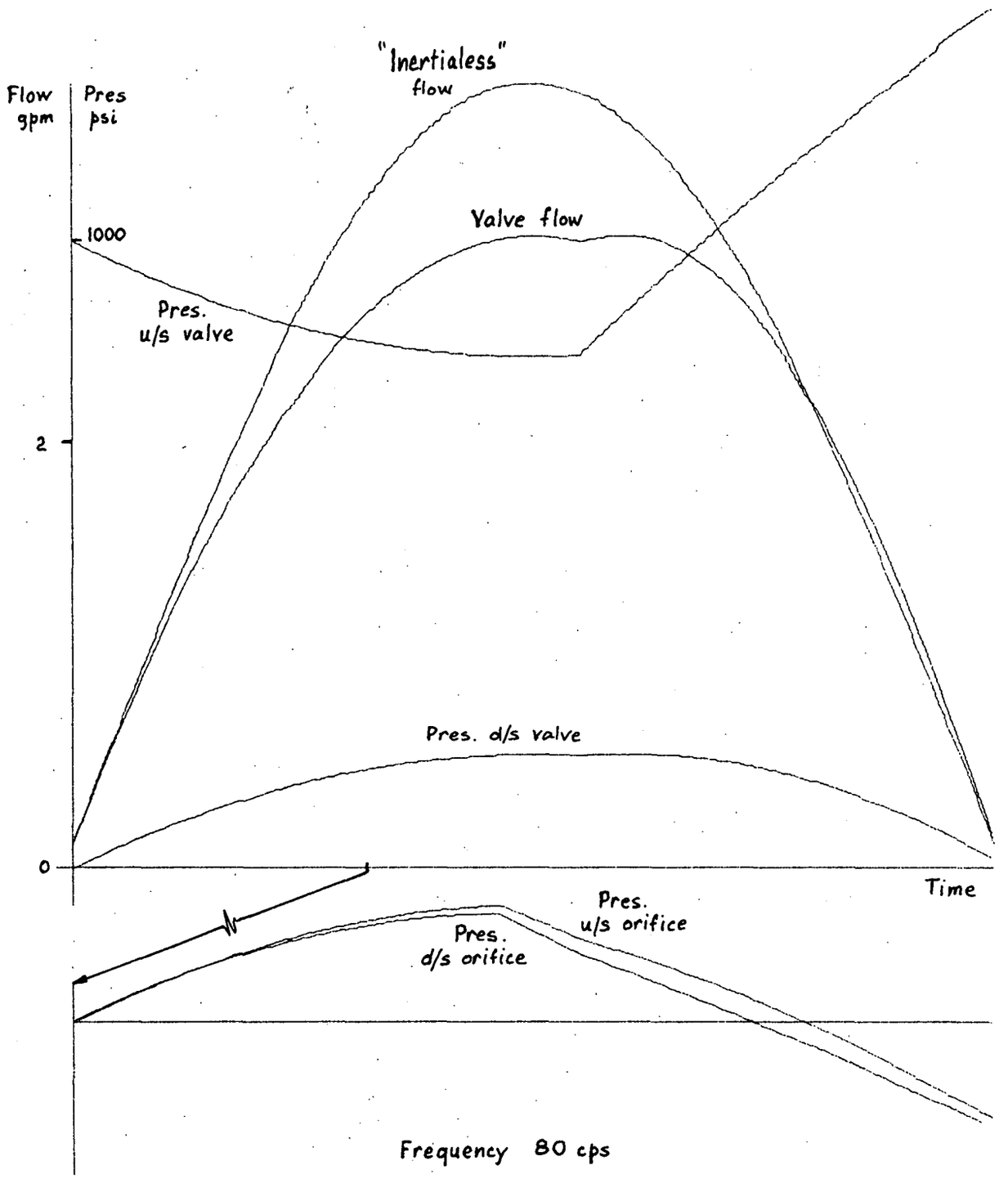
"Inertialess"
flow
Flow
gpm
Pres
psi
1000
Valve flow
Pres.
u/s valve
2
Pres. d/s valve
0
Time
Pres.
u/s orifice
Pres.
d/s orifice
Frequency 80 cps

Figure 4.38

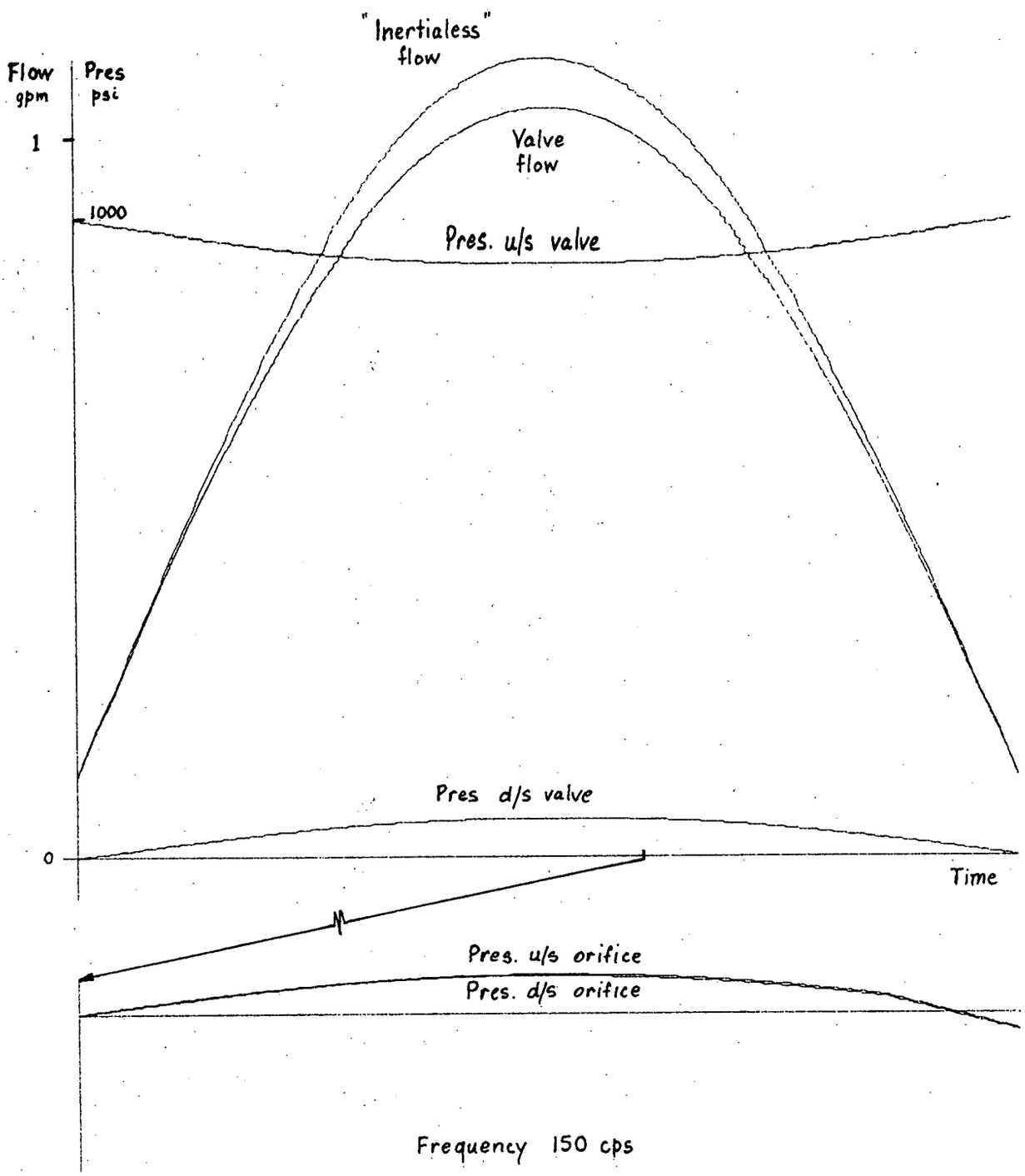
"Inertialess" flow
Flow gpm
Pres psi
1
1000
Valve flow
Pres. u/s valve
Pres d/s valve
0
Time
Pres. u/s orifice
Pres. d/s orifice
Frequency 150 cps

Figure 4.39

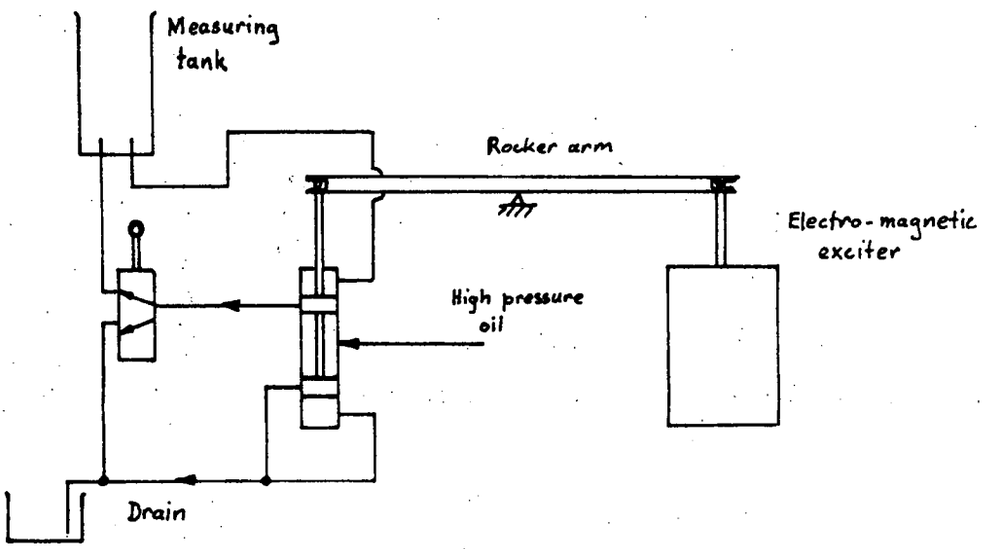

Figure 4.40

Hose connections for dynamic tests

This was set to give a constant displacement amplitude from 5 to 54.2 Hz and thereafter a constant acceleration amplitude. The feedback was derived from a small piezoelectric accelerometer mounted on the valve spool. The signal from this was scaled to 10 mV/g, and, in the case of constant displacement operation, integrated twice, to give the required control signal. This was rectified and integrated to yield an average signal amplitude which, by comparison with a preset value, controlled the output of the signal generator. In this regard the equipment differed from that normally associated with this type of system for it only controlled the average amplitude of vibration and in no way "waveshaped" it. This was a disadvantange in many instances for the waveshape was often very poor.

The behaviour of the system was monitored by recording on a U.V. recorder, the acceleration and displacement of the spool, the transmitted force and the pressure downstream of the valve. The galvanometers in this unit had a flat frequency response up to 300 cps. Some of the resultant traces are shown in figures 4.41 to 4.48. The force trace is the force being transmitted by the rocker arm. These figures show

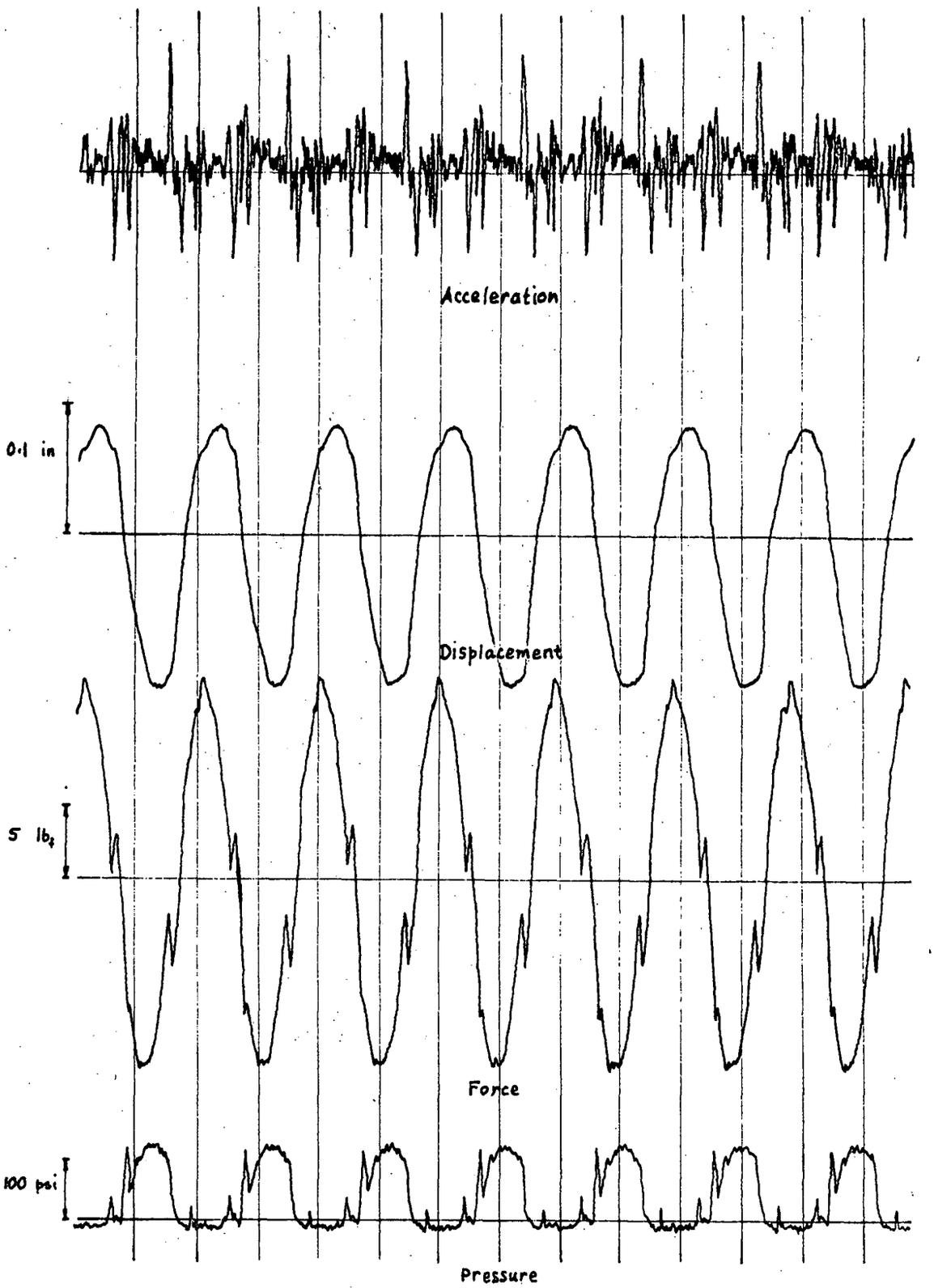

Frequency 5 cps
Port B

Figure 4.41

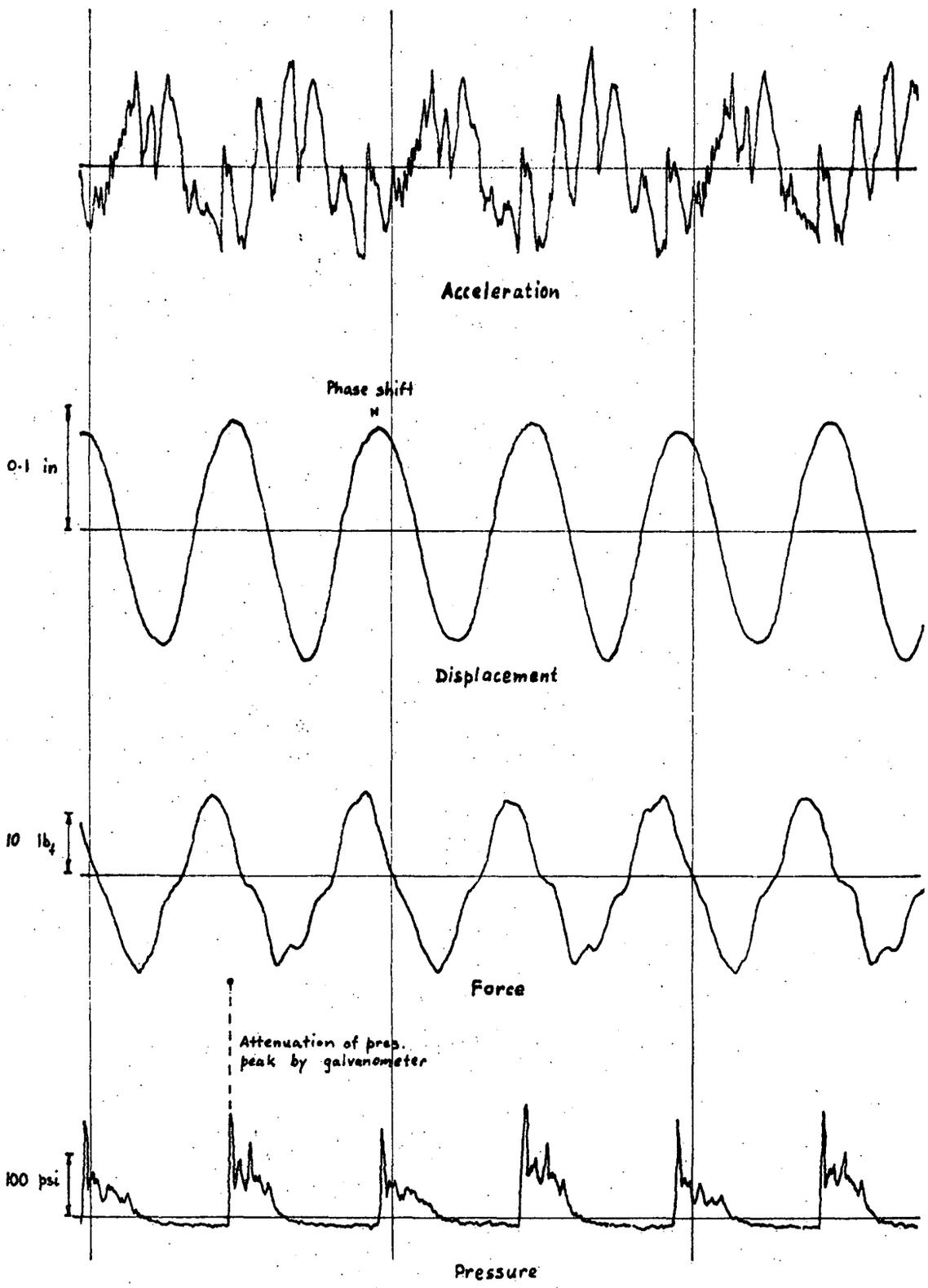
Acceleration
Phase shift
0.1 in
Displacement
10 lb$_f$
Force
Attenuation of pres. peak by galvanometer
100 psi
Pressure
Frequency 20 cps
Port A

Figure 4.42

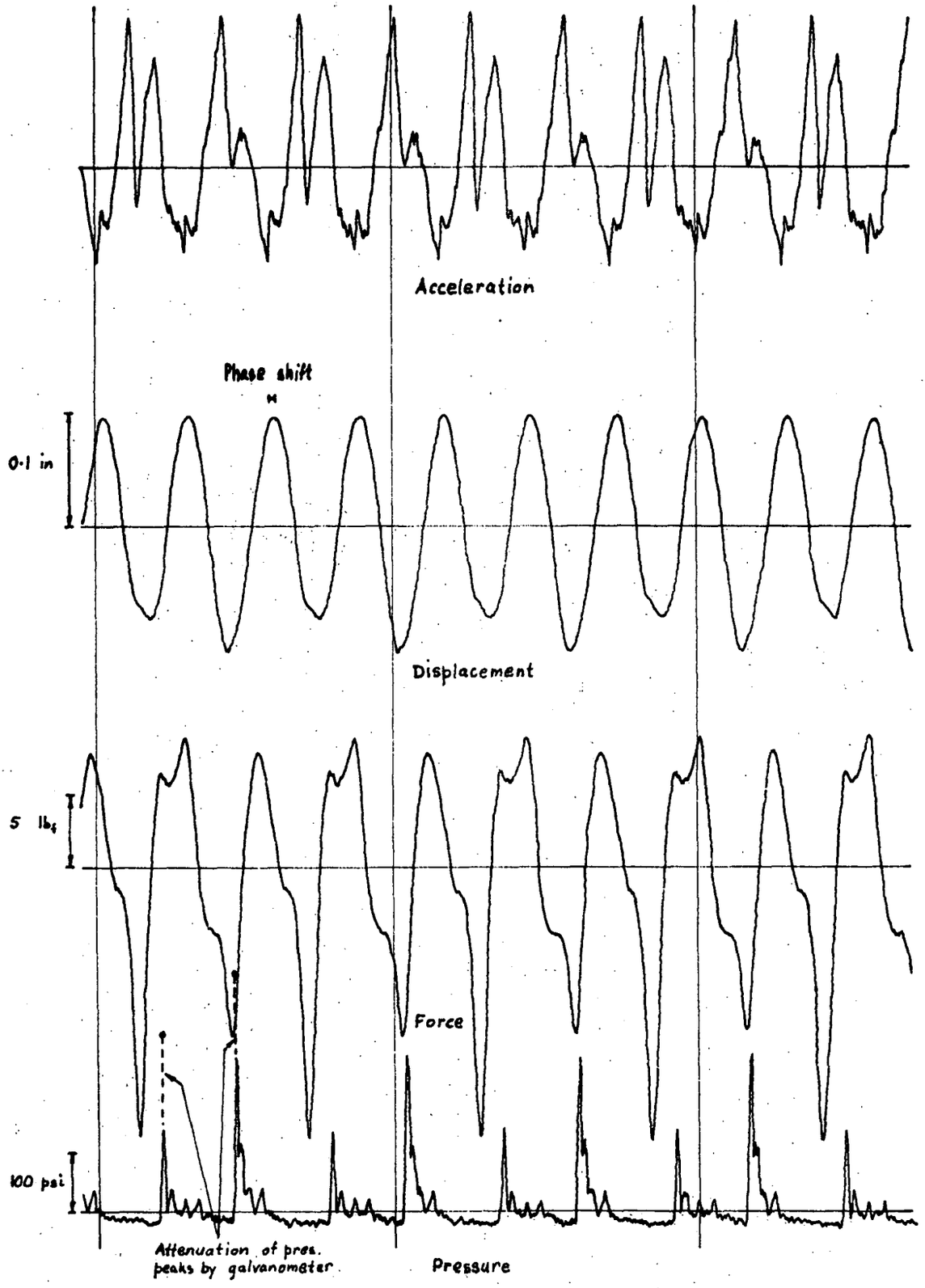

Frequency 35 cps
Port B

Figure 4.43

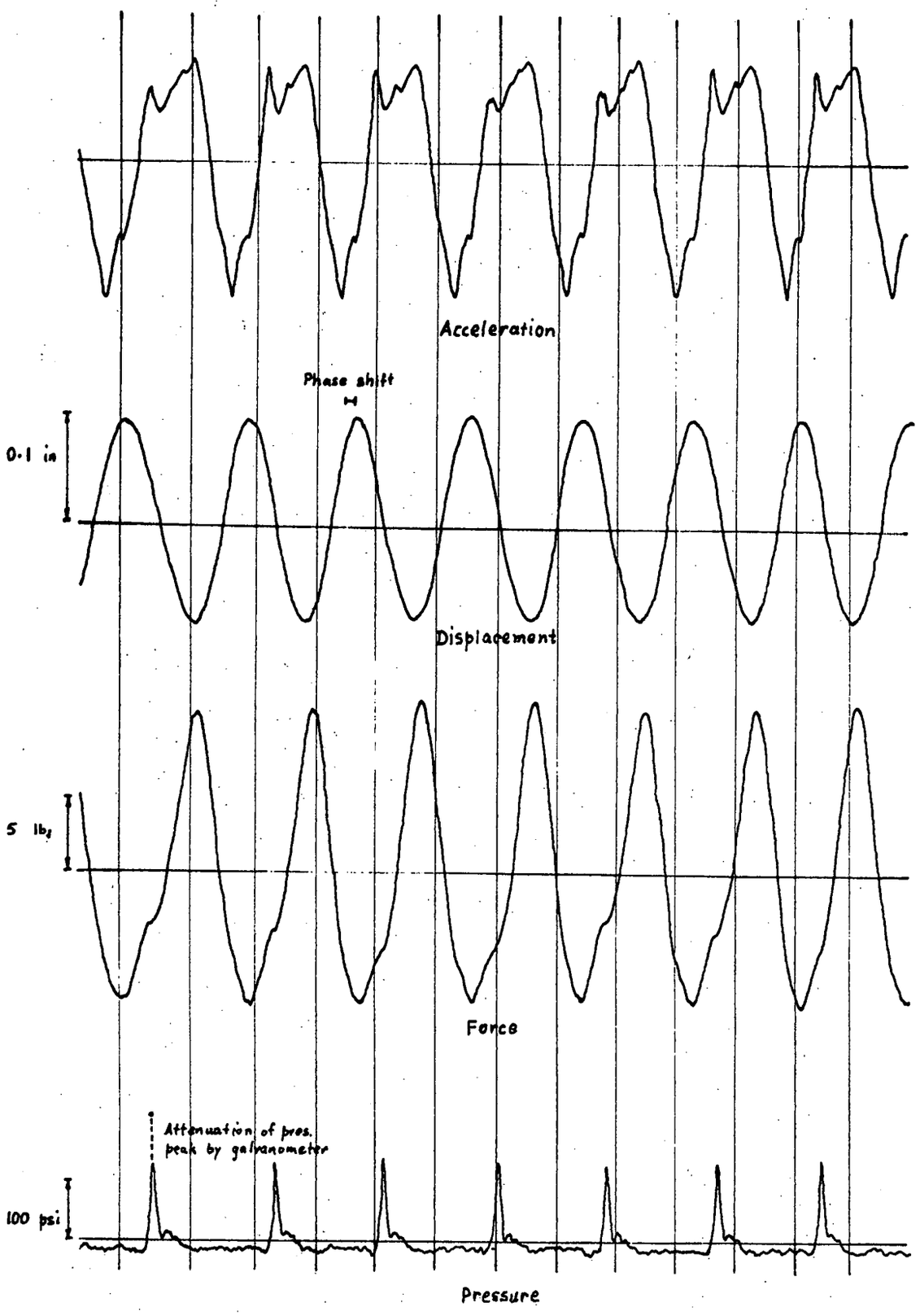

Frequency 55 cps
Port A

Figure 4.44

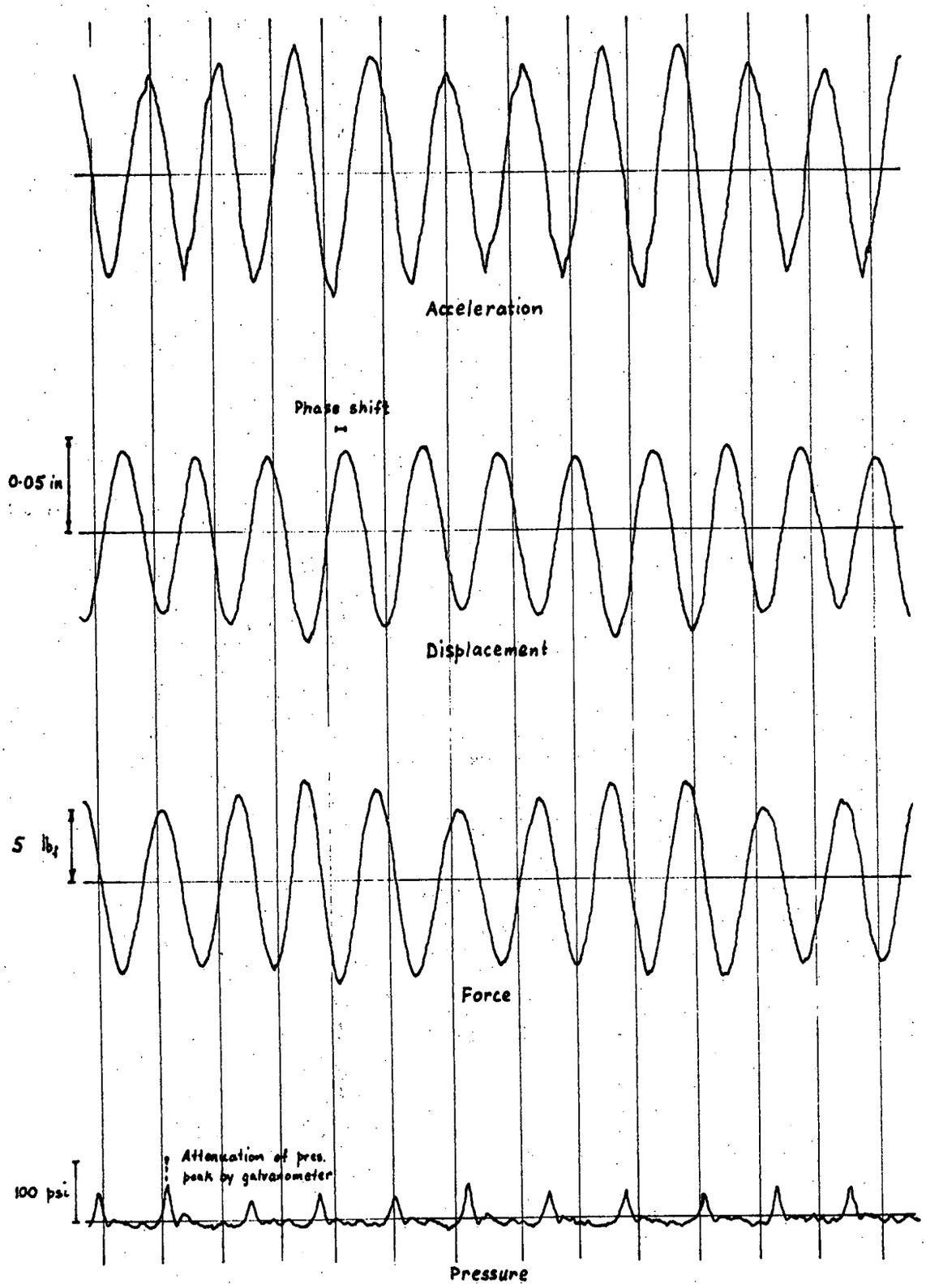

Frequency 80 cps
Port A

Figure 4.45

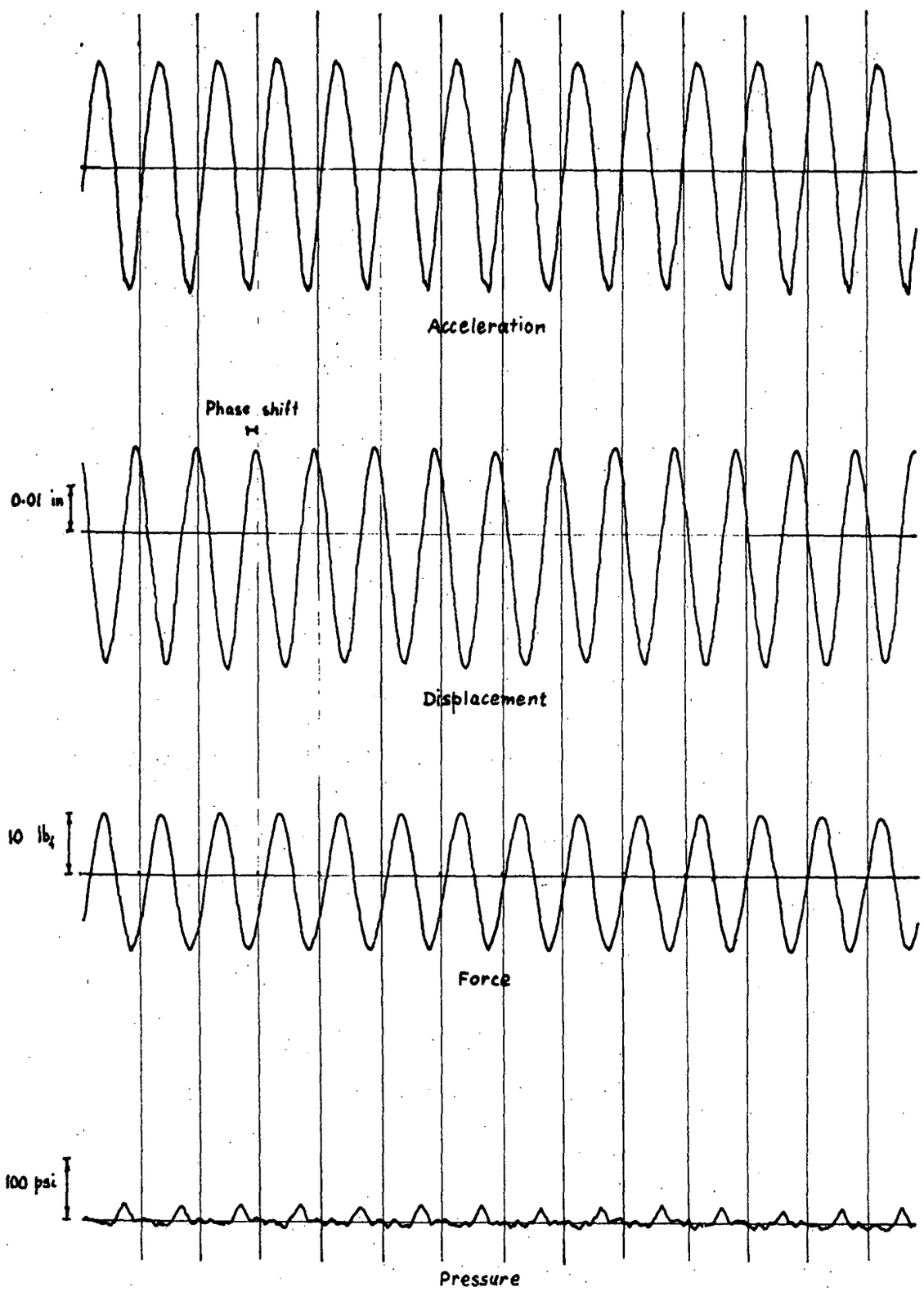

Frequency 100 cps
Port A

Figure 4.46

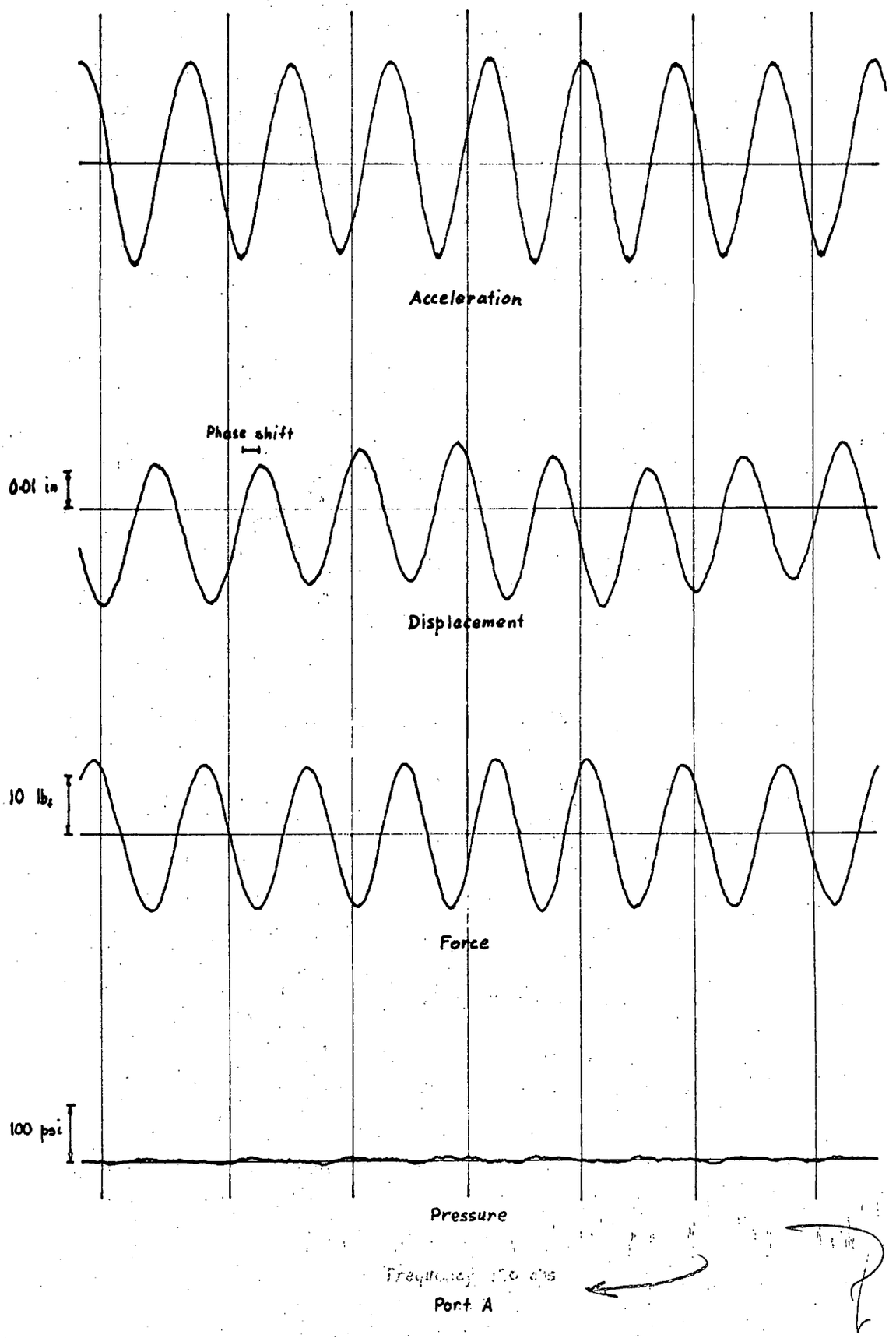
Acceleration
Phase shift
0·01 in
Displacement
10 lbs
Force
100 psi
Pressure
Frequency (c.p.s)
Port A

Figure 4.47

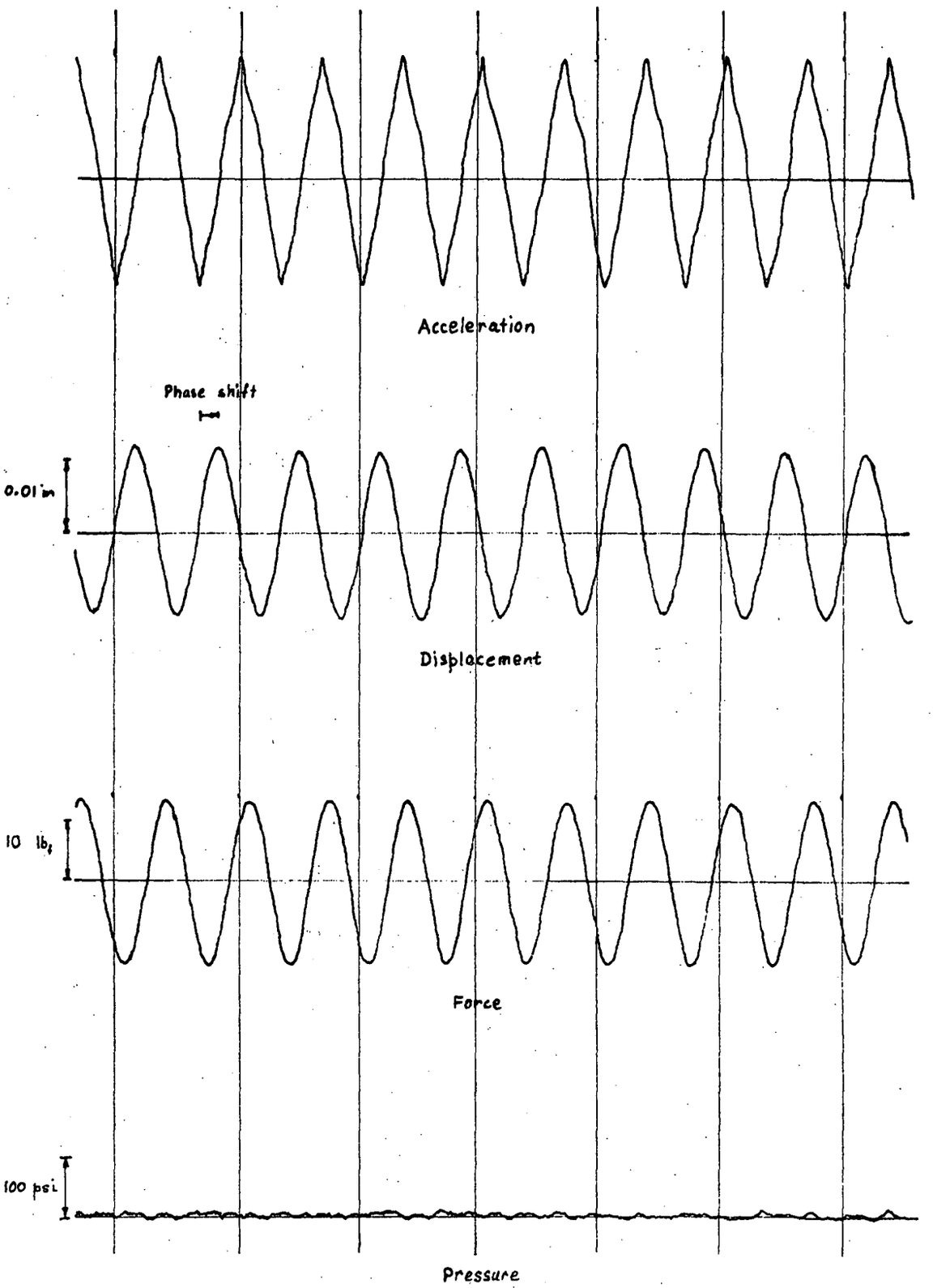

Frequency 150 cps
Port A

Figure 4.48

quite clearly the difficulty in obtaining "clean" waveshapes with the two-land configuration of the valve spool. Distortion is particularly evident in the frequency ranges 25 to 95, 60 to 90 and 110 to 140 Hz.

These figures also show one of the disadvantages of the U.V. recorder galvanometers. Some of the measured variables changed so rapidly that the galvanometers could not follow them and consequently the peaks were attenuated. This was particularly noticeable with the pressure traces and to a more limited extent with the acceleration traces. To overcome this difficulty these variables were displayed on a CRO and peak readings taken from this. The galvanometers also distorted "square-edged" traces due to a slight amount of overshoot and subsequent damped oscillation. Fortunately this effect was not of much importance in this experiment. In any case all questionable traces were displayed on the CRO to check the waveshape and amplitude.

The phase shifts indicated on the displacement traces were caused by the displacement transducer. This had a filter with a fairly low pass-band in the output stage. Consequently at the higher frequencies the output not only became shifted but also became attenuated, the attenuation becoming quite severe at frequencies above approximately 100 Hz. A displacement transducer with a much higher internal carrier frequency would be desirable.

The large amount of "noise" in the acceleration traces at the lower frequencies was attributed to chatter caused by the small clearances in the connections at each end of the rocker arm. The bearing at the centre of the rocker arm also wore quite badly during the experiment and the resultant slack at this point no doubt contributed to the "noise". It is probably present at all frequencies. However the very much large accelerations at the higher frequencies mask the small amount of chatter present.

One of the most interesting aspects of these results is the comparison between the shapes and amplitudes of the pressure traces in figures 4.41 to 4.48, and those of the modified method of characteristics model, figures 4.35 to 4.39. Considering the limitations of the

model in making no allowance for friction or cavitation, the similarity is remarkable, particularly at the lower frequencies. The corresponding pressure traces of figures 4.35 to 4.39 are those just upstream of the fixed orifice. It would be of even more interest to see what effect the inclusion of friction in the model would have.

Besides recording the variables presented in figures 4.41 to 4.48, the average oil flow through each valve port was measured. This was achieved by directing the flow into the measuring tank and timing a given level change. Figure 4.49 shows the experimental results plotted together with the results obtained from the various mathematical models. To overcome some of the effects of poor waveshape and more particularly, any slight offset in the mean position of the valve spool relative to its central position, the flow results from each port at each frequency, were averaged before plotting. As can be seen the overall agreement between the models and experimental results was reasonable.

One point which is also apparent, is the occurrence of two peaks in the experimental points; one at approximately 15 - 30 cps and the other at 90 - 110 cps. At these frequencies the oil coming from the valve had a very creamy appearance, due to large numbers of very small gas bubbles in the oil. There was also a distinct change in the noise made by the system at these frequencies. This was thought to be due to severe cavitation. This would certainly explain some of the gas bubbles, as they would come out of solution with cavitation and then remain for a considerable time because of the difficulty of reabsorption. However, there was also some pumping of air into the end-chambers of the valve, through the annular clearances between the valve spool and end-caps. This could be observed by pouring oil on to the end-cap to "seal" the annular groove. While the oil pool lasted there was a marked decrease in the number of gas bubbles in the oil coming from the valve. In any case, the presence of these bubbles of gas in the oil could explain the higher flow readings at these frequencies, for the apparent oil volume in the measuring tank would be increased by these bubbles.

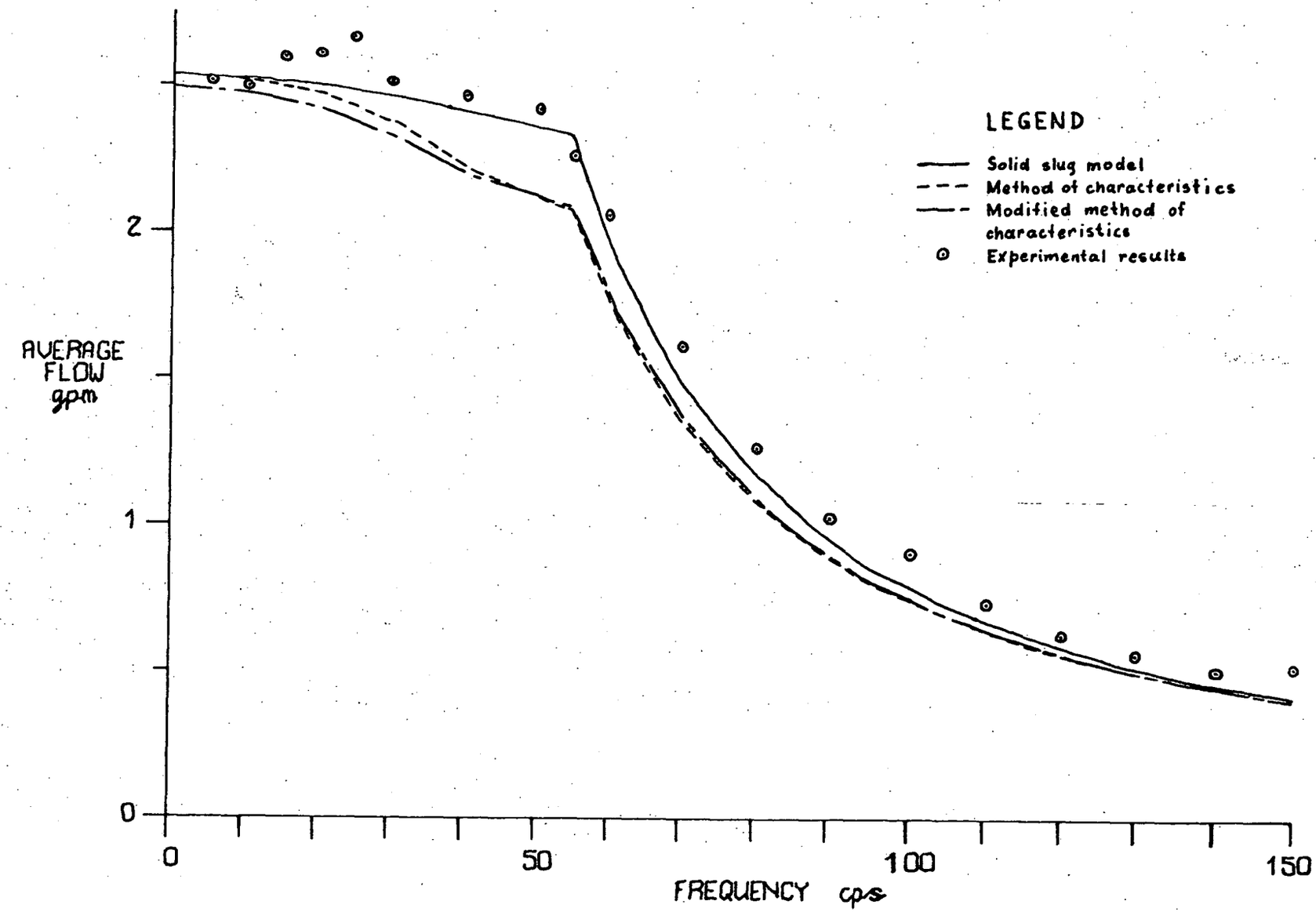
LEGEND
Solid slug model
Method of characteristics
Modified method of characteristics
Experimental results
AVERAGE FLOW gpm
2
1
0
0
50
100
150
FREQUENCY cps

Figure 4.49

It is also of particular interest to note that the experimental results, besides being slightly higher overall than the model results, follow more closely the general shape of the solid slug model rather than the method of characteristics models. This was somewhat unexpected, for it was thought that the method of characteristics should have given a more accurate result. It may be that the exclusion of friction from the method of characteristics models has caused some of the discrepancy. It could also be that the discrepancy in the overall shapes of the curves is not significant, for the large distortion of the valve waveshapes at many frequencies could easily have masked the true shape of the average flow results.

On the other hand the overall trend for the experimental flow results to be higher than the model results can not readily be ignored. It is difficult to justify increasing the discharge coefficients of the models above those used, unless of course the dynamic behaviour of the valve is assumed to be significantly different from the static behaviour. It could be that the average pressure upstream of the valve was higher than the nominal pressure of 1000 psi, for, although there were no pressure tappings upstream which would allow proper dynamic measurements, the bourdon-tube pressure gauge showed considerable high frequency fluctuations, the mean of which was greater than 1000 psi. In fact at certain frequencies there appeared to be resonance type effects. These were probably caused by the valve moving with a frequency near a submultiple, or multiple, of the pump piston frequency. It might help to move the accumulator, perhaps towards the experimental system, in order to more effectively damp out these pressure fluctuations. In any case if this were done the extra length of hose between the accumulator and pump would help to damp out any disturbances from the experimental system before they could reach the pump and possibly upset the operation of the pressure compensator.

One further point of interest which has not been shown by the results already presented was the occurrence of a resonance between the valve spool, rocker-arm and exciter element. There were two

resonant frequencies observed; one at 25 cps and the other at 95 cps approximately. From the results already presented in Chapter 3 together with those from the mathematical models, for the frequencies considered here the back pressures in the oil lines may be assumed small and the oil flows nearly in phase with the valve displacement. Under these conditions the flow reaction force may be thought of as a spring type force acting on the valve spool. The overall system then looks somewhat like the two-mass, two-spring system sketched in figure 4.50.

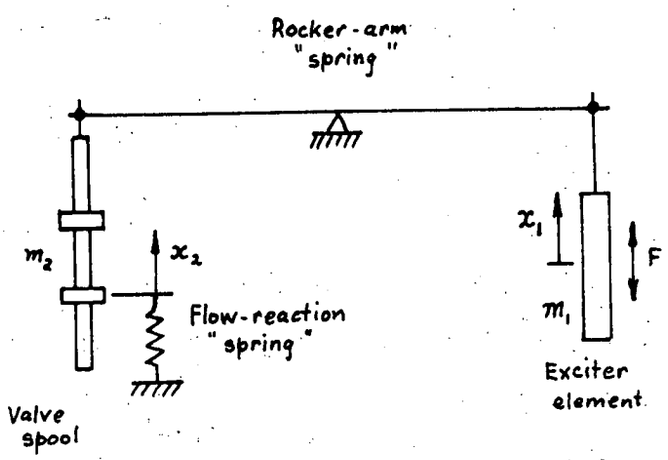

Figure 4.50

Valve spool and exciter element

as two-mass, two-spring system

By inserting values for the masses, spring-stiffnesses and spool displacements the system can be analysed. This was done and the driving forces, transmitted forces and resonant frequencies compared with those observed experimentally. At low frequencies there was good agreement both between the lower resonant frequency and the exciter force required. However at the higher frequencies it was found that the agreement could only be maintained by increasing the "flow-reaction" spring stiffness. It is doubtful whether this in reality occurs. However as previously mentioned, because of the peculiar construction of this valve, the valve spool had a pumping action on any oil trapped in the end chambers, and it would be

expected that this pumping action would be dependent on frequency. Hence it is very likely that the effective increase required by the "flow-reaction" force was caused by this pumping action on the oil in the end chambers. There would also be viscous damping present at the valve spool and this would alter the response, although by not enough to explain the observed discrepancy.

A comparison was made too, between the transmitted forces predicted by this model and those observed experimentally. Although this was somewhat difficult due to the variability and distortion of the experimental force results the overall trend was in good agreement, provided an increasing spring stiffness was used in the model.

Finally, it should be noted that before any attempt can be made to "waveshape" the valve displacement by some form of feedback, this resonance effect would need to be overcome. This could be done either by stiffening the rocker-arm quite considerably, or by coupling the exciter directly to the valve spool. The later would be preferable in many respects.

------ooo------

CONCLUSIONS

It was somewhat disappointing that the more specific aim of the project, viz. the construction of a fluid-powered vibrating testing machine, could not be completed in the available time. That progress should be slow ought perhaps, to be expected with any developmental project, although the relative isolation of Tasmania undoubtedly contributed. Nevertheless the general aim of constructing an hydraulic test facility and of gaining experience in the assembly and use of hydraulic components and systems was achieved. In fact a great deal of experience has been gained particularly in the design and construction of hydraulic valves.

Basic Hydraulic System

The basic hydraulic system is now at a workable stage. Either individual components or whole systems can be studied simply by making the necessary connections. However one problem still remains. There is an urgent need for an efficient oil cooling system, preferably automatically controlled. During this project the oil temperature proved difficult to maintain within reasonable limits. This not only made it difficult to obtain repeatable observations but also limited the maximum length of time during which any experimental run could be conducted.

Furthermore with an efficient oil cooling system the oil pressure could be increased to 2000 psi, using the existing equipment. This would be very desirable as many of the problems associated with hydraulic components become more pronounced at the higher pressures. However, with components constructed within the department leakage might prove to be a problem at the higher pressures. Nevertheless it should be possible to overcome this, at least in part, by proper regard to tolerances and careful manufacture.

One other problem which arose during the dynamic tests was the occurrence of quite pronounced pressure pulsations upstream of the

experimental valve, even with the accumulator in the system. This could disturb the results obtained from any dynamic-type experiment and should be studied. It might be possible to reduce the pulsations by moving the accumulator closer to the main high-pressure hydraulic line, as well as closer to the experimental system. Studies of the actual accumulator capacity have shown that it should be adequate for the types of experiments envisaged.

Four-way Valves

The fluted form of construction used for the four-way valves has proved very effective. The relatively long stroke for reasonable oil flows, made the displacement measurements very much easier, particularly the dynamic measurements. It did, however, have the disadvantage that at the higher frequencies the acceleration required to maintain the stroke length became very large, and it was necessary to operate with a constant acceleration and decreasing stroke at frequencies above 54.2 Hz.

Static tests showed the flow-displacement behaviour to closely follow the "orifice-flow" equation, characteristic of the more usual "square-land" type of valve. The discharge coefficient was slightly higher at 0.72, but this was to be expected as the slot through which the oil flowed was far from an orifice type restriction. Although the flow reaction forces were higher than the equivalent "square-land" configuration, they were relatively small compared to the forces available from the electromagnetic exciter and consequently did not cause any real problem. Leakage flows were small, being less than 2% of the maximum flow. However if the pressure were increased to 2000 psi or higher leakage might present a problem. In this event the manufacture and particularly the final lapping operations would need to be closely watched.

One real disadvantage with the fluted valve design was the accurate positioning of the ends of the slots. This could prove a serious problem with any hardened valve spool, for the slots would

need to be machined before hardening, and any subsequent distortion, combined with the final grinding to "true" the spool, would considerably change the position of the ends of the slots. To date the valve spools have not been hardened and consequently this problem has not been serious. Furthermore the valve ports have been machined after the spool, to suit the position of the ends of the slots. It might be possible with hardened valve spools to finally grind the slots to give the desired result.

Mathematical Models

The "solid-slug" models of both the vibration tester and the pulsating "pipe-flow" problem proved very difficult to handle in a digital computer due to numerical instability. Because of this it is doubtful whether this model is of much use, particularly for the analysis of the vibration tester. For the pulsating "pipe-flow" problem, the solution was forced through the unstable regions to give results which agreed well with the experimental results. However the main interest in this model would appear to be as a problem in numerical instability rather than a practical means of analysing the hydraulic circuits studied here.

The compressible fluid model of the vibration tester on the other hand, proved very much easier to handle, and the results from this model were quite exciting. Not only was the model relatively easy to handle in a digital computer, but the predicted outputs were very close to those expected and certainly far superior to any predicted by linearized models. To be efficient however, the procedure would require a variable step size for the integration. This could be achieved along the lines discussed in Chapter 4, using the pressure increments at each step to control the step size.

The compressible fluid model also has the great advantage that both Coloumb and viscous friction effects can be easily incorporated in the equations. Furthermore it is of a convenient

form for "patching up" on a suitable analogue computer. In this respect, the analogue computer in the Electrical Engineering Department of the University is now at a stage at which this should be possible, and it would be of considerable interest to do this.

For the pulsating "pipe-flow" problem there is no doubt that the method of characteristics is one of the best means of analysis. It is readily handled in a digital computer and the results obtained are generally more realistic than other methods. In this particular project time did not permit the inclusion of friction terms within the model. Nevertheless the comparison between the pressures predicted and those observed experimentally was excellent. The flow results did not compare as well with the experimental results as those from the solid slug model. But, as mentioned in Chapter 4, this may not be significant.

It should also be possible to use the method of characteristics to analyse the vibration tester. However the moving boundary presented by the ram could prove difficult to follow within the computer. It is also doubtful whether this method would offer any advantages in computation time or accuracy of results over those of the compressible fluid model for the small pipe lengths envisaged in the final type of vibration testing machine. Nevertheless this aspect warrants further investigation.

General

A small, high-speed, digital computer has recently been purchased by the Civil and Mechanical Engineering Department and this has opened up many new and exciting possibilities with regard to this particular test facility. For instance the computer could be used to advantage for the more usual jobs of data-logging, monitoring, analysing or controlling some system or test program on a system. However it is the field of feedback similation that is perhaps of most interest with respect to this project. For

instance the computer could be used to simulate pressure feedback to the valve spool. This would be done by sensing oil pressures at appropriate points in the system, calculating, in the computer, the force that would have been exerted on the spool by these pressures had they been feed back, and then modifying the signal to the electromagnetic exciter to simulate the addition of this force. This would have the great advantage that many quite complex feedback arrangements could be simulated and studied without having to go to the expense and trouble of producing valves with the necessary small internal passageways. However the rocker-arm mechanism used to couple the exciter to the valve spool would have to be stiffened very considerably in order to overcome the resonance effects, with the associated phase reversals, observed in these experiments. Better still would be to couple the exciter directly to the spool.

Finally a comment on the flow nomograph presented in Appendix 1. It is of some interest that many of the persons involved in estimating, "in the field", such things as orifice-type flows, often have a very poor understanding of mathematics. Furthermore they are particularly confused by the units required for the variables in such an equation in order to make it consistent. It is to these people that a nomograph is most useful. In fact just such a situation was one of the main incentives in preparing the nomograph. In practice it has proved quite reliable for fluids from oil and water through to liquid nitrogen. The errors have been 10% or less, provided the limitations of the nomograph have not been exceeded.

------ooo------

Appendix 1

Turbulent Orifice Flow Nomograph

A nomograph is a graphical device for solving an equation by means of a straight line laid across three or more calibrated scales which represent the variables in the equation.

The form of nomograph chosen in this case was the three variable parallel line form shown below.

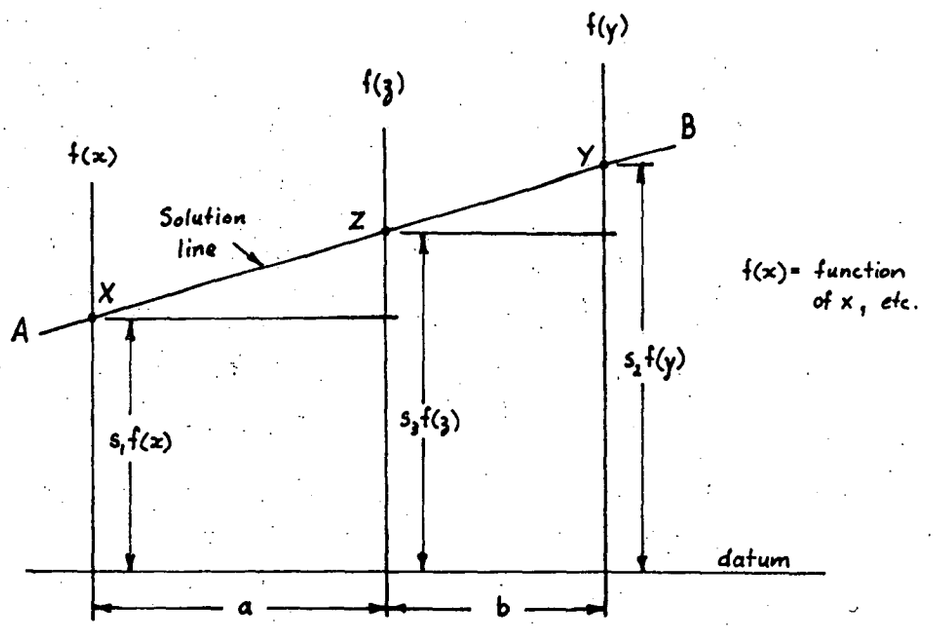

This nomograph can be used to solve equations of the form

$$f(z) = f(x) + f(y) \qquad (1)$$

The chart has to be constructed therefore, in such a way that a line (line AB for instance) through values X and Y will yield the correct solution Z. If s_i is the scale to which the i_{th} function is plotted, then by simple geometry, from the above diagram

$$\frac{s_2 f(y) - s_3 f(z)}{b} = \frac{s_3 f(z) - s_1 f(x)}{a}$$

or

$$bs_1 f(x) + a s_2 f(y) = (a + b)s_3 f(z)$$

However if this is to represent equation (1) then

$$bs_1 = as_2 = (a + b)s_3$$

or

$$\frac{a}{b} = \frac{s_1}{s_2} \tag{2}$$

and therefore

$$s_3 = \frac{s_1 s_2}{s_1 + s_2} \tag{3}$$

Hence once the scales for the functions of x and y have been chosen the ratio of a to b and the scale of the third functions are automatically set from equations 2 and 3.

It is now possible to set up the equations for the flow nomograph. However as only three variables can be dealt with at a time it is first necessary to split the orifice flow equation into two as below

$$q = k\sqrt{p/\rho} \tag{4}$$

$$Q = Aq \tag{5}$$

where p = pressure drop across the orifice

ρ = fluid density

k = constant (includes the discharge coefficient)

A = orifice area

q = flow/unit area

Q = total flow

The same procedure is used on both equations 4 and 5 and hence only equation 4 will be discussed below.

In order to convert equation 4 into the form of equation 1, take logs, i.e.

$$\log(q) = \log(k) + 1/2\log(p) - 1/2\log(\rho)$$

Therefore put

$$f(x) = \log(q/k)$$

$$f(y) = 1/2\log(\rho)$$

$$f(z) = 1/2\log(p)$$

Similarly for equation 5.

The "log" equations are then in the form required and hence by choosing the range and scales for the variables and functions the nomograph can be constructed. The resulting nomograph is presented on the following page.

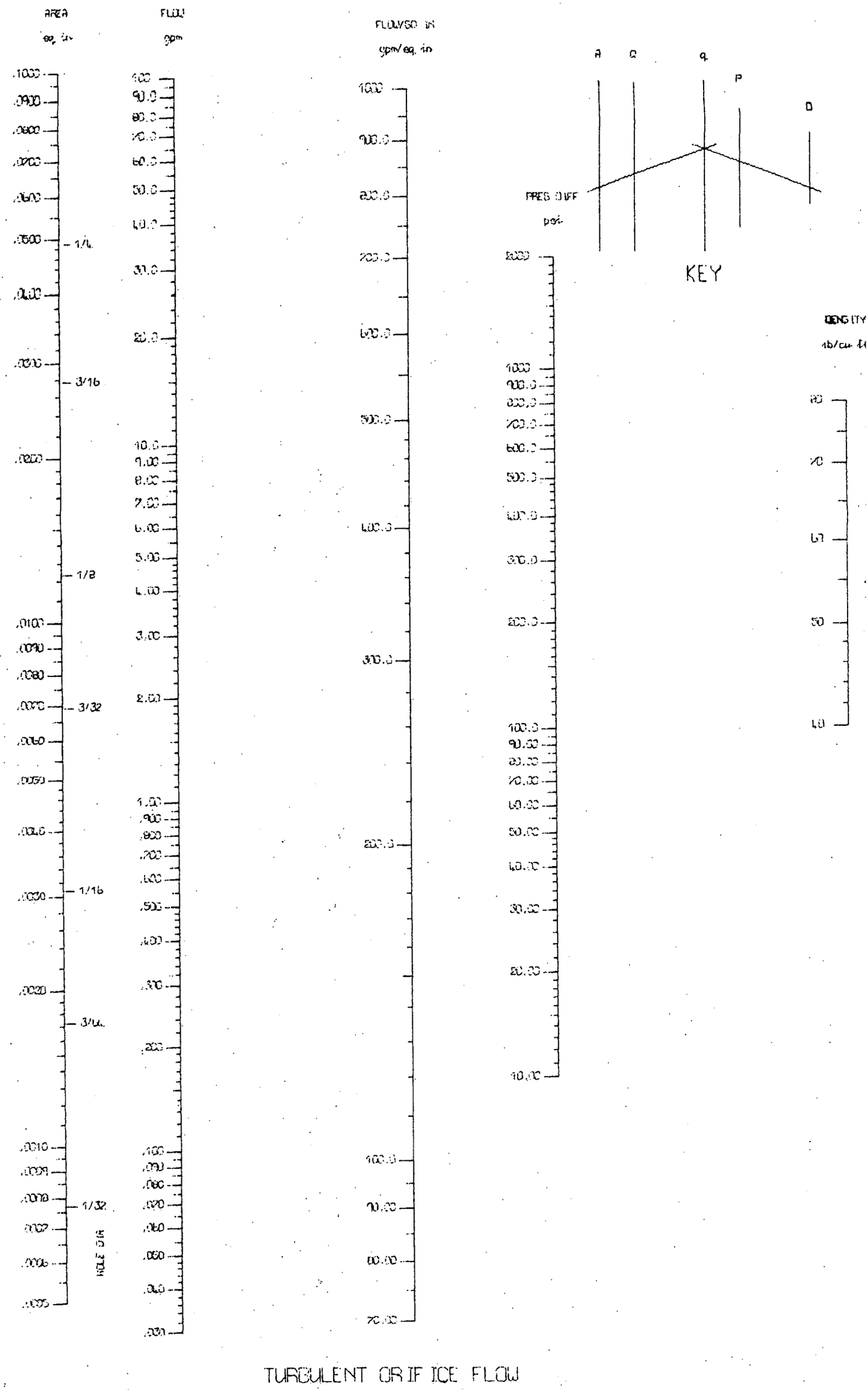

TURBULENT ORIFICE FLOW

$Q = CA\sqrt{2P/D}$ $(C = 0.65)$

IFJ
1971

Appendix 2

Second Order Runge-Kutta Integration Procedure

Consider the differential equation given by

$$\frac{dy}{dx} = f(x, y)$$

with initial condition y_o.

The second order Runge-Kutta process gives an approximate solution at $x + h$ by the following equations:

$$k_o = hf(x_o, y_o)$$

$$k_1 = hf(x_o + h, y_o + k_o)$$

$$y_1 = y_o + 0.5(k_o + k_1)$$

This process can be repeated over and over again by using the new value of y as the initial value in the following step. The truncation error at each step can be shown to be of order h^3.

The technique can also be extended to higher order differential equations by writing the equation as a set of first order equations. For example

$$y'' = f(x, y', y)$$

$$\text{where } y' = \frac{dy}{dx}$$

can be rewritten as the two first order equations

$$v' = f(x, v, y)$$

$$y' = v$$

The procedure is then precisely as before only vectors are used instead of scalers. For example at the first step k_o becomes a column vector rather than a single value, and this vector is used to generate a column vector for k_1 etc. The "solution" at the first step is the column vector

$$\begin{bmatrix} v \\ y \end{bmatrix}$$

Appendix 3

Parameters used in the Mathematical Models

Vibration Tester

Servo A	Servo B	
A = 3	1.5	(ram area) sq.in.
M = 50	20	(ram mass) lbm
C_1 = 150	10	(valve const.) $in^2/\sqrt{psi}$
p = 1000	1000	(supply pres.) psi
$\beta/V = 10^{\pm 4}$	10^{+4}	(bulk mod./volume) lbf/in^5

Solid Slug Model

Cd = 0.72	(discharge coef)	
k = 0.0975	(port area scale factor)	sq.in./in.
ρ = 53	(density)	lb_m/ft^3
p = 1000	(supply press.)	psi
A = 0.196	(hose cross-sect. area)	sq.in.
x_0 = 0.0015	(valve "underlap")	in.
mI = 0.36	(upstream oil mass)	lbm.
mII= 0.72	(downstream oil mass)	lbm.
Q_r = 0.1	(leakage flow during "dead" half cycle)	gpm.

Input amplitude

x = 0.1 for f < 54.2 Hz

then $x = 294/f^2$ f > 54.2 Hz (const. accel. of 30 g.)

Method of Characteristics

	Original	Modified		
C_d	= 0.72	0.73		
k	= 0.0975	0.0975		sq.in./in.
p	= 1000	1000		psi
ρ	= 53	53		lb_m/ft^3
x_o	= 0.0015	0.0015		in.
A	= 0.196	0.196		sq.in.
l_1	= 60	60	(upstream hose length)	in.
l_2	= 120	70	(downstream hose length)	in.
l_3	= -	50	(2nd downstream hose length)	in.
A_o	= -	0.035	(Area downstream orifice)	sq.in.
a	= 2900	2900	(wave velocity)	fps
Q_r	= 0.1	0.1		gpm

Input amplitude :- as for solid slug model.

------ ooo ------

References

1. Ratier-Forest Co. "Oscillating solenoid controls hydraulic slave" Machine Design, May, 1968.

2. Coombes, J.E.M. "Hydraulic remote position - controllers" J. Instn. Elec. Engrs., 1947, 94, 270.

3. Royle, J.K. "Inherent non-linear effects in hydraulic control systems with inertia loading" Proc. Instn. Mech. Engrs., 1959, 173, 257.

4. Butler, R. "Theoretical analysis of the response of a loaded hydraulic relay" Proc. Instn. Mech. Engrs., 1959, 173, 429.

5. Turnbull, D.E. "The response of a loaded hydraulic servomechanism" Proc. Instn. Mech. Engrs., 1959, 173, 270.

6. Martin, H.R. and Lichtarowicz, A. "Theoretical investigation into the prevention of cavitation in hydraulic actuators" Proc. Instn. Mech. Engrs, 1966-67, 181, (No. 18) 423.

7. Walters, R. "Hydraulic and electro-hydraulic servo systems" Iliffe Books Ltd., 1967.

8. Guillon, M. "Hydraulic servo systems", Butterworth & Co., 1969.

9. Reeves, E.I. "Analysis of the effects of nonlinearity in a valve controlled hydraulic drive" Trans. Am. Soc. Mech. Engrs., 1957, 79.

10. Ashley, A.C. and Mills, B. "Frequency response of an electro hydraulic vibrator with inertial load" Jl. Mech. Engng. Sci. 1966, 8, (No. 3), 27.

11. Lambert, T.H. and Davies, R.M. "Investigations of the response of an hydraulic servomechanism with inertial load" Jl. Mech. Engng. Sci. 1963, 5, (No. 3), 281.

12. Blackburn, J.F., Reethof, G., and Shearer, J.L. "Fluid Power Control" MIT Press, 1969

13. Bellman, R.E. "Introduction to Matrix Analysis" McGraw-Hill, 1960.

14. Rosenbrock and Storey "Computational Techniques for Chemical Engineers" Pergamon Press.

15. Smith, G.D. "Numerical Solutions of Partial Differential Equations" Oxford Uni. Press, 1969.

16. Streeter, V.L. and Wylie, E.B. "Hydraulic Transients" McGraw-Hill Book Co., 1967.

------ ooo ------

Refer to Montgomery + Lichtarowicz